
[All ETDs from UAB](#)

[UAB Theses & Dissertations](#)

2010

Functional Determinants Of The Porin Mspa And Its Role In Permeabilizing Mycobacterial Outer Membranes

Jason Huff

University of Alabama at Birmingham

Follow this and additional works at: <https://digitalcommons.library.uab.edu/etd-collection>

Recommended Citation

Huff, Jason, "Functional Determinants Of The Porin Mspa And Its Role In Permeabilizing Mycobacterial Outer Membranes" (2010). *All ETDs from UAB*. 1994.

<https://digitalcommons.library.uab.edu/etd-collection/1994>

This content has been accepted for inclusion by an authorized administrator of the UAB Digital Commons, and is provided as a free open access item. All inquiries regarding this item or the UAB Digital Commons should be directed to the [UAB Libraries Office of Scholarly Communication](#).

FUNCTIONAL DETERMINANTS OF THE PORIN MSPA AND ITS ROLE IN
PERMEABILIZING MYCOBACTERIAL OUTER MEMBRANES

by

JASON HUFF

MICHAEL NIEDERWEIS, COMMITTEE CHAIR
KEVIN DYBVIG
GUILLERMO MARQUES
ANDRIES STEYN
CHARLES TURNBOUGH

A DISSERTATION

Submitted to the graduate faculty of The University of Alabama at Birmingham,
in partial fulfillment of the requirements for the degree of
Doctor of Philosophy

BIRMINGHAM, ALABAMA

2010

FUNCTIONAL DETERMINANTS OF THE PORIN MSPA AND ITS ROLE IN PERMEABILIZING MYCOBACTERIAL OUTER MEMBRANES

JASON HUFF

MICROBIOLOGY

ABSTRACT

Mycobacterium tuberculosis (*Mtb*) infects one third of the global population and causes approximately 2,000,000 Tuberculosis-related deaths annually. Mycobacteria are Gram positive organisms but contain a unique outer membrane (OM) which is functionally similar but structurally different from those of Gram negative bacteria. The mycobacterial OM presents an efficient permeability barrier towards hydrophilic solutes. Slow permeation kinetics of hydrophilic molecules through membranes and several discoveries of cell wall channel-forming proteins indicate that mycobacterial OMs are functionalized by proteins.

MspA is the primary porin of *M. smegmatis* and mediates diffusion of small, hydrophilic nutrients and antibiotics across the OM. Unlike porins of Gram negative bacteria, MspA forms a large, octameric β -barrel and represents the founding member of a new class of OM proteins. *Mtb* does not encode Msp homologs and functions of *Mtb* OM proteins are unknown. Therefore, MspA serves to model transport of hydrophilic compounds across mycobacterial OMs.

Here, the periplasmic L6 loop and the constriction zone were identified as determinants of transport through the MspA channel. The L6 loop affected transport of ions, monosaccharides, voltage-gating, expression, and channel stability, but was dispensable for porin function. Conversely, the constriction zone mutant MspA D90L was highly impaired for channel activity. As the role of the hydrophilic pathway across

the OM during *Mtb* infection was unknown, we expressed MspA wt and D90L in *Mtb* during mouse infections to determine whether increased permeability would be beneficial due to increased nutrient uptake or detrimental due to toxic solute influx. Surface exposure of functional pores drastically reduced virulence, suggesting that toxic solute influx outweighs the benefits of increased nutrient uptake during infection. Because genes that reduce fitness are selected against *in vivo*, stable gene integration is required. Therefore, we constructed a new series of phage-based plasmids capable of multiple, stable integrations in mycobacterial chromosomes. When used in tandem, these vectors provide increased global expression of terminator-protected gene cassettes.

Thus, this work describes how porins functionalize the hydrophilic pathway across mycobacterial OMs and defines low OM permeability as required for *Mtb* virulence. Additionally, new genetic tools were generated to enhance *in vivo* examination of genes in mycobacteria.

TABLE OF CONTENTS

	<i>Page</i>
ABSTRACT	ii
LIST OF TABLES	vi
LIST OF FIGURES	vii
LIST OF BOXES	x
INTRODUCTION	1
Medical significance of <i>Mycobacterium tuberculosis</i>	1
The mycobacterial outer membrane.....	2
Outer membrane proteins of Gram negative bacteria	3
Porins of Gram negative bacteria.....	6
Outer membrane proteins of <i>M. tuberculosis</i>	7
<i>Mycobacterium smegmatis</i> porin A	8
Stable gene integration for <i>M. tuberculosis</i> infection studies.....	12
Aims of dissertation	13
References.....	15
FUNCTIONS OF THE PERIPLASMIC LOOP OF THE PORIN MSPA FROM <i>MYCOBACTERIUM SMEGMATIS</i>	21
OPEN PORES IN THE OUTER MEMBRANE DRASTICALLY REDUCE VIRULENCE OF <i>MYCOBACTERIUM TUBERCULOSIS</i>	50
TAKING PHAGE INTEGRATION TO THE NEXT LEVEL AS A GENETIC TOOL FOR MYCOBACTERIA.....	90
MYCOBACTERIAL OUTER MEMBRANES: IN SEARCH OF PROTEINS	123
SUMMARY AND CONCLUSIONS	149
<i>M. tuberculosis</i> pathogenesis and the mycobacterial cell envelope	149
<i>M. tuberculosis</i> resides in macrophage phagosomes	149
Requirement of surface lipids and proteins	150
Rationale for thesis project	150

Translocation determinants of MspA.....	151
MspA loop L6 is a molecular determinant of translocation	151
Role of the L6 loop in voltage-dependent gating.....	152
Role of the constriction zone in voltage gating	154
Implications of voltage gating for biotechnology.....	154
The L6 loop is required for expression in the outer membrane.....	156
The constriction zone is a molecular determinant of translocation	160
<i>In vivo</i> examination of the hydrophilic pathway across the outer membrane of <i>M. tuberculosis</i>	161
Investigating the requirement of the cell wall for virulence	162
Outer membrane permeabilization by MspA reduces virulence.....	164
Antimycobacterial phagosomal constituents	165
Identification of <i>M. tuberculosis</i> outer membrane proteins and their physiological roles in nutrient acquisition	166
An alternative paradigm for <i>M. tuberculosis</i> pathogenesis and its implications for solute uptake.....	168
Postulates for translational research in the treatment of Tuberculosis	170
A new series of integration-proficient vectors.....	171
Chromosomal vs. episomal gene expression	172
Increased global expression from mycobacterial chromosomes	172
Alternative means of increasing gene expression.....	174
Conclusions.....	176
References.....	177

LIST OF TABLES

<i>Table</i>	<i>Page</i>
FUNCTIONS OF THE PERIPLASMIC LOOP OF THE PORIN MSPA FROM <i>MYCOBACTERIUM SMEGMATIS</i>	
1	Oligonucleotides used in this work.....31
OPEN PORES IN THE OUTER MEMBRANE DRASTICALLY REDUCE VIRULENCE OF <i>MYCOBACTERIUM TUBERCULOSIS</i>	
1	Bacterial strains and plasmids used in this study.....64
TAKING PHAGE INTEGRATION TO THE NEXT LEVEL AS A GENETIC TOOL FOR MYCOBACTERIA	
S1	Primers used in this study100
1	Strains and plasmids used in this study.....105
2	Transformation efficiencies108

LIST OF FIGURES

Figure *Page*

INTRODUCTION

1 Structure of MspA.....9

FUNCTIONS OF THE PERIPLASMIC LOOP OF THE PORIN MSPA FROM

MYCOBACTERIUM SMEGMATIS

1 Schematic representation of the deletions in the periplasmic loop 6 of MspA30

2 Expression of MspA loop deletion mutants in the porin mutant *M. smegmatis* ML16
.....32

3 Single channel recordings of purified MspA loop deletion mutants in lipid bilayers
.....33

4 Analysis of single channel conductances of purified MspA deletion mutants34

5 Voltage gating properties of purified MspA L6 deletion mutants.....36

6 Surface accessibility and *in vivo* function of MspA L6 deletion mutants39

OPEN PORES IN THE OUTER MEMBRANE DRASTICALLY REDUCE

VIRULENCE OF MYCOBACTERIUM TUBERCULOSIS

1 Expression of *mspA* in *M. tuberculosis*.....65

S1 Detection of MspA expression in *M. tuberculosis* by blot over-exposure65

2 Virulence of *M. tuberculosis* chromosomally expressing *mspA* during mouse

	infections.....	66
3	Virulence of <i>M. tuberculosis</i> episomally expressing <i>mspA</i> during mouse infections	68
4	Expression of Leucine mutants in <i>M. smegmatis</i>	70
5	Single channel analysis of MspA D90L and D90L/D91L.....	71
6	Diffusion of glucose through MspA D90L and D90L/D91L into liposomes.....	72
7	Activity of MspA D90L and D90L/D91L <i>in vivo</i>	74
8	Surface accessibility of MspA, MspA D90L, and OmpA in <i>M. tuberculosis</i> by whole cell ELISA.....	76
9	Virulence of <i>M. tuberculosis</i> expressing functional or transport-impaired MspA channels.....	77

TAKING PHAGE INTEGRATION TO THE NEXT LEVEL AS A GENETIC TOOL
FOR MYCOBACTERIA

1	Genomic organization of the mycobacteriophage L5 bacterial attachment site and crossover with the phage attachment site.....	93
2	Plasmid map of integration vector pML1342	104
3	Identification of positive clones by visualization of plasmid-encoded reporter genes	109
4	Expression of <i>gfp_m²⁺</i> from episomal and integrative vectors in <i>M. smegmatis</i>	110
5	Expression of <i>gfp_m²⁺</i> from episomal and integrative vectors in <i>M. tuberculosis</i>	111
6	Mycobacteriophage attachment sites in <i>M. smegmatis</i> and <i>M. tuberculosis</i> chromosomes	113
S1	Activity of <i>xylE_m</i> integrated at <i>M. smegmatis</i> L5, Giles and Ms6 <i>attB</i> sites	114
S2	Recombination of a plasmid containing L5 <i>attP</i> and L5 <i>attB</i> in <i>E. coli</i>	116
7	Co-transformation and superintegration in <i>M. tuberculosis</i>	118

MYCOBACTERIAL OUTER MEMBRANES: IN SEARCH OF PROTEINS

1	Cryo-electron microscopy of the mycobacterial cell envelope.....	128
2	Models of the mycobacterial outer membrane and cell envelope.....	129
3	Structure of the porin MspA of <i>M. smegmatis</i>	133

LIST OF BOXES

<i>Box</i>		<i>Page</i>
	MYCOBACTERIAL OUTER MEMBRANES: IN SEARCH OF PROTEINS	
1	The cryo-electron tomography (CET) technique.....	127

INTRODUCTION

Medical significance of *Mycobacterium tuberculosis*. Nearly two million people annually succumb to infection with *Mycobacterium tuberculosis*, the causative agent of Tuberculosis, while about one third of the global population harbors latent infections (24). Though a vaccine exists in the nearly genetically identical *M. bovis* BCG (>99.9%), its efficacy is limited to protection in children but remains ineffective against the primary form of the disease, adult pulmonary tuberculosis (66). Treatment of *M. tuberculosis* infections requires combination therapy consisting of up to four drugs for a minimum duration of six months. The rise of the HIV pandemic in recent decades has caused a resurgence in *M. tuberculosis* infections, often in the poorest and most rural areas of the globe. The prohibitively high cost of treatment combined with rising HIV coinfection rates, ineffective protection by the BCG vaccine, and emergence of multiple drug resistant strains (MDR) and extensively drug resistant strains (XDR) warrant the labeling of *M. tuberculosis* as a Global Emergency by the World Health Organization (37).

After inhalation into the lung, *M. tuberculosis* is phagocytosed by resident alveolar macrophages where it is contained in immune cell aggregates called granulomas. *M. tuberculosis* can survive in these macrophages because it inhibits the maturation of the phagosome and prevents fusion with acidic, bactericidal lysosomes (60). However, with the onset of the adaptive immune response, stimulation of macrophages via IFN- γ overrides the blockade of phagosome maturation and enables them to destroy the bacteria in lysosomal compartments by delivery of bactericidal compounds including reactive nitrogen and oxygen intermediates (RNIs and ROIs), protons, defensins and cathelicidins. The life-long persistent infection established by *M. tuberculosis* begs the

question of how the organism survives in such a harsh environment containing many noxious molecules.

The mycobacterial outer membrane. Although technically Gram positive, mycobacteria contain a unique outer membrane. This outer membrane contains some of the longest fatty acids found in nature called mycolic acids which are esterified to an arabinogalactan-peptidoglycan copolymer in the cell wall. These massive, covalently linked lipids account for the low fluidity and low permeability of the rigid cell wall (39). Though the idea that esterified mycolic acids and other extractable phospholipids are arranged to form a second membrane was first proposed by Minnikin in 1982 (46), direct proof by visualization remained elusive for years. Only very recently did cryoelectron tomography and microscopy of ultrathin vitreous sections produce the first visualizations of the mycobacterial outer membrane and confirm the existence of this unique subcellular compartment (30, 87). Interestingly, the outer membrane measured about 8 nm thick, much too thin to house fully extended mycolic acids that contain acyl chains of up to 60 carbon atoms. To account for this, several models, each with limited experimental support, were proposed including intercalating extractable lipids, extension of mycolic acid heads beneath the inner leaflet into the putative periplasm (30), and folded conformations of the mycolic acid acyl chains (87). Though functionally similar, the composition and architecture of the mycobacterial outer membrane is thus significantly different from the outer membrane found in Gram negative bacteria.

The requirement of outer membrane lipids for virulence of *M. tuberculosis* is well established (1, 23). The critical role of lipids is not surprising given that almost one-third of the *M. tuberculosis* genome is devoted to lipid metabolism (10). For instance, lipid

effectors suppress production of pro-inflammatory cytokines (54, 65, 68), inhibit phagosome maturation by several methods (20, 84), and are required for resistance to IFN- γ -independent immunity (50). The outer membrane constituted by esterified mycolic acids and extractable lipids is a primary constituent of the mycobacterial cell wall that renders them approximately 1,000-fold less permeable to small, hydrophilic compounds such as cephalosporins in comparison to Gram negative bacteria such as *Escherichia coli* (34). Expectedly, mutants devoid in synthesis of extractable lipids or with altered biogenesis of mycolic acids (the latter are essential (61)) increase permeability (9, 33) and/or highly reduce virulence of *M. tuberculosis* (15, 22, 67). Thus, the unique outer membrane lipids of mycobacteria serve both structural and effector functions required for virulence and antibiotic resistance.

The efficient cell wall barrier surrounding the bacterium presents a seemingly contradictory problem as *M. tuberculosis* must still acquire nutrients while resisting the uptake of toxic compounds. To meet these needs, Gram negative bacteria such as *E. coli* employ over 60 proteins to functionalize the outer membrane. Many transport functions performed in the outer membrane are essential as intrinsic permeation rates for many solutes across membranes are too slow to be physiologically relevant (55). With its highly efficient permeability barrier, *M. tuberculosis* must also functionalize the outer membrane with proteins. Consistent with this assumption, over 140 proteins were predicted to be outer membrane proteins in *M. tuberculosis* (76) and channel-forming proteins have been observed in cell wall extracts (72, 75, 82).

Outer membrane proteins of Gram negative bacteria. Gram negative bacteria such as *E. coli* functionalize the outer membrane with proteins that perform a wide array

of functions. These functions range from nutrient uptake, assembly of the membrane and complexes therein, secretion of molecules, and cell-adhesion (for further review, see (55)). As they are exposed at the cell surface, many outer membrane proteins also serve as phage receptors and are antigens. Thus, outer membrane proteins provide first-line interactions with the environment.

Nearly all outer membrane proteins with known structures have no hydrophobic α -helices and contain amphipathic β -strands that arrange to form very rigid β -barrels (71). Loops link β -strands on both sides of the membrane in most simple β -barrel structures. However, some proteins contain larger soluble domains likely important for function such as corks, hatches, and peptidoglycan binding domains (7). High β -content allows for exceptional stability of outer membrane proteins, which can be resistant to many denaturants such as detergents, urea, pH and heat (27). Because of this, many outer membrane proteins retain channel activity after cellular extraction when reconstituted in artificial lipid bilayers.

Many nutrients are either scarce or very large, making passive diffusion processes impossible to sustain growth. Thus, energy is required for the uptake of nutrients such as iron and vitamin B₁₂. However, ATP is generated and sequestered in the cytosol, therefore making direct accessibility to energy problematic for outer membrane proteins. To solve this problem, energy-dependent outer membrane transporters link to the inner membrane ATPase ExbBD via the periplasmic energy transducer TonB. For instance, binding of iron-loaded ferrichrome to the *E. coli* siderophore receptor FhuA induces its interaction with TonB (47). The combination of ligand binding and energy transduced by TonB induces conformational changes in FhuA, which may include hatch domain

movement or disorganization, thereby initiating transport of the siderophore through the barrel. Periplasmic binding proteins then shuttle released iron-loaded siderophores to inner membrane transport pumps in a multi-step import process (7). In an alternative method, the promiscuous drug exporter TolC links directly from the outer membrane to the inner membrane pump AcrB via the periplasmic adapter AcrA, resulting in efficient, energy-dependent expulsion of toxic compounds across both membranes in a single step (56).

While energy is required for transport across the outer membrane for large or scarce molecules or against concentration gradients, Gram negative bacteria have also developed interesting energy-independent mechanisms for nutrient acquisition. Outer membrane transporters in this category require no periplasmic adaptors or inner membrane ATPases, but rather rely on intrinsic properties of strategically positioned side chains for both substrate specificity and mechanism of transport. The fatty acid transporter FadL of *Pseudomonas aeruginosa* presents a unique uptake model where substrates are first captured at a low affinity binding site at the protein exterior, diffuse through a hydrophobic channel in the barrel to a high affinity binding pocket, and are laterally released through the barrel wall into the outer membrane via a spontaneous conformational change in an interior kinked strand (26). *E. coli* LamB, also known as "maltoporin," contains a succession of aromatic residues spiraling down the length of the barrel (70). This so-called "greasy slide" interacts with oligosaccharides via Van der Waals forces (17) while charged residues called the "polar track" transiently form hydrogen bonds with sugar hydroxyl groups (16), thus guiding the substrate through the specific diffusion channel. These and other examples highlight the ability of Gram

negative bacteria to selectively take up substrates while resisting influx of toxic compounds across the ATP-inaccessible compartment of the outer membrane.

Porins of Gram negative bacteria. Diffusion of small and hydrophilic compounds across the outer membrane of Gram negative bacteria is mediated by porins. These energy-independent channel proteins allow non-specific diffusion of hydrophilic compounds approx. 600 Da or less (36). The general porins (also called classical porins) of *E. coli* consist of monomeric β -barrels which trimerize to form three-pore functional units. Structures of the three primary porins OmpF, PhoE (11), and OmpC (3) show that barrel monomers are joined together via an external loop called a latch which folds over the top of the adjacent barrel. Another loop referred to as L3 folds back into the barrel creating a narrowing or constriction of the open pore. Loss or alteration of porins often results in increased antibiotic resistance (13) and a decrease in nutrient uptake and growth rate (40, 41).

Referring to porins as non-specific, general diffusion pathways may be misleading. While porins are by definition not specific for any particular substrate, they do have substrate preferences, are not passive pores but rather contain dynamic features, and their activity is regulated at every level in the cell. For instance, the *E. coli* porin OmpF prefers cations while PhoE prefers anions (5), despite a 72% amino acid sequence similarity. Anionic preference likely explains the expression of PhoE during phosphate starvation (85). The transport properties of OmpF differ from OmpC with OmpF conducting ions in artificial lipid bilayers more efficiently than OmpC (8) and is more permeable to larger compounds in whole cells (58) and liposomes (57). For an excellent review of channel activity experiments in artificial lipid bilayers and liposomes, see (83).

Interestingly, expression of OmpF is repressed while OmpC is increased under conditions of high osmolarity (35), acidic pH (28), and low oxygen (44). These results imply that conditions encountered by *E. coli* during infection in the gastrointestinal tract induce adjustments to lower permeability by switching to the more restrictive channel OmpC, thus decreasing influx of toxic solutes such as bile salts (55, 62).

Outer membrane permeability is not altered simply by the exchange of porins with channels of apparently different size. In fact, the recent crystal structure of OmpC showed its channel size and geometry to be nearly identical to that of OmpF (3). Therefore, electrostatic potential and amino acid side chain arrangement must at least partially account for the different channel properties of OmpF and OmpC. In agreement, molecular dynamics simulations defined distinct pathways for flowing counterions in the OmpF channel lumen (31). Additionally, mutation of a single key residue in PhoE can drastically alter ion selectivity without affecting localization or single channel conductance (4). The channel lumen of OmpF can also be directly occluded by channel-blocking polyamines (14, 32) or by dynamically folding extracellular loops in response to pH and possibly voltage (2, 49). These experiments show that passage through a general porin must account for dynamic regulatory mechanisms as well as electrostatic properties within the barrel lumen. Thus, porins are better characterized as preferential diffusion pores rather than permissive based upon size alone.

Outer membrane proteins of *M. tuberculosis*. Despite the wealth of knowledge about outer membrane proteins in Gram negative bacteria, extremely little is known about their counterparts in mycobacteria. More than 15 years before the visualization of the outer membrane, channel-forming proteins were evident in the mycobacterial cell

wall (82). This result argued for the existence of an outer membrane as open channels inserted in the inner membrane would likely disrupt the proton gradient and efflux essential nutrients (52). OmpATb (Rv0899) was the first identified channel-forming protein in the cell wall of *M. tuberculosis* and was originally proposed to be a porin based upon weak homology with the monomeric porin OmpA of *E. coli* and its small single channel conductance of 0.7 nS (72). It is also the first reported outer membrane virulence factor of *M. tuberculosis* (64). Surprisingly, the pore-forming activity of OmpATb is reduced while its expression is increased at low pH (48, 64). The apparent contrast between activity and expression may be explained in that OmpATb is required for normal adaptation to low pH and is induced during infection (64). These results suggest an alternative function for this protein (51).

Rv1698 was the second confirmed pore-forming protein identified in the outer membrane of *M. tuberculosis*. This protein produced large channels in artificial lipid bilayers (4.5 nS single channel conductance) and at least partially complemented the porin defects of a *M. smegmatis* porin mutant (75). Though nothing is yet known about the function of Rv1698, homologues exist in all corynebacteria, suggesting it plays an important role in functionalizing outer membranes of these mycolic acid-producing bacteria. In addition, Rv1973 was identified by bioinformatics and experimentally determined to be an outer membrane protein of *M. tuberculosis* (76). Despite its annotation as a mycobacterial cell entry (mce) protein, nothing is yet known about the function of this protein.

***Mycobacterium smegmatis* porin A.** The fast growing, non-pathogenic saprophyte *M. smegmatis* contains at least four highly homologous porins called MspA,

B, C, and D (53). The primary porin of *M. smegmatis* is MspA, which has a large single channel conductance of 4.6 nS (78). Deletion of *msp* genes results in reduced nutrient uptake, slower growth, and resistance to hydrophilic antibiotics (12, 79, 80, 86). Heterologous expression of *mspA* in slow growing mycobacteria increases nutrient uptake, growth, and sensitivity to antibiotics (43). These results show that MspA can serve as a model for transport of hydrophilic solutes across mycobacterial outer membranes.

The MspA crystal structure (Fig. 1) (19) is unique in comparison to all crystal structures of outer membrane proteins solved thus far. Despite the structural dissimilarity, the primary features of porins found in Gram negative bacteria are evident in MspA. It is a large β -barrel channel that spans the outer membrane and contains both periplasmic and extracellular loops that connect adjacent β -strands.

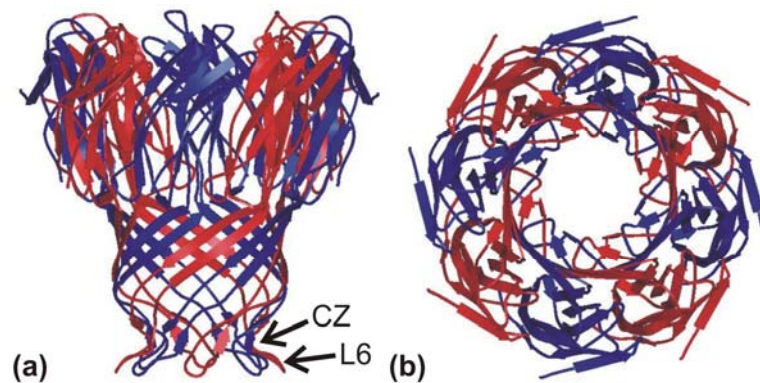


Figure 1. Structure of MspA. A) Side view of the MspA octamer. Alternating monomers are highlighted in red and blue. Arrows in the crystal structure represent β -strands. The three distinct β -barrels are evident from this view. CZ: constriction zone; L6: periplasmic loop L6. B) Top-down view of the MspA octamer. This view displays the hollow channel of the porin which is narrowed by the constriction zone. PDB accession code: 1UUN.

Contrary to the trimeric porins of Gram negative bacteria, MspA is an octameric porin with only one channel per octamer. While no inward folding loop constricts the barrel similar to the L3 loop of OmpF, MspA instead contains a constriction zone derived from a narrowing of the channel. Interestingly, this most constricted region of the pore is lined by 16 aspartic acid residues, which likely explains the cation preference of MspA (53). Each MspA monomer contains an unusually large periplasmic loop positioned at the base of the barrel referred to as the L6 loop. Interestingly, the L6 loop, which is accessible in whole cells to biotinylation agents (42) and may be flexible, is positioned just below the constriction zone. Together, the periplasmic loop L6 and the constriction zone may play important roles in the transport properties of MspA in a similar manner that flexible loops and luminal residues of porins from Gram negative bacteria do. These features show that MspA is the founding member of a new class of outer membrane proteins and highlight the concept that mycobacterial outer membrane proteins are functionally similar but structurally unique in comparison to those of Gram negative bacteria. Novel structure also suggests that mycobacterial outer membrane proteins likely function by novel mechanisms.

No Msp homologs or other known general porins are encoded by the genome of *M. tuberculosis* (10). However, permeation rates of small and hydrophilic compounds across lipid bilayers are assumed to be too slow to be physiologically relevant (55). This indicates that the outer membrane of *M. tuberculosis* is functionalized by proteins, as evidenced by the existence of channel-forming proteins identified in this compartment. Identification and characterization of such proteins would be critical to our understanding

of the physiology of *M. tuberculosis* and its environmental interactions during infection. In the absence of identified genuine porins in *M. tuberculosis* or other slowly growing mycobacteria, MspA serves to model the transport of small and hydrophilic molecules across mycobacterial outer membranes.

The growth rate of the vaccine strain *M. bovis* BCG is increased upon expression of *mspA* (43). However, the growth rate is not increased to that of the fast growing, non-pathogenic *M. smegmatis*. This suggests that the slow growth rate of members of the *M. tuberculosis* complex is not due to slow nutrient uptake alone and that other factors such as slow DNA elongation (29), slow RNA and protein synthesis (6, 25), and presence of the DNA-binding protein MDBPI (45) may also account for slow growth. It has yet to be determined if slow growth is a requirement for, the result of, or correlated with virulence. Expression of *mspA* in *M. tuberculosis* expectedly increased not only the growth rate but also susceptibility to hydrophilic and hydrophobic antibiotics (43). The apparent problem is that *M. tuberculosis* must acquire nutrients for growth and replication while resisting the uptake of toxic compounds. Mechanisms by which *M. tuberculosis* achieves this balance of permeability and resistance have not been reported.

The increased antibiotic sensitivity upon *mspA* porin expression begs the question whether *M. tuberculosis* utilizes high impermeability to resist noxious compounds encountered during infection at the expense of nutrient uptake. Deletion of *msp* genes from *M. smegmatis* enhanced intracellular survival in macrophages (74). Reduced permeability to a ubiquitin-derived peptide (63) and nitric oxide (18) at least partially account for increased survival of *M. smegmatis* lacking porins in macrophages. Conversely, expression of *mspA* in *M. bovis* BCG resulted in increased survival in

macrophages (73), suggesting that the mechanisms governing intracellular survival in relation to outer membrane permeability are different between fast growing, non-pathogenic mycobacteria and slow growing, virulent mycobacteria. It is unclear whether the survival of *M. tuberculosis* in mice would be enhanced from increased nutrient uptake or be compromised due to increased permeability to toxic solutes. Both outcomes were previously observed for *M. bovis* BCG *in vitro*, and results of such experiments would help to define the physiology of *M. tuberculosis* during infection.

Stable gene integration for *M. tuberculosis* infection studies. Introduction of foreign genes or genes for complementation is performed to generate vaccine candidates or examine functions of their protein products. For example, heterologous expression of *mspA* in *M. tuberculosis* sheds light on the role of the hydrophilic pathway across the outer membrane during infection. The easiest method of introducing genes into mycobacteria is by transformation of multi-copy episomal expression vectors. However, episomal vectors cannot be selected for during infection and may be subsequently lost, thus skewing the results of often very time consuming and expensive infection studies. Therefore, stable expression of introduced genes is required for infection experiments and can be achieved by plasmid integration in the host chromosome.

The most commonly used method to integrate genes into mycobacterial chromosomes is by use of phage-encoded integration machinery. The mycobacteriophage L5 genome includes all the components necessary for integration in the genomes of *M. tuberculosis* and *M. smegmatis*. The phage encoded integrase (*int*) mediates site-specific recombination between the phage attachment site *attP* and the homologous bacterial attachment site *attB* located in the *glyV* tRNA gene (38). A mycobacterial-encoded

integration host factor (mIHF) is jointly required for integration (59). Because *attP* and *attB* are homologous, the *glyV* gene is reconstituted at the newly formed *attL* site, thereby avoiding deleterious effects on the host (38). For a visual representation of phage integration into mycobacterial chromosomes, refer to Figure 1 on page 93. Sequence reconstitution but not functional reconstitution of *attB* occurs at the *attL* site after integration ((38) and Dr. Graham Hatfull, personal communication). Taken together, plasmids containing the mycobacteriophage L5 *int* gene and *attP* site can be integrated into mycobacterial chromosomes.

Several caveats exist when attempting to generate stable, high-level expression from integrated constructs. Continuous expression of the L5 integrase destabilizes integrated plasmids (77) and disproportionately low expression levels are often observed ((81) and Mailaender, unpublished results). Furthermore, the number of genes that can be integrated is limited (69). Several methods to curtail these pitfalls have been developed ranging from separately expressing integrase genes (77), integrating an additional *attB* site into the genome (69), or integrating multiple genes at different mycobacteriophage attachment sites (21). To date, however, no integrative plasmid has been developed that satisfies all the requirements needed to increase expression, maintain plasmid stability, be genetically modular, and adaptable to alternative integration machinery.

Aims of dissertation. MspA is the founding member of a new class of mycobacterial outer membrane proteins and serves as a model for transport of small and hydrophilic solutes across this membrane. Mechanisms governing transport through the MspA channel are currently unknown. Crystal structure analysis and biotinylation accessibility studies identified the periplasmic loop L6 as a possible functional

determinant of MspA. We therefore examined the role of the L6 loop in solute transport, expression, and stability of MspA. As the physiology of *M. tuberculosis* during infection is poorly defined, we expressed *mspA* in *M. tuberculosis* during mouse infections as a tool to examine the role of the hydrophilic pathway across the outer membrane and its effects on virulence. To integrate stable, high-level expression plasmids in mycobacterial chromosomes for infection studies and to compare gene expression from different locations in mycobacterial chromosomes, a new series of vectors were generated which contain bidirectional intrinsic transcriptional terminators flanking an expression cassette, removable integrase genes monitorable by a backbone reporter gene, and are adaptable to multiple phage integration sites. Additionally, the current progress of determining mycobacterial cell wall architecture and attributing function to its resident proteins, as well as a discussion of putative outer membrane proteins, are reviewed.

REFERENCES

1. **Barry, C. E.** 2001. Interpreting cell wall 'virulence factors' of *Mycobacterium tuberculosis*. Trends Microbiol **9**:237-41.
2. **Basle, A., R. Qutub, M. Mehrazin, J. Wibbenmeyer, and A. H. Delcour.** 2004. Deletions of single extracellular loops affect pH sensitivity, but not voltage dependence, of the *Escherichia coli* porin OmpF. Protein Eng Des Sel **17**:665-72.
3. **Basle, A., G. Rummel, P. Storici, J. P. Rosenbusch, and T. Schirmer.** 2006. Crystal structure of osmoporin OmpC from *E. coli* at 2.0 Å. J Mol Biol **362**:933-42.
4. **Bauer, K., M. Struyve, D. Bosch, R. Benz, and J. Tommassen.** 1989. One single lysine residue is responsible for the special interaction between polyphosphate and the outer membrane porin PhoE of *Escherichia coli*. J. Biol. Chem. **264**:16393-8.
5. **Benz, R., A. Schmid, and R. E. Hancock.** 1985. Ion selectivity of gram-negative bacterial porins. J. Bacteriol. **162**:722-7.
6. **Bercovier, H., O. Kafri, and S. Sela.** 1986. Mycobacteria possess a surprisingly small number of ribosomal RNA genes in relation to the size of their genome. Biochem Biophys Res Commun **136**:1136-41.
7. **Braun, V., and F. Endriss.** 2007. Energy-coupled outer membrane transport proteins and regulatory proteins. Biometals **20**:219-31.
8. **Buehler, L. K., S. Kusumoto, H. Zhang, and J. P. Rosenbusch.** 1991. Plasticity of *Escherichia coli* porin channels. Dependence of their conductance on strain and lipid environment. J. Biol. Chem. **266**:24446-50.
9. **Camacho, L. R., P. Constant, C. Raynaud, M. A. Laneelle, J. A. Triccas, B. Gicquel, M. Daffé, and C. Guilhot.** 2001. Analysis of the phthiocerol dimycocerosate locus of *Mycobacterium tuberculosis*. Evidence that this lipid is involved in the cell wall permeability barrier. J. Biol. Chem. **276**:19845-54.
10. **Cole, S. T., R. Brosch, J. Parkhill, T. Garnier, C. Churcher, D. Harris, S. V. Gordon, K. Eiglmeier, S. Gas, C. E. Barry, 3rd, F. Tekaia, K. Badcock, D. Basham, D. Brown, T. Chillingworth, R. Connor, R. Davies, K. Devlin, T. Feltwell, S. Gentles, N. Hamlin, S. Holroyd, T. Hornsby, K. Jagels, and B. G. Barrell.** 1998. Deciphering the biology of *Mycobacterium tuberculosis* from the complete genome sequence. Nature **393**:537-44.
11. **Cowan, S. W., T. Schirmer, G. Rummel, M. Steiert, R. Ghosh, R. A. Paupit, J. N. Jansonius, and J. P. Rosenbusch.** 1992. Crystal structures explain functional properties of two *E. coli* porins. Nature **358**:727-33.
12. **Danilchanka, O., M. Pavlenok, and M. Niederweis.** 2008. Role of porins for uptake of antibiotics by *Mycobacterium smegmatis*. Antimicrob Agents Chemother **52**:3127-34.
13. **Davin-Regli, A., J. M. Bolla, C. E. James, J. P. Lavigne, J. Chevalier, E. Garnotel, A. Molitor, and J. M. Pages.** 2008. Membrane permeability and regulation of drug "influx and efflux" in enterobacterial pathogens. Curr Drug Targets **9**:750-9.
14. **delaVega, A. L., and A. H. Delcour.** 1995. Cadaverine induces closing of *E. coli* porins. Embo J **14**:6058-65.

15. **Dubnau, E., J. Chan, C. Raynaud, V. P. Mohan, M. A. Laneelle, K. Yu, A. Quemard, I. Smith, and M. Daffé.** 2000. Oxygenated mycolic acids are necessary for virulence of *Mycobacterium tuberculosis* in mice. *Mol Microbiol* **36**:630-7.
16. **Dumas, F., R. Koebnik, M. Winterhalter, and P. van Gelder.** 2000. Sugar transport through maltoporin of *Escherichia coli*. Role of polar tracks. *J Biol Chem* **275**:19747-51.
17. **Dutzler, R., Y. F. Wang, P. Rizkallah, J. P. Rosenbusch, and T. Schirmer.** 1996. Crystal structures of various maltooligosaccharides bound to maltoporin reveal a specific sugar translocation pathway. *Structure* **4**:127-34.
18. **Fabrino, D. L., C. K. Bleck, E. Anes, A. Hasilik, R. C. Melo, M. Niederweis, G. Griffiths, and M. G. Gutierrez.** 2009. Porins facilitate nitric oxide-mediated killing of mycobacteria. *Microbes Infect* **11**:868-75.
19. **Faller, M., M. Niederweis, and G. E. Schulz.** 2004. The structure of a mycobacterial outer-membrane channel. *Science* **303**:1189-92.
20. **Fratti, R. A., J. Chua, I. Vergne, and V. Deretic.** 2003. *Mycobacterium tuberculosis* glycosylated phosphatidylinositol causes phagosome maturation arrest. *Proc Natl Acad Sci USA* **100**:5437-42.
21. **Freitas-Vieira, A., E. Anes, and J. Moniz-Pereira.** 1998. The site-specific recombination locus of mycobacteriophage Ms6 determines DNA integration at the tRNA(Ala) gene of *Mycobacterium* spp. *Microbiology* **144** (Pt 12):3397-406.
22. **Glickman, M. S., J. S. Cox, and W. R. Jacobs, Jr.** 2000. A novel mycolic acid cyclopropane synthetase is required for cording, persistence, and virulence of *Mycobacterium tuberculosis*. *Mol Cell* **5**:717-27.
23. **Guenin-Mace, L., R. Simeone, and C. Demangel.** 2009. Lipids of pathogenic Mycobacteria: contributions to virulence and host immune suppression. *Transbound Emerg Dis* **56**:255-68.
24. **Harries, A. D., and C. Dye.** 2006. Tuberculosis. *Ann. Trop. Med. Parasitol.* **100**:415-31.
25. **Harshey, R. M., and T. Ramakrishnan.** 1977. Rate of ribonucleic acid chain growth in *Mycobacterium tuberculosis* H37Rv. *J. Bacteriol.* **129**:616-22.
26. **Hearn, E. M., D. R. Patel, B. W. Lepore, M. Indic, and B. van den Berg.** 2009. Transmembrane passage of hydrophobic compounds through a protein channel wall. *Nature* **458**:367-70.
27. **Heinz, C., H. Engelhardt, and M. Niederweis.** 2003. The core of the tetrameric mycobacterial porin MspA is an extremely stable beta-sheet domain. *J. Biol. Chem.* **278**:8678-8685.
28. **Heyde, M., and R. Portalier.** 1987. Regulation of major outer membrane porin proteins of *Escherichia coli* K 12 by pH. *Mol. Gen. Genet.* **208**:511-7.
29. **Hiriyan, K. T., and T. Ramakrishnan.** 1986. Deoxyribonucleic acid replication time in *Mycobacterium tuberculosis* H37Rv. *Arch. Microbiol.* **144**:105-9.
30. **Hoffmann, C., A. Leis, M. Niederweis, J. M. Pitzko, and H. Engelhardt.** 2008. Disclosure of the mycobacterial outer membrane: Cryo-electron tomography and vitreous sections reveal the lipid bilayer structure. *Proc. Natl. Acad. Sci. U S A* **105**:3963-3967.

31. **Im, W., and B. Roux.** 2002. Ions and counterions in a biological channel: A molecular dynamics simulation of OmpF porin from *Escherichia coli* in an explicit membrane with 1 M KCl aqueous salt solution. *J. Mol. Biol.* **319**:1177-97.
32. **Iyer, R., Z. Wu, P. M. Woster, and A. H. Delcour.** 2000. Molecular basis for the polyamine-OmpF porin interactions: inhibitor and mutant studies. *J Mol Biol* **297**:933-45.
33. **Jackson, M., C. Raynaud, M. A. Laneelle, C. Guilhot, C. Laurent-Winter, D. Ensergueix, B. Gicquel, and M. Daffé.** 1999. Inactivation of the antigen 85C gene profoundly affects the mycolate content and alters the permeability of the *Mycobacterium tuberculosis* cell envelope. *Mol Microbiol* **31**:1573-87.
34. **Jarlier, V., and H. Nikaido.** 1990. Permeability barrier to hydrophilic solutes in *Mycobacterium chelonae*. *J. Bacteriol.* **172**:1418-1423.
35. **Kawaji, H., T. Mizuno, and S. Mizushima.** 1979. Influence of molecular size and osmolarity of sugars and dextrans on the synthesis of outer membrane proteins O-8 and O-9 of *Escherichia coli* K-12. *J Bacteriol* **140**:843-7.
36. **Koebnik, R., K. P. Locher, and P. van Gelder.** 2000. Structure and function of bacterial outer membrane proteins: barrels in a nutshell. *Mol. Microbiol.* **37**:239-53.
37. **Laughon, B. E.** 2007. New tuberculosis drugs in development. *Curr Top Med Chem* **7**:463-73.
38. **Lee, M. H., L. Pascopella, W. R. Jacobs, Jr., and G. F. Hatfull.** 1991. Site-specific integration of mycobacteriophage L5: integration-proficient vectors for *Mycobacterium smegmatis*, *Mycobacterium tuberculosis*, and bacille Calmette-Guerin. *Proc Natl Acad Sci USA* **88**:3111-5.
39. **Liu, J., C. E. Barry, 3rd, G. S. Besra, and H. Nikaido.** 1996. Mycolic acid structure determines the fluidity of the mycobacterial cell wall. *J. Biol. Chem.* **271**:29545-51.
40. **Liu, X., and T. Ferenci.** 1998. Regulation of porin-mediated outer membrane permeability by nutrient limitation in *Escherichia coli*. *J. Bacteriol.* **180**:3917-22.
41. **Lutkenhaus, J. F.** 1977. Role of a major outer membrane protein in *Escherichia coli*. *J Bacteriol* **131**:631-7.
42. **Mahfoud, M., S. Sukumaran, P. Hülsmann, K. Grieger, and M. Niederweis.** 2006. Topology of the porin MspA in the outer membrane of *Mycobacterium smegmatis*. *J Biol Chem* **281**:5908-15.
43. **Mailaender, C., N. Reiling, H. Engelhardt, S. Bossmann, S. Ehlers, and M. Niederweis.** 2004. The MspA porin promotes growth and increases antibiotic susceptibility of both *Mycobacterium bovis* BCG and *Mycobacterium tuberculosis*. *Microbiology* **150**:853-864.
44. **Matsubara, M., S. I. Kitaoka, S. I. Takeda, and T. Mizuno.** 2000. Tuning of the porin expression under anaerobic growth conditions by his-to-Asp cross-phosphorelay through both the EnvZ-osmosensor and ArcB-anaerosensor in *Escherichia coli*. *Genes Cells* **5**:555-69.
45. **Matsumoto, S., M. Furugen, H. Yukitake, and T. Yamada.** 2000. The gene encoding mycobacterial DNA-binding protein I (MDPI) transformed rapidly growing bacteria to slowly growing bacteria. *FEMS Microbiol Lett* **182**:297-301.

46. **Minnikin, D. E.** 1982. Lipids: Complex lipids, their chemistry, biosynthesis and roles, p. 95-184. In C. Ratledge and J. Stanford (ed.), The biology of the mycobacteria: Physiology, identification and classification, vol. I. Academic Press, London.
47. **Moock, G. S., J. W. Coulton, and K. Postle.** 1997. Cell envelope signaling in *Escherichia coli*. Ligand binding to the ferrichrome-iron receptor FhuA promotes interaction with the energy-transducing protein TonB. J Biol Chem **272**:28391-7.
48. **Molle, V., N. Saint, S. Campagna, L. Kremer, E. Lea, P. Draper, and G. Molle.** 2006. pH-dependent pore-forming activity of OmpATb from *Mycobacterium tuberculosis* and characterization of the channel by peptidic dissection. Mol Microbiol **61**:826-37.
49. **Müller, D. J., and A. Engel.** 1999. Voltage and pH-induced channel closure of porin OmpF visualized by atomic force microscopy. J. Mol. Biol. **285**:1347-51.
50. **Murry, J. P., A. K. Pandey, C. M. Sasseti, and E. J. Rubin.** 2009. Phthiocerol dimycocerosate transport is required for resisting interferon-gamma-independent immunity. J Infect Dis **200**:774-82.
51. **Niederweis, M.** 2003. Mycobacterial porins - new channel proteins in unique outer membranes. Mol. Microbiol. **49**:1167-77.
52. **Niederweis, M.** 2008. Nutrient acquisition by mycobacteria. Microbiology **154**:679-692.
53. **Niederweis, M., S. Ehrt, C. Heinz, U. Klöcker, S. Karosi, K. M. Swiderek, L. W. Riley, and R. Benz.** 1999. Cloning of the *mspA* gene encoding a porin from *Mycobacterium smegmatis*. Mol. Microbiol. **33**:933-945.
54. **Nigou, J., C. Zelle-Rieser, M. Gilleron, M. Thurnher, and G. Puzo.** 2001. Mannosylated lipoarabinomannans inhibit IL-12 production by human dendritic cells: evidence for a negative signal delivered through the mannose receptor. J Immunol **166**:7477-85.
55. **Nikaido, H.** 2003. Molecular basis of bacterial outer membrane permeability revisited. Microbiol. Mol. Biol. Rev. **67**:593-656.
56. **Nikaido, H.** 2009. Multidrug resistance in bacteria. Annu Rev Biochem **78**:119-46.
57. **Nikaido, H., and E. Y. Rosenberg.** 1983. Porin channels in *Escherichia coli*: studies with liposomes reconstituted from purified proteins. J. Bacteriol. **153**:241-52.
58. **Nikaido, H., E. Y. Rosenberg, and J. Foulds.** 1983. Porin channels in *Escherichia coli*: studies with beta-lactams in intact cells. J. Bacteriol. **153**:232-40.
59. **Pedulla, M. L., M. H. Lee, D. C. Lever, and G. F. Hatfull.** 1996. A novel host factor for integration of mycobacteriophage L5. Proc Natl Acad Sci USA **93**:15411-6.
60. **Pieters, J.** 2008. *Mycobacterium tuberculosis* and the macrophage: maintaining a balance. Cell Host Microbe **3**:399-407.
61. **Portevin, D., C. De Sousa-D'Auria, C. Houssin, C. Grimaldi, M. Chami, M. Daffe, and C. Guilhot.** 2004. A polyketide synthase catalyzes the last condensation step of mycolic acid biosynthesis in mycobacteria and related organisms. Proc. Natl. Acad. Sci. USA **101**:314-9.

62. **Pratt, L. A., W. Hsing, K. E. Gibson, and T. J. Silhavy.** 1996. From acids to *osmZ*: multiple factors influence synthesis of the OmpF and OmpC porins in *Escherichia coli*. *Mol Microbiol* **20**:911-7.
63. **Purdy, G. E., M. Niederweis, and D. G. Russell.** 2009. Decreased outer membrane permeability protects mycobacteria from killing by ubiquitin-derived peptides. *Mol Microbiol* **73**:844-57.
64. **Raynaud, C., K. G. Papavinasundaram, R. A. Speight, B. Springer, P. Sander, E. C. Böttger, M. J. Colston, and P. Draper.** 2002. The functions of OmpATb, a pore-forming protein of *Mycobacterium tuberculosis*. *Mol. Microbiol.* **46**:191-201.
65. **Reed, M. B., P. Domenech, C. Manca, H. Su, A. K. Barczak, B. N. Kreiswirth, G. Kaplan, and C. E. Barry, 3rd.** 2004. A glycolipid of hypervirulent tuberculosis strains that inhibits the innate immune response. *Nature* **431**:84-7.
66. **Rook, G. A., K. Dheda, and A. Zumla.** 2005. Immune responses to tuberculosis in developing countries: implications for new vaccines. *Nat Rev Immunol* **5**:661-7.
67. **Rousseau, C., T. D. Sirakova, V. S. Dubey, Y. Bordat, P. E. Kolattukudy, B. Gicquel, and M. Jackson.** 2003. Virulence attenuation of two Mas-like polyketide synthase mutants of *Mycobacterium tuberculosis*. *Microbiology* **149**:1837-47.
68. **Rousseau, C., N. Winter, E. Pivert, Y. Bordat, O. Neyrolles, P. Ave, M. Huerre, B. Gicquel, and M. Jackson.** 2004. Production of phthiocerol dimycocerosates protects *Mycobacterium tuberculosis* from the cidal activity of reactive nitrogen intermediates produced by macrophages and modulates the early immune response to infection. *Cell Microbiol* **6**:277-87.
69. **Saviola, B., and W. R. Bishai.** 2004. Method to integrate multiple plasmids into the mycobacterial chromosome. *Nucleic Acids Res* **32**:e11.
70. **Schirmer, T., T. A. Keller, Y. F. Wang, and J. P. Rosenbusch.** 1995. Structural basis for sugar translocation through maltoporin channels at 3.1 Å resolution. *Science* **267**:512-4.
71. **Schulz, G. E.** 2000. β -Barrel membrane proteins. *Curr. Opin. Struct. Biol.* **10**:443-7.
72. **Senaratne, R. H., H. Mobasheri, K. G. Papavinasundaram, P. Jenner, E. J. Lea, and P. Draper.** 1998. Expression of a gene for a porin-like protein of the OmpA family from *Mycobacterium tuberculosis* H37Rv. *J. Bacteriol.* **180**:3541-3547.
73. **Sharbati-Tehrani, S., B. Meister, B. Appel, and A. Lewin.** 2004. The porin MspA from *Mycobacterium smegmatis* improves growth of *Mycobacterium bovis* BCG. *Int J Med Microbiol* **294**:235-45.
74. **Sharbati-Tehrani, S., J. Stephan, G. Holland, B. Appel, M. Niederweis, and A. Lewin.** 2005. Porins limit the intracellular persistence of *Mycobacterium smegmatis*. *Microbiology* **151**:2403-10.
75. **Siroy, A., C. Mailaender, D. Harder, S. Koerber, F. Wolschendorf, O. Danilchanka, Y. Wang, C. Heinz, and M. Niederweis.** 2008. Rv1698 of

- Mycobacterium tuberculosis* represents a new class of channel-forming outer membrane proteins. J. Biol. Chem. **283**:17827-37.
76. **Song, H., R. Sandie, Y. Wang, M. A. Andrade-Navarro, and M. Niederweis.** 2008. Identification of outer membrane proteins of *Mycobacterium tuberculosis*. Tuberculosis **88**:526-44.
 77. **Springer, B., P. Sander, L. Sedlacek, K. Ellrott, and E. C. Böttger.** 2001. Instability and site-specific excision of integration-proficient mycobacteriophage L5 plasmids: development of stably maintained integrative vectors. Int J Med Microbiol **290**:669-75.
 78. **Stahl, C., S. Kubetzko, I. Kaps, S. Seeber, H. Engelhardt, and M. Niederweis.** 2001. MspA provides the main hydrophilic pathway through the cell wall of *Mycobacterium smegmatis*. Mol. Microbiol. **40**:451-464 (Authors' correction appeared in *Mol. Microbiol.* **57**, 1509).
 79. **Stephan, J., J. Bender, F. Wolschendorf, C. Hoffmann, E. Roth, C. Mailänder, H. Engelhardt, and M. Niederweis.** 2005. The growth rate of *Mycobacterium smegmatis* depends on sufficient porin-mediated influx of nutrients. Mol. Microbiol. **58**:714-730.
 80. **Stephan, J., C. Mailaender, G. Etienne, M. Daffe, and M. Niederweis.** 2004. Multidrug resistance of a porin deletion mutant of *Mycobacterium smegmatis*. Antimicrob. Agents Chemother. **48**:4163-70.
 81. **Stover, C. K., V. F. de la Cruz, T. R. Fuerst, J. E. Burlein, L. A. Benson, L. T. Bennett, G. P. Bansal, J. F. Young, M. H. Lee, G. F. Hatfull, and et al.** 1991. New use of BCG for recombinant vaccines. Nature **351**:456-60.
 82. **Trias, J., V. Jarlier, and R. Benz.** 1992. Porins in the cell wall of mycobacteria. Science **258**:1479-81.
 83. **van Gelder, P., F. Dumas, and M. Winterhalter.** 2000. Understanding the function of bacterial outer membrane channels by reconstitution into black lipid membranes. Biophys Chem **85**:153-67.
 84. **Vergne, I., J. Chua, and V. Deretic.** 2003. Tuberculosis toxin blocking phagosome maturation inhibits a novel Ca²⁺/calmodulin-PI3K hVPS34 cascade. J Exp Med **198**:653-9.
 85. **Wanner, B. L., and R. McSharry.** 1982. Phosphate-controlled gene expression in Escherichia coli K12 using MudI-directed lacZ fusions. J Mol Biol **158**:347-63.
 86. **Wolschendorf, F., M. Mahfoud, and M. Niederweis.** 2007. Porins are required for uptake of phosphates by *Mycobacterium smegmatis*. J Bacteriol **189**:2435-2442.
 87. **Zuber, B., M. Chami, C. Houssin, J. Dubochet, G. Griffiths, and M. Daffe.** 2008. Direct visualization of the outer membrane of native mycobacteria and corynebacteria. J Bacteriol **190**:5672-5680.

FUNCTIONS OF THE PERIPLASMIC LOOP OF THE PORIN MSPA FROM
MYCOBACTERIUM SMEGMATIS

by

JASON HUFF, MIKHAIL PAVLENOK, SUJA SUKUMARAN, AND MICHAEL
NIEDERWEIS

Journal of Biological Chemistry [jbc.M808599200]

Copyright

2009

by

American Society for Microbiology

Used by permission

Format adapted for dissertation

ABSTRACT

MspA is the major porin of *Mycobacterium smegmatis* and mediates diffusion of small and hydrophilic solutes across the outer membrane. The octameric structure of MspA, its sharply defined constriction zone, and a large periplasmic loop L6 represent novel structural features. L6 consists of 13 amino acids and is directly adjacent to the constriction zone. Deletion of 3, 5, 7, 9, and 11 amino acids of the L6 loop resulted in functional pores that restored glucose uptake and growth of a porin mutant of *M. smegmatis*. Lipid bilayer experiments revealed that all mutant channels were noisier than wt MspA indicating that L6 is required for pore stability *in vitro*. Voltage-gating of the *E. coli* porin OmpF was attributed to loops that collapse into the channel in response to a strong electrical field. Here, we show that deletion mutants $\Delta 7$, $\Delta 9$ and $\Delta 11$ had critical voltages similar to wt MspA. This demonstrated that the L6 loop is not the primary voltage-dependent gating mechanism of MspA. Surprisingly, large deletions in L6 resulted in three- to six-fold less extractable pores, whereas small deletions did not alter expression levels of MspA. Pores with large deletions in L6 were more permissive for glucose than smaller deletion mutants, while their single channel conductance was similar to that of wt MspA. These results indicate that translocation of ions through the MspA pore is governed by different mechanisms than that of neutral solutes. This is the first study identifying a molecular determinant of solute translocation in a mycobacterial porin.

INTRODUCTION

Mycobacteria have a unique outer membrane composed of covalently attached mycolic acids and a variety of other loosely associated lipids. Visualized by cryo-electron tomography (13), the outer membrane of mycobacteria is an efficient permeability barrier that renders them intrinsically resistant to many drugs and toxic compounds. As is the case for gram-negative bacteria, this permeability barrier must be functionalized by outer membrane proteins. While over 60 outer membrane proteins are known to exist in *E. coli* {Molloy, 2000 #5876, very few have been described in mycobacteria to date.

The major protein of *Mycobacterium smegmatis* is MspA {Ojha, 2007 #18555}, which is the primary member of the nearly identical Msp (*Mycobacterium smegmatis* porin) proteins. Msp proteins account for approximately 80% of detergent-extractable proteins at 100°C (11) in wt *M. smegmatis* mc²155. MspA represents the main pathway for small and hydrophilic solutes and nutrients across the outer membrane (34). One hallmark of MspA is its extremely high stability. Functional pores are detectable at temperatures up to 100°C, a pH range from 0-14, and resist the action of denaturing agents such as 2% SDS (10), thus providing the utility of MspA for nanotechnological applications. However, it is unknown how *M. smegmatis* utilizes Msp porins to functionalize the outer membrane in varying conditions or what parts of the channel determine substrate translocation. It is our goal to understand the translocation determinants of the MspA channel.

The crystal structure revealed that eight monomers comprise one functional MspA pore (9). Like all other known outer membrane proteins (18), MspA contains a β -barrel that spans the outer membrane. A novel feature of MspA is the constriction zone where

the region of the channel with the smallest diameter is lined by at least 16 aspartic acid residues, likely explaining the cation preference of MspA (26). Most porins of gram-negative bacteria display large, extracellular loops and much smaller periplasmic loops (3, 7, 31, 39). In contrast, the single 13 amino acid periplasmic loop of MspA, herein referred to as L6, is larger than the extracellular loops (Fig. 1). Additionally, the L6 loop is positioned adjacent to the 1 nm wide constriction zone whereas the smaller extracellular loops surround a vestibule opening of 4.8 nm in diameter (9). The L6 loop was also found to be exposed to the periplasmic space via biotinylation of cysteine mutants (22).

It is unknown what the role of this unusual periplasmic loop is. It was shown that MspA exhibited voltage gating (8), suggesting that, in response to a strong electric field, the channel undergoes a conformational change that restricts ionic conductance through the pore. While the rest of MspA is primarily comprised of a rigid β -barrel, the periplasmic loop L6 appeared to be a likely candidate for mediating such channel gating.

Many outer membrane proteins have also been shown to utilize soluble periplasmic domains for functional purposes. For example, OmpA of *E. coli* contains a C-terminal domain that binds peptidoglycan (17) while TolC links to inner membrane efflux pumps via its large periplasmic domain (21). It may be that the loop L6 due to its larger size also serves as a binding site for proteins or other effector molecules that aid in transport processes across the cell envelope of *M. smegmatis*.

To examine the role of the periplasmic loop of MspA, we constructed five mutants with symmetric deletions of 3, 5, 7, 9, or 11 amino acids in L6. The function of these mutants was analyzed both *in vitro* and *in vivo*.

MATERIALS AND METHODS

Chemicals and enzymes. Chemicals were of the highest purity available from Merck (Germany), Roth (Germany), Invitrogen (USA), or Sigma (USA) unless otherwise noted. The detergent *n*-octylpolyoxyethylene (*n*-octyl-POE) was from Alexis (USA). Oligonucleotides were obtained from Integrated DNA Technologies (USA).

Bacterial strains and growth conditions. *M. smegmatis* ML16, which lacks the porin genes *mspA*, *mspC*, and *mspD* (36) was grown at 37°C in 7H9 liquid medium (BD Biosciences) supplemented with 0.2% glycerol and 0.05% Tween 80 or on 7H10 agar (BD Biosciences) supplemented with 0.2% glycerol, unless otherwise indicated.

Escherichia coli DH5 α was used for cloning experiments and was routinely grown in Luria-Bertani broth (LB) at 37°C. Hygromycin was used in concentrations of 50 μ g/ml and 200 μ g/ml for *M. smegmatis* and *E. coli*, respectively.

Construction of MspA loop 6 deletion mutants. The L6 deletion mutants were constructed using the plasmid pMN016, which carries the *p_{smyc}-mspA* transcriptional fusion (36) as a template. Psmyc1 and pMS-seq1 were used as end primers along with appropriate mutagenesis primers to perform a two-step PCR. Separate PCR amplifications of the upstream and downstream portions of the gene flanking the deletion were performed. Then, the two purified PCR products were amplified and ligated together in the same reaction using ampliligase (Epicentre). Mutated *mspA* genes were then ligated into SphI and HindIII double digested pMN016 to generate the plasmids pML905-pML909. Primers and resulting plasmids are listed in Table 1. All plasmids were verified by sequencing the entire *mspA* gene before they were transformed into the porin mutant *M. smegmatis* ML16 for protein production.

Expression, extraction, and purification of MspA mutants. The wild-type (wt) *mspA* gene (pMN016) and the mutated *mspA* genes (pML905-pML909) were constitutively expressed in *M. smegmatis* ML16. This strain contains at least 15-fold less Msp porins in the outer membrane (36). To examine whether the five L6 deletion mutants were expressed in ML16, a selective extraction procedure was employed that yields predominantly MspA when whole cells of *M. smegmatis* are heated in POPO5 buffer (300 mM NaH₂PO₄/Na₂HPO₄, 0.3 mM Na₂EDTA, 150 mM NaCl, 0.5% (w/v) *n*-octyl-POE) at a cell density of 100 µl/10 mg cells (wet weight) to 100°C for 30 min (11). Protein extracts were separated on a denaturing 10% polyacrylamide gel and stained with Coomassie Blue. Quantitative image analysis of protein gel bands by pixel densitometry was performed using Labworks 4.6 (UVP, Inc.) software. Wt and mutant MspA proteins were purified as previously described (11). Briefly, protein extracts were precipitated in acetone and resuspended in AOPO5 buffer (25 mM HEPES/NaOH, 10 mM NaCl, 0.5% *n*-octyl-POE, pH 7.5). Proteins were then loaded onto a 1.7 mL POROS 20HZ anion-exchange column (Perceptive Biosystems) and eluted off in a salt concentration gradient ranging from 0.76 M to 1.02 M NaCl. Buffers were then exchanged by gel filtration in AOPO5.

Lipid bilayer and voltage gating experiments. The channel activity of the proteins was measured in lipid bilayer experiments as described (11). In all single channel conductance experiments, 1 M KCl was used as the electrolyte. The single channel conductances of at least 100 pores reconstituted from a freshly diluted solution of purified proteins were analyzed in several diphytanoyl phosphatidylcholine (Avanti Polar Lipids) membranes with a constant applied voltage of -10 mV. Where applicable, the *cis*

side of the cuvette was defined as the side with the positive electrode. In voltage gating experiments, the applied voltage increased from 0 mV to -60 mV or +60 mV in 10 mV increments. Using Ag/AgCl electrodes, the membrane current under the voltage clamp was measured with a current amplifier (Keithley 428 current amplifier) and digitized by a desktop computer equipped with Keithley Metrabyte STA 1800U interface. Data were recorded using a macro and the software Test Point 4.0 (Keithley). Analysis of the current traces was carried out using a macro based on the Igor Pro 5.03 software (written by Dr. Harald Engelhardt). For all measurements where the conductance fluctuations (noise) due to individual pore insertion were negligible, the entire current trace with 50-100 pores was analyzed. However, for analysis of the pores where insertion of an individual pore created fluctuations (noise) in the recording, only the initial 10-20 pores were used. The steps recorded in four to six membranes were pooled to generate the final distribution plots (SigmaPlot 9.0). The noise suppression factor was constant for all measurements.

Growth assays in minimal media. Growth on solid media was performed by inoculating primary cultures in HdB liquid medium with 0.05% Tween 80 and supplemented with 1% glucose. Cultures were filtered through a 5 μ m filter and grown overnight in beveled flasks on a shaker at 37°C. Cultures were then filtered again through a 5 μ m filter, serially diluted in HdB with 0.05% Tween 80 and no glucose, and plated onto HdB solid media supplemented with 1% glucose. Pictures at 12.5 x magnification were taken after five days of incubation in a sealed container at 37°C.

Growth in liquid medium was performed by inoculating 5 mL primary cultures in HdB with 0.025% Tyloxapol and 0.2% glucose. Cultures were filtrated with a 5 μ m filter

and grown overnight. Cultures were then diluted in triplicate in 30 mL of HdB with 0.025% Tyloxapol and 0.2% glucose in beveled flasks and incubated on a shaker at 37°C. At indicated time points, samples of each culture were taken and the optical density at 600 nm was recorded using a photometer and cuvettes with a 1 cm path length.

Enzyme-linked immunosorbent assay (ELISA). To confirm expression and localization of MspA mutants, a sandwich-type enzyme-linked immunosorbent assay (ELISA) using whole cells of *M. smegmatis* ML16 was adapted from a previously described whole cell ELISA protocol (34). Cells were grown to an OD₆₀₀ of about 0.8, harvested by centrifugation, washed with TBST (0.01 M Tris-HCl pH 8, 0.15 M NaCl, 0.05% Tween 20), and resuspended in coating buffer (50 mM NaHCO₃ pH 9.6) to an OD₆₀₀ of about 10. Wells of a maxisorp plate (NUNC-Immuno™ MaxiSorp™ Surface, Nalge Nunc International) were coated with 100 µL of a 1:2,000 dilution of MspA pAb 813 (26) for 1 hr at 37°C to trap cells. After blocking with 5% powdered skim milk in TBST for 1 hour, approximately 10⁸ cells were loaded into each well and incubated at 37°C for 1 hour. Unbound cells were removed by washing three times with TBST, and bound cells were incubated with 100 µL of a 1:20 dilution of MspA mAb P2 (will be published elsewhere) for 1 hr at 37°C. Cells were washed three times and then incubated with a 1:2,000 dilution of horseradish peroxidase conjugated goat anti-mouse antibody (Sigma) for 1 hr at 37°C. After washing three times, 50 µL of O-phenylenediamine substrate (Sigma) were added to each well and the plate was incubated at room temperature in the dark until a yellow color developed (~20 min). The reaction was then stopped with 50 µL of 1M H₂SO₄. The plate was centrifuged (3,000 rpm, 5 min), the

supernatant was removed to a new microtiter plate, and the absorbance was read at 490 nm using a microplate reader (Synergy HT, Bio-TEK Instrument Inc, USA).

Glucose uptake measurements. Glucose uptake measurements were carried out as previously described (34, 35). To reduce aggregation and clumping, all *M. smegmatis* cells were filtered through a 5 μm pore-size filter (Sartorius) and grown to an OD_{600} of about 0.8 in the presence of 1 mM glucose. Cells were harvested ($3000 \times g$ at 4°C for 10 min), washed once in uptake buffer (2 mM PIPES (pH 6.5), 0.05 mM MgCl_2), and resuspended in the same buffer to an OD_{600} of about 0.4. Radio-labeled [^{14}C] glucose and unlabeled glucose were mixed and added to the cell suspension to a final concentration of 20 μM . Cells were then incubated at 37°C for 5 min. At the indicated time points, 1 ml samples were removed to 3 mL kill buffer (0.1 M LiCl, 6.7% formalin). Cells were captured on a 0.45 μm pore-size filter (Sartorius) and counted in a liquid scintillation counter. All experiments were performed in triplicate. The mean dry weight of the cells in these samples was 0.6 ± 0.2 mg. The glucose uptake rate was expressed as nmol/mg cells/min and was determined by fitting a straight line to the first 4 data points (from 1 to 4 min). Uptake rates at the individual concentrations, K_m and v_{max} values for the overall transport and a minimal estimate of the permeability coefficient were determined as described previously (15, 34).

RESULTS

Construction of *mspA* L6 deletion mutants. The crystal structure of MspA (9) revealed a single loop (L6) at the periplasmic end of the monomer (Fig. 1). To determine whether L6 contributes to the translocation of small and hydrophilic compounds through the MspA channel, symmetric deletions centered around Pro97 were constructed in this loop.

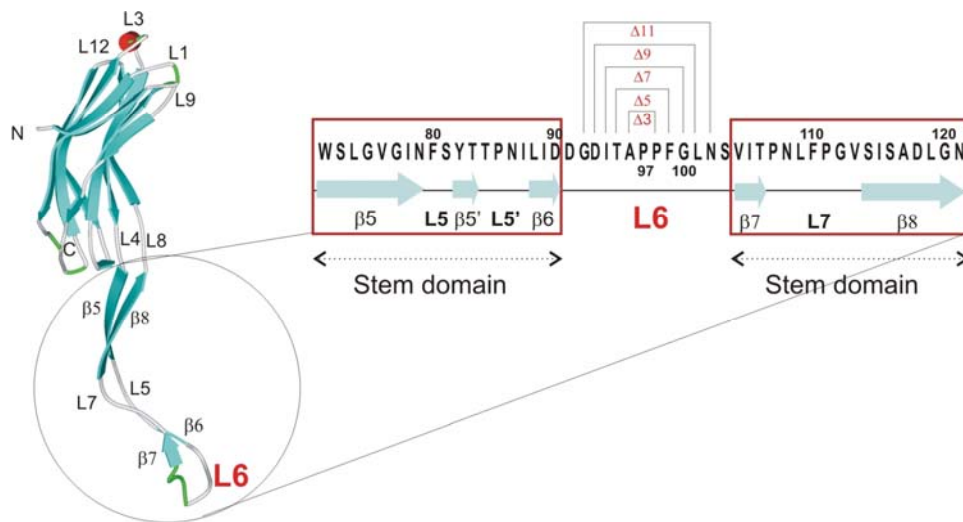


Figure 1. Schematic representation of the deletions in the periplasmic loop 6 of MspA. The assignment of the secondary structural elements was taken from the crystal structure of MspA (9). The arrows represent the β -sheets, lines represent the loops, and the red cylinder represents the L3 helix. The periplasmic loop is marked as L6, and the primary sequence of the loop 6 and stem domain is shown to the right. Deletion of amino acids 96–98, 95–99, 94–100, 93–101, and 92–102 generated the *mspA* mutants $\Delta 3$, $\Delta 5$, $\Delta 7$, $\Delta 9$, and $\Delta 11$, respectively.

The resulting *mspA* mutant genes were cloned into pMN016, which contains a *p_{smyc}-mspA* transcriptional fusion (36). Using appropriate mutagenesis primers (Table 1), $\Delta A96$ -P98,

Δ T95-F99, Δ I94-G100, Δ D93-L101, and Δ G92-N102 were constructed (Fig. 1).

Henceforth, these mutants are referred to as Δ 3, Δ 5, Δ 7, Δ 9, and Δ 11, respectively.

Mutant	Plasmid	Primer pair for fragment A (5'-3')	Primer pair for fragment B (5'-3')
Δ 3	pML905	TTCGGCCTGAACTCGGTCATCACC CGACCAGCACGGCATAACATC (psmyc1)	GGTGATGTCACCGTCGTCGATCAGG CGTTCTCGGCTCGATGATCC (pMS-seq1)
Δ 5	pML906	GGCCTGAACTCGGTCATCACCCCG CGACCAGCACGGCATAACATC	GATGTCACCGTCGTCGATCAGGATG CGTTCTCGGCTCGATGATCC
Δ 7	pML907	CTGAACTCGGTCATCACCCCGAAC CGACCAGCACGGCATAACATC	GTCACCGTCGTCGATCAGGATGTTT CGTTCTCGGCTCGATGATCC
Δ 9	pML908	AACTCGGTCATCACCCCGAACCTG CGACCAGCACGGCATAACATC	ACCGTCGTCGATCAGGATGTTCCGG CGTTCTCGGCTCGATGATCC
Δ 11	pML909	TCGGTCATCACCCCGAACCTGTTC CGACCAGCACGGCATAACATC	GTCGTCGATCAGGATGTTCCGG CGTTCTCGGCTCGATGATCC

Table 1. Oligonucleotides used in this work.

Expression of L6 deletion mutants in *M. smegmatis*. For expression of the *mspA* genes encoding the loop deletion mutants the porin triple mutant *M. smegmatis* ML16 was used, which lacks the *mspA*, *mspC*, and *mspD* genes. The amount of porins in the outer membrane is reduced by approximately 15-fold in this strain (36). To examine whether the loop deletion mutants were expressed in ML16, a selective extraction procedure was utilized that yields predominantly MspA when whole cells of *M. smegmatis* are heated with 0.5% octyl-POE to 100°C (11). Whole cell extracts of these mutants were separated on a denaturing 10% polyacrylamide gel and stained with Coomassie Blue. Almost no Msp porins were detected in extracts of *M. smegmatis* ML16 carrying the empty vector pMS2 (16) (Fig 2, lane “no MspA”), indicating a very low background expression of *mspB*. Expression of wt *mspA* in ML16 using the vector pMN016 (lane wt) yields MspA levels similar to that in wt *M. smegmatis* mc²155 (22, 36). Mutants with the smallest deletions in the periplasmic loop (Δ 3, Δ 5 and Δ 7) had

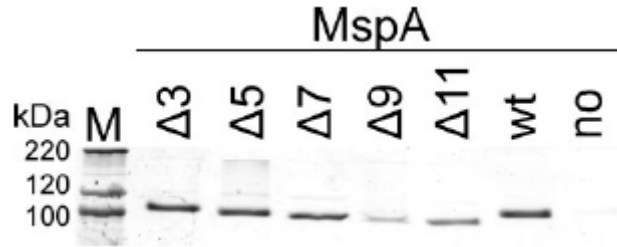


Figure 2. Expression of MspA deletion mutants in the porin mutant *M. smegmatis* ML16. Comparison of detergent extracts by SDS-polyacrylamide gel electrophoresis is shown. MspA proteins were selectively extracted from the porin mutant *M. smegmatis* ML16 ($\Delta mspA$, $\Delta mspC$, and $\Delta mspD$) (36) at 100 °C in a buffer containing 0.5% *n*-octyl-POE, separated on a 10% polyacrylamide gel, and stained with Coomassie Blue. Lane M contains the protein mass marker (Mark12; Invitrogen). The expression vector pMN016 (wt *mspA*, wt lane), the empty vector pMS2 (no MspA lane), and the mutated *mspA* genes (pMN016 derivatives, lanes $\Delta 3$ - $\Delta 11$) were constitutively expressed in ML16. The part of the gel containing the bands of octameric MspA is shown. The intensity of the monomeric band was identical for all MspA proteins. The amount of the loop deletion mutants was quantified by image analysis and normalized to wt MspA. For mutants $\Delta 3$, $\Delta 5$, $\Delta 7$, $\Delta 9$, and $\Delta 11$, expression was 104, 94, 91, 17, and 40% of wt, respectively. The background signal (no MspA) was 0.2% of that of wt MspA.

expression levels similar to that of wt *mspA* (Fig. 2). However, expression of mutants harboring larger deletions was significantly reduced in comparison to wt *mspA* (Fig. 2). Quantitative image analysis of the bands representing the MspA octamer showed that $\Delta 3$, $\Delta 5$ and $\Delta 7$ had expression levels that were 104, 94 and 91% of wt levels, while $\Delta 9$, $\Delta 11$ and the empty vector had expression levels that were 17, 40 and 0.2% of wt (Fig. 2). It should be noted that the intensity of the monomeric band was similar for all mutants and the wt. The same quantitative expression patterns were obtained in several other Coomassie Blue-stained protein gels. Further, expression of all loop deletion mutants was confirmed via Western blot using the Msp-specific antiserum pAK813 (not shown). These results demonstrated that all mutants were expressed in *M. smegmatis* ML16 and

were stable during heat extraction. The much lower expression of $\Delta 9$ and $\Delta 11$ indicated the importance of the periplasmic loop for MspA expression in the outer membrane.

Analysis of channel activity in artificial lipid bilayers. Lipid bilayer experiments provide direct evidence whether a particular protein forms channels within a lipid membrane (26). To determine whether the mutated MspA proteins formed functional pores, the genes were overexpressed in *M. smegmatis* ML16 and proteins were purified by a two-step chromatographic protocol as previously described (11). No pores were recorded in control experiments when only detergent-containing buffer was added to the lipid bilayer (not shown). As can be seen in Figure 3, all mutants formed open

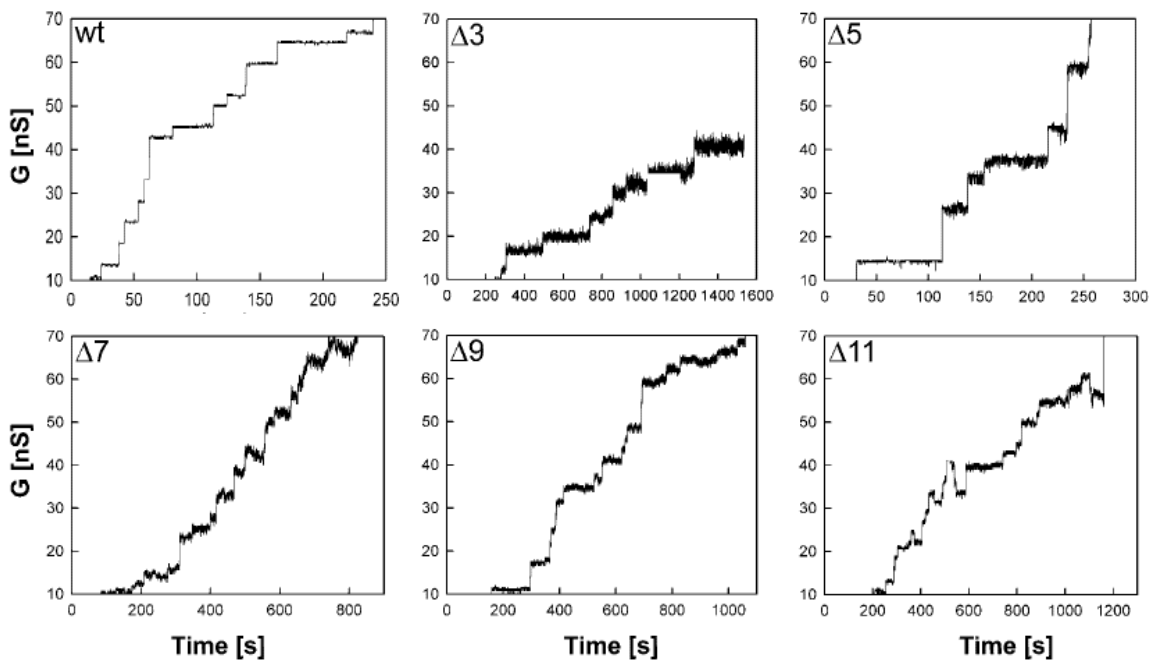


Figure 3. Single channel recordings of purified MspA loop deletion mutants in lipid bilayers. Single-channel recordings of a diphytanoyl phosphatidylcholine membrane in the presence of 0.02, 500, or 0.1 ng/ml of wt, $\Delta 3$, and $\Delta 5$ - $\Delta 11$ purified MspA protein, respectively. Protein solutions were added to both sides of the membrane, and data were collected from at least five different membranes. The membrane current was measured in an aqueous solution of 1 M KCl with an applied transmembrane potential of -10 mV.

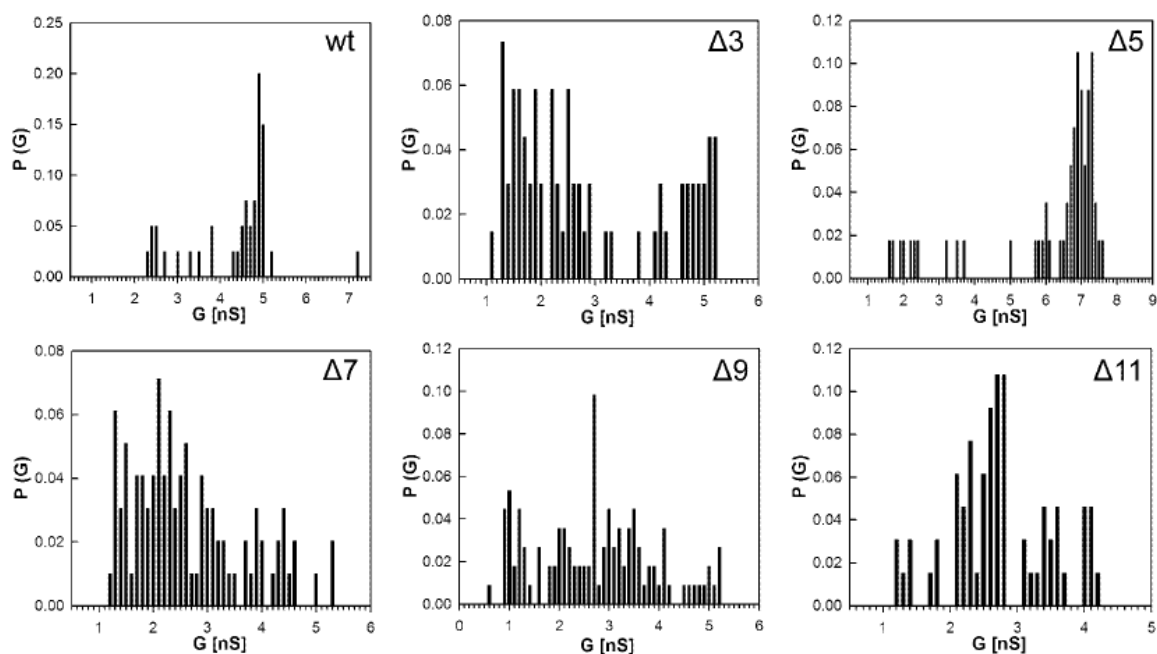


Figure 4. Analysis of single channel conductances of purified MspA deletion mutants. Analysis of the probability P of a conductance step G for single channel events. The average single channel conductances were 4.9, 1.3, and 5.1 (bimodal), 7.0, 2.1, 2.6, and 2.8 nS for wt, $\Delta 3$, $\Delta 5$, $\Delta 7$, $\Delta 9$, and $\Delta 11$, respectively.

channels in artificial lipid bilayers. All loop deletion mutants produced noisier channels. In contrast to wt and the other deletion mutants, loss of conductance events were much more frequent in $\Delta 11$. Individual conductance steps were plotted to determine the probability of conductance for single channels. Significant changes in the single channel conductance were observed for all mutants. A reduced ability to conduct ions was apparent for $\Delta 7$, $\Delta 9$, and $\Delta 11$, which were determined to be 2.1, 2.6, and 2.8 nS in 1 M KCl, respectively (Fig. 4). In contrast, the ion conductance of $\Delta 5$ was much higher with a peak at 7.0 nS. The $\Delta 3$ mutant displayed a bimodal distribution of ionic conductances

with one species conducting ions near wt levels and the other reduced to levels similar to $\Delta 7$, $\Delta 9$ and $\Delta 11$. These experiments showed that L6 has a considerable effect on the single channel conductance of purified MspA and the stability of the pores in artificial bilayers.

Voltage-dependent channel closure. It was shown that MspA inserts unidirectionally into lipid membranes and that the MspA channel closes at voltages exceeding -20 mV and +40 mV (8). To investigate the role of the periplasmic loop in voltage gating of MspA, approximately 100 pores of purified MspA were reconstituted into artificial lipid bilayers after addition of protein in the *cis* side of the cuvette. Ionic conductance through the channels was measured at increasing voltage magnitudes and alternating polarities. In this experiment, wt MspA channels closed starting at voltages of +30 mV and -20 mV (Fig. 5). These values are consistent with those previously published (8). Upon deletion of the periplasmic loop, different voltage gating responses were observed. $\Delta 3$ formed stable pores and did not gate at positive voltages up to +50 mV and was less sensitive to negative voltages, gating at -40 mV. Voltages above +50 mV could not be used as no membrane was obtained under in those conditions. $\Delta 5$ was also less sensitive to positive voltages, undergoing closure events only after +40 mV were applied. However, negative voltage resulted in gating similar to wt.

Conversely, both $\Delta 7$ and $\Delta 9$ were slightly more sensitive and gated at lower voltages. $\Delta 7$ began to close at 20 mV in both polarities. $\Delta 9$ was also affected by voltages of both polarities, undergoing gating events with voltages of +20 mV and -10 mV.

Most importantly, the gating properties of $\Delta 11$ were similar to that of wt MspA with evidence of gating events at +30 mV and -20 mV. This mutant has lost almost the

entire L6 loop. These data show that L6 affects the voltage-dependent gating properties of MspA but is not the primary gating mechanism.

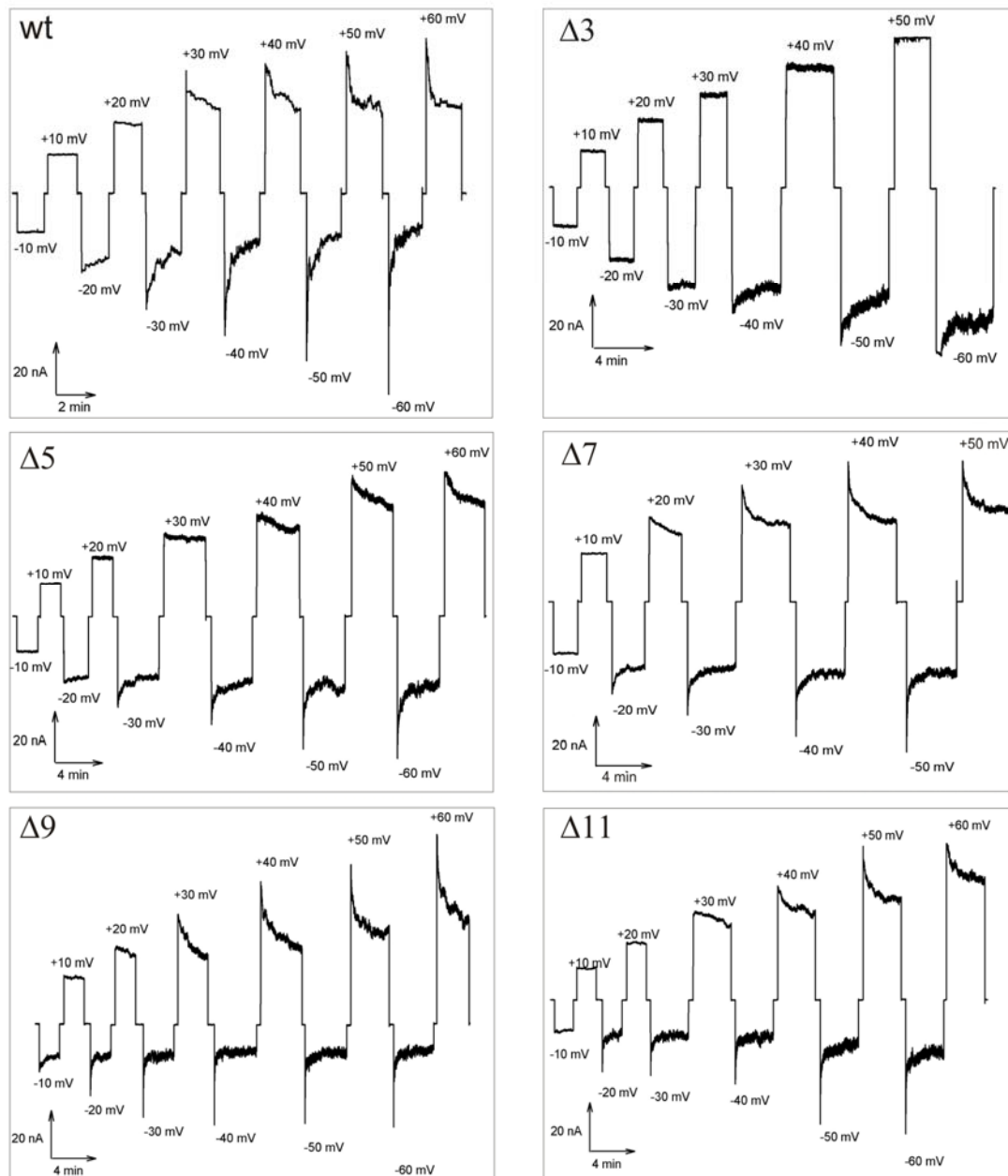


Figure 5. Voltage gating properties of purified MspA L6 deletion mutants. Purified MspA was added to the *cis*-side of a diphytanoyl phosphatidylcholine membrane.

Increasingly positive (upper traces) and negative (lower traces) voltages were applied to the membrane when ~100 channels were reconstituted into the membrane. The membrane current was recorded at each applied voltage. The critical voltage at which the channels began to close (V_c) was determined to be the voltage where conductance decreased after an initial spike. The wt was measured to have a V_c of +30 and -20 mV. For the L6 mutants $\Delta 5$, $\Delta 7$, $\Delta 9$, and $\Delta 11$, V_c was approximately +40/-30, +20/-20, +20/-20, and +30/-20 mV, respectively. The $\Delta 3$ mutant did not gate at positive voltages before membrane breakage, whereas gating occurred at -40 mV.

Activity of the loop deletion mutants *in vivo*. The periplasmic L6 loop of MspA has been shown to affect the conductance properties and stability of the pore in artificial membranes. To determine if the loop alterations influenced the channel function *in vivo*, the growth defect of the triple porin mutant *M. smegmatis* ML16 was exploited in growth complementation assays. Strains of ML16 complemented with MspA loop deletion mutants were grown to mid log phase, filtered to obtain single cell suspensions, and plated onto minimal HdB media supplemented with 1.0% glucose as the sole carbon source. Representative colony pictures showed that wt *mspA* gave rise to full size colonies in contrast to the empty vector (Fig. 6A). Colonies formed by *M. smegmatis* ML16 containing L6 deletion mutants had a similar size as those containing wt MspA indicating functional expression of the L6 mutants. To quantify the growth rates, the same strains were grown in HdB liquid medium containing 0.025% Tyloxapol and supplemented with 0.2% glucose as the sole carbon source. All mutants complemented the growth defect of ML16 with similar growth kinetics as wt MspA (Fig. 6B). These results are consistent with the growth experiments on agar plates and show that the L6 loop is dispensable for porin function *in vivo*. Thus, all L6 deletion mutants appear to be fully functional *in vivo* despite their different *in vitro* properties.

Surface accessibility of loop deletion mutants. As shown in Fig. 2, large deletions in L6 resulted in a reduced number of extractable pores in *M. smegmatis* ML16. To determine if L6 deletion mutants were efficiently inserted into the outer membrane of *M. smegmatis* and that loop alterations did not result in pores more resistant to extraction, the surface-accessibility of each mutant was examined by whole cell capture ELISA. Cells expressing MspA were bound to wells of a microtiter plate by a polyclonal MspA antibody. Surface-exposed MspA was detected with a monoclonal MspA antibody. As ML16 complemented with the empty vector expresses no MspA in the outer membrane, no capture above background was detected. Conversely, wt MspA was clearly detectable (Fig. 6C). Mutant pores with smaller deletions in L6 ($\Delta 3$ - $\Delta 7$) were better detected on the cell surface of *M. smegmatis* than wt MspA. In contrast, larger deletions of the periplasmic loop resulted in decreased surface detection. These results reflect the expression pattern in Fig. 2 indicating that the L6 deletion mutants are localized in the outer membrane and are extractable.

Uptake of glucose. To determine whether the periplasmic loop of MspA is important for the translocation of small molecules *in vivo*, we examined the accumulation of glucose by whole cells as a reference solute for porin activity (23, 34, 36). *M. smegmatis* ML16 strains expressing MspA L6 deletion mutants were incubated with a 20 μ M mixture of unlabelled and 14 C-labelled glucose. Accumulation of glucose was measured over time and normalized to the dry weight of the cells. As previously shown, the porin mutant ML16 was almost completely deficient for glucose uptake (36). Expression of wt *mspA* in ML16 increased glucose uptake rates by 50-fold (Fig. 6D). L6 deletion mutants partially complemented the porin defect of ML16 with uptake rates

ranging from 50-80% of that mediated by wt MspA. These results are consistent with the growth experiments and showed that all L6 mutants were functionally expressed in the outer membrane and enabled diffusion of glucose *in vivo*.

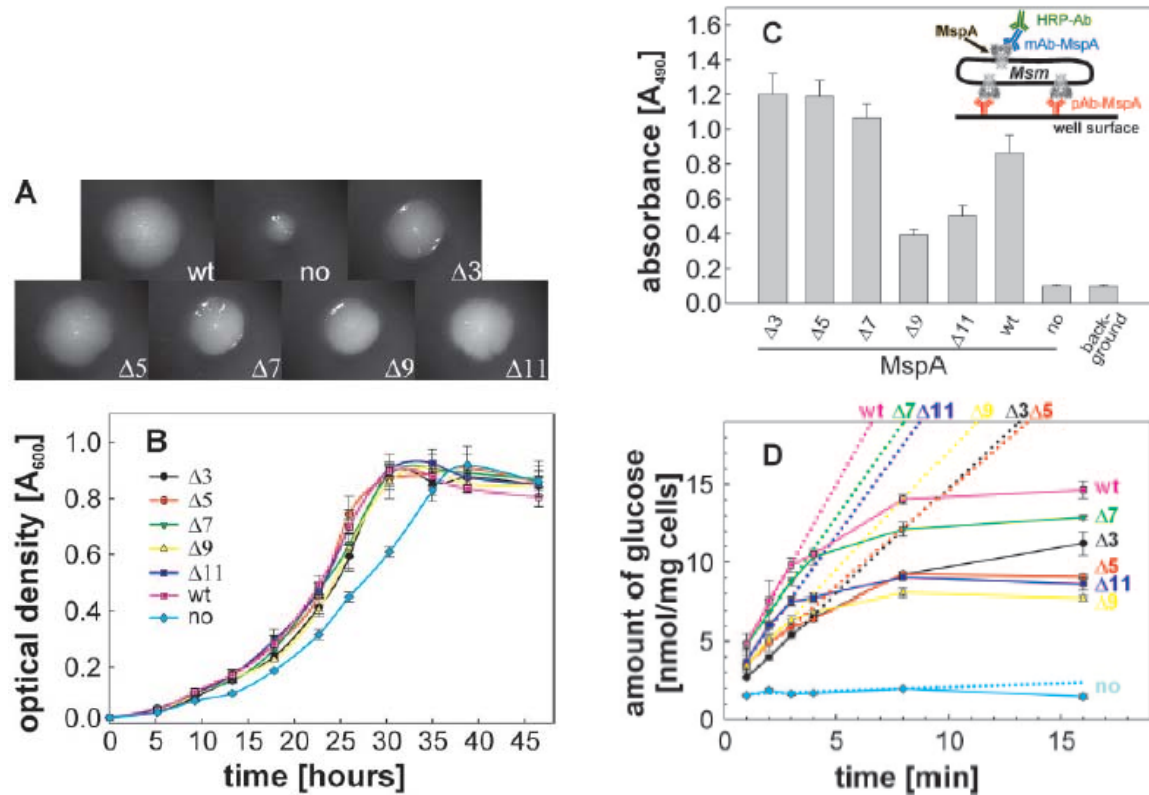


Figure 6. Surface accessibility and *in vivo* function of MspA L6 deletion mutants. A) growth on agar plates and colony morphology. *M. smegmatis* ML16 complemented with MspA L6 deletion mutants were grown on HdB minimal medium supplemented with 1% glucose. After 5 days of incubation at 37 °C, pictures of representative colonies were taken at 12.5 X magnification. B) growth in liquid medium. Triplicate cultures in beveled flasks were inoculated to an A_{600} of 0.02 in HdB liquid medium, 0.025% tyloxapol, and supplemented with 0.2% glucose. The optical density at 600 nm was recorded at the indicated time points during growth at 37 °C. C) surface accessibility of MspA mutants by whole cell capture ELISA. The experimental set-up is drawn as an insert. Wells of a Maxisorp 96-well microtiter plate were coated with an MspA antiserum to which ML16 cells expressing MspA were then “captured.” The anti-MspA mAb P2 was used for detection of surface-exposed MspA in combination with a secondary antibody conjugated with horseradish peroxidase. D) uptake of glucose. ML16 complemented with MspA mutants were grown to an A_{600} of ~0.8 and incubated with a 20- μ M mixture of

nonlabeled and [^{14}C] glucose. At the indicated time points, 1 ml of the cell suspensions were removed, filtered, and counted on a scintillation counter. The dotted lines represent the best fit for the first four time points (1–4 min). Uptake rates for wt, no MspA, $\Delta 3$, $\Delta 5$, $\Delta 7$, $\Delta 9$, and $\Delta 11$ were determined to be 2.5, 0.05, 1.3, 1.2, 2.0, 1.5, and 2.0 nmol/mg cells/min, respectively.

DISCUSSION

This study marks the first analysis of a molecular determinant of channel activity for a mycobacterial porin. The large periplasmic loop L6 is directly adjacent to the constriction zone of MspA (Fig. 1) and might influence the channel conductance of the pore and its gating properties by dynamic motions. Indeed, deletions in L6 resulted in altered single channel conductances of the purified proteins reconstituted in artificial bilayers. All mutants with the exception of $\Delta 5$ had a reduced single channel conductance in 1 M KCl compared to wt MspA (Fig. 4). It appears to be counter-intuitive that deletion of a possibly occluding loop resulted in decreased conductance. One explanation might be that residues lining the entire barrel lumen from the vestibule to the periplasmic tip of MspA are required for an optimal, ordered flow of ions through the channel as previously shown for OmpF in a molecular dynamics study (14). An alternative explanation is that the L6 loop is required for stabilizing the constriction zone. The observation that all channels of the loop deletion mutants are much more noisy than wt MspA is consistent with both mechanisms and supports the conclusion that the L6 loop is required for a stable MspA pore. In light of this interpretation, the larger channel conductance of the $\Delta 5$ mutant (T95-F99) might result from a different stabilization of the constriction zone by sequence-specific effects which are not present in the other loop deletion mutants. A simple alternative explanation is the increased propensity of $\Delta 5$ to aggregate as indicated by a high molecular weight band above that of the octamer (Fig. 2). Thus, more than one functional pore of the $\Delta 5$ mutant might simultaneously insert into the artificial lipid bilayer and cause a higher conductance value. It should be noted that bi- or multimodal

distributions of apparent single channel conductances have also been observed for other porins such as PhoE of *E. coli* (38).

Voltage-gating is a fundamental feature of β -barrel membrane channels (1). This phenomenon was observed for porins in gram-negative bacteria and has received a lot of attention because the elucidation of its molecular mechanism helps to understand the translocation of ions through these pores (29). The deletion mutants $\Delta 7$, $\Delta 9$ and $\Delta 11$, in which the L6 loop was mostly or completely removed, had critical voltages (V_c) very similar to wt MspA (Fig. 5). This clearly demonstrated that the L6 loop is not the primary voltage-dependent gating mechanism of MspA. This observation rules out the motion of loops that fold back to gate the pore as discussed for OmpF of *E. coli* as a mechanism underlying voltage gating (24). In the aforementioned study, large extracellular loops were found to collapse in response to high voltage and block the OmpF pore (24). However, deletion of any single of the seven extracellular loops of OmpF only affected the pH sensitivity of the pores but did not significantly alter voltage gating (2). These experiments did not rule out redundancy of extracellular loops for channel closure. A similar argument does not apply to MspA because MspA has only one periplasmic loop per monomer. A voltage-induced conformational change of the smaller extracellular loops (3 to 6 amino acids) as an alternative mechanism cannot block the wide vestibule opening with a diameter of 4.8 nm (9). Several reports suggested that individual residues close to the constriction zone of the OmpF pore are involved in voltage gating (5, 27, 37). This may hold true also for MspA since minor changes in voltage-dependent gating were observed for the loop deletion mutants which have either altered spacing or numbers of charged residues (Fig. 1). These alterations may also explain why the $\Delta 3$ mutant closed at

significantly higher positive voltages than wt MspA (Fig. 5). The discovery of voltage gating in MspA as another β -barrel protein with no structural similarities to either porins of gram-negative bacteria nor β -barrel toxins such as α -haemolysin of *Staphylococcus aureus* (19, 33) supports the hypothesis that voltage gating might indeed be an intrinsic property of β -barrel proteins as first described by Lakey and co-workers (1). Hence, our finding favors a mechanism in which an externally applied voltage perturbs the electric field in β -barrel pores that is required for ion translocation (1). It should be noted that it is unclear both for porins of gram-negative bacteria (32) and for mycobacteria (8) whether voltage-dependent gating is physiologically relevant.

Expression of MspA in *M. smegmatis* was also affected by mutations in L6 (Fig. 2). However, all mutants were still extracted from the outer membrane, albeit at differing levels, indicating that the localization of the protein was not altered. This conclusion is confirmed by the observation that all loop deletion mutants were functionally active and complemented an Msp porin triple mutant of *M. smegmatis* similar to wt MspA (Fig. 6). While small deletions in L6 did not alter expression levels and surface accessibility of MspA, large deletions in L6 ($\Delta 9$ and $\Delta 11$) resulted in three- to six-fold less extracted pores. A reduced number of pores in the outer membrane for $\Delta 9$ and $\Delta 11$ was confirmed by whole cell ELISA (Fig. 6C) excluding the possibility that these mutants were less extractable by our standard method. It is unlikely that reduced transcription of the genes accounts for this observation as all mutants were expressed from the same genetic constructs. Hence, these experiments demonstrated that deletion of the L6 loop reduced the levels of MspA in the outer membrane of *M. smegmatis*. In gram-negative bacteria, insertion of proteins into the outer membrane is accomplished by a machinery composed

of an assembly factor such as Omp85 of *N. meningitidis* and YaeT of *E. coli* and other proteins (4, 30). This assembly complex inserts OmpF of *E. coli* in a reversed orientation compared to *in vitro* experiments (12). It has recently been shown that the assembly factor Omp85 recognizes its outer membrane protein substrates by a species-specific C-terminal motif (28). A similar mechanism might exist in mycobacteria and may involve interactions of the periplasmic loop of MspA with a yet unknown outer membrane protein assembly machinery of *M. smegmatis*.

All loop deletion mutants complemented the growth defect of the porin triple mutant *M. smegmatis* ML16 on solid and in liquid HdB minimal media supplemented with glucose (Fig. 6A and B), demonstrating functional pores *in vivo*. It is concluded that the L6 loop is dispensable for porin function in *M. smegmatis*. However, larger deletions of L6 resulted in MspA proteins that enable a faster uptake of glucose than smaller loop deletion mutants (Fig. 6D). This is in apparent contrast to the expression levels since much fewer pores are found in the outer membrane for these mutants (Fig. 6C). Normalization to the amount of extractable protein resulted in uptake rates for glucose of 2.5, 1.3, 1.3, 2.2, 8.8, and 5.0 nmol/mg cells/min for wt, $\Delta 3$, $\Delta 5$, $\Delta 7$, $\Delta 9$, and $\Delta 11$, respectively. This shows that large deletions in L6 result in pores two- to three-fold more permissive for translocation of glucose. It might be speculated that while large deletions in L6 do not increase the conductance of small ions *in vitro*, they may remove a blockade to neutral and larger solutes such as glucose. These results indicate that the molecular mechanisms governing the translocation of ions are different from those of neutral solutes. It should be noted that the lipid environment in the outer membrane of

M. smegmatis and in the lipid bilayer experiments are very different and is likely to influence the translocation of solutes as shown for the porin OmpF of *E. coli* (20).

The periplasmic portions of many outer membrane proteins of gram-negative bacteria, such as TolC (21) and OmpA (17), have been shown to interact with periplasmic and/or inner membrane effectors. Demonstration that deletion of almost the entire periplasmic loop in $\Delta 11$ results in a pore still capable of complementing a porin mutant growth defect shows that the periplasmic loop is not essential for docking of periplasmic or inner membrane effectors required for growth.

In conclusion, the L6 loop affects expression of MspA in the outer membrane and its permeability to both ions and larger, neutral solutes *in vitro*. It is not, however, required for channel function in whole cells nor is it the primary mechanism for voltage-dependent gating. The role of the periplasmic loop L6 in substrate translocation is not surprising given its large size and proximity to the constriction zone. MspA is the prototype of a new family of porins with more than 30 members identified solely in mycolic acid-containing bacteria (25) and has excellent perspectives in nanotechnological applications due to its extraordinary biophysical and biochemical properties (6, 40). In addition to the periplasmic loop L6, the constriction zone represents another structural novelty of MspA. Hence, work is underway to elucidate the role of the constriction zone in translocation of solutes through the MspA pore.

ACKNOWLEDGEMENTS

We gratefully acknowledge Ying Wang for excellent technical assistance. This work was supported by the National Human Genome Research Institute (NIH) grant HG004145 to MN. JH was supported by a fellowship from the NIH training grant “Basic Mechanisms of Lung Diseases” (NHLBI T32 HL07553).

REFERENCES

1. **Bainbridge, G., I. Gokce, and J. H. Lakey.** 1998. Voltage gating is a fundamental feature of porin and toxin beta-barrel membrane channels. *FEBS Lett* **431**:305-8.
2. **Basle, A., R. Qutub, M. Mehrazin, J. Wibbenmeyer, and A. H. Delcour.** 2004. Deletions of single extracellular loops affect pH sensitivity, but not voltage dependence, of the *Escherichia coli* porin OmpF. *Protein Eng Des Sel* **17**:665-72.
3. **Basle, A., G. Rummel, P. Storici, J. P. Rosenbusch, and T. Schirmer.** 2006. Crystal structure of osmoporin OmpC from *E. coli* at 2.0 Å. *J Mol Biol* **362**:933-42.
4. **Bos, M. P., V. Robert, and J. Tommassen.** 2007. Biogenesis of the gram-negative bacterial outer membrane. *Annu Rev Microbiol* **61**:191-214.
5. **Bredin, J., N. Saint, M. Mallea, E. D. G. Molle, J. M. Pages, and V. Simonet.** 2002. Alteration of pore properties of *Escherichia coli* OmpF induced by mutation of key residues in anti-loop 3 region. *Biochem J* **363**:521-8.
6. **Butler, T. Z., M. Pavlenok, I. M. Derrington, M. Niederweis, and J. H. Gundlach.** 2008. Single-molecule DNA detection with an engineered MspA protein nanopore. *Proc Natl Acad Sci U S A* **105**:20647-52.
7. **Cowan, S. W., T. Schirmer, G. Rummel, M. Steiert, R. Ghosh, R. A. Paupit, J. N. Jansonius, and J. P. Rosenbusch.** 1992. Crystal structures explain functional properties of two *E. coli* porins. *Nature* **358**:727-33.
8. **Engelhardt, H., C. Heinz, and M. Niederweis.** 2002. A tetrameric porin limits the cell wall permeability of *Mycobacterium smegmatis*. *J. Biol. Chem.* **277**:37567-37572.
9. **Faller, M., M. Niederweis, and G. E. Schulz.** 2004. The structure of a mycobacterial outer-membrane channel. *Science* **303**:1189-92.
10. **Heinz, C., H. Engelhardt, and M. Niederweis.** 2003. The core of the tetrameric mycobacterial porin MspA is an extremely stable beta-sheet domain. *J. Biol. Chem.* **278**:8678-8685.
11. **Heinz, C., and M. Niederweis.** 2000. Selective extraction and purification of a mycobacterial outer membrane protein. *Anal. Biochem.* **285**:113-120.
12. **Hoenger, A., J. M. Pages, D. Fourel, and A. Engel.** 1993. The orientation of porin OmpF in the outer membrane of *Escherichia coli*. *J. Mol. Biol.* **233**:400-13.
13. **Hoffmann, C., A. Leis, M. Niederweis, J. M. Plitzko, and H. Engelhardt.** 2008. Disclosure of the mycobacterial outer membrane: Cryo-electron tomography and vitreous sections reveal the lipid bilayer structure. *Proc. Natl. Acad. Sci. U S A* **105**:3963-3967.
14. **Im, W., and B. Roux.** 2002. Ions and counterions in a biological channel: A molecular dynamics simulation of OmpF porin from *Escherichia coli* in an explicit membrane with 1 M KCl aqueous salt solution. *J. Mol. Biol.* **319**:1177-97.
15. **Jarlier, V., and H. Nikaido.** 1990. Permeability barrier to hydrophilic solutes in *Mycobacterium chelonae*. *J. Bacteriol.* **172**:1418-1423.
16. **Kaps, I., S. Ehrt, S. Seeber, D. Schnappinger, C. Martin, L. W. Riley, and M. Niederweis.** 2001. Energy transfer between fluorescent proteins using a co-expression system in *Mycobacterium smegmatis*. *Gene* **278**:115-24.
17. **Koebnik, R.** 1995. Proposal for a peptidoglycan-associating alpha-helical motif in the C-terminal regions of some bacterial cell-surface proteins. *Mol. Microbiol.* **16**:1269-70.
18. **Koebnik, R., K. P. Locher, and P. van Gelder.** 2000. Structure and function of bacterial outer membrane proteins: barrels in a nutshell. *Mol. Microbiol.* **37**:239-53.

19. **Korchev, Y. E., G. M. Alder, A. Bakhranov, C. L. Bashford, B. S. Joomun, E. V. Sviderskaya, P. N. Usherwood, and C. A. Pasternak.** 1995. *Staphylococcus aureus* alpha-toxin-induced pores: channel-like behavior in lipid bilayers and patch clamped cells. *J Membr Biol* **143**:143-51.
20. **Korkmaz, F., S. Koster, O. Yildiz, and W. Mantele.** 2008. The Role of Lipids for the Functional Integrity of Porin: An FTIR Study Using Lipid and Protein Reporter Groups. *Biochemistry*.
21. **Koronakis, V., J. Li, E. Koronakis, and K. Stauffer.** 1997. Structure of TolC, the outer membrane component of the bacterial type I efflux system, derived from two-dimensional crystals. *Mol Microbiol* **23**:617-26.
22. **Mahfoud, M., S. Sukumaran, P. Hülsmann, K. Grieger, and M. Niederweis.** 2006. Topology of the porin MspA in the outer membrane of *Mycobacterium smegmatis*. *J Biol Chem* **281**:5908-15.
23. **Mailaender, C., N. Reiling, H. Engelhardt, S. Bossmann, S. Ehlers, and M. Niederweis.** 2004. The MspA porin promotes growth and increases antibiotic susceptibility of both *Mycobacterium bovis* BCG and *Mycobacterium tuberculosis*. *Microbiology* **150**:853-864.
24. **Müller, D. J., and A. Engel.** 1999. Voltage and pH-induced channel closure of porin OmpF visualized by atomic force microscopy. *J. Mol. Biol.* **285**:1347-51.
25. **Niederweis, M.** 2008. Mycobacterial porins, p. 153-165. *In* M. Daffe and J.-M. Reyat (ed.), *The mycobacterial cell envelope*. ASM Press, Washington, DC.
26. **Niederweis, M., S. Ehrt, C. Heinz, U. Klöcker, S. Karosi, K. M. Swiderek, L. W. Riley, and R. Benz.** 1999. Cloning of the *mspA* gene encoding a porin from *Mycobacterium smegmatis*. *Mol. Microbiol.* **33**:933-945.
27. **Phale, P. S., A. Philippsen, C. Widmer, V. P. Phale, J. P. Rosenbusch, and T. Schirmer.** 2001. Role of charged residues at the OmpF porin channel constriction probed by mutagenesis and simulation. *Biochemistry* **40**:6319-25.
28. **Robert, V., E. B. Volokhina, F. Senf, M. P. Bos, P. Van Gelder, and J. Tommassen.** 2006. Assembly factor Omp85 recognizes its outer membrane protein substrates by a species-specific C-terminal motif. *PLoS Biol* **4**:e377.
29. **Robertson, K. M., and D. P. Tieleman.** 2002. Molecular basis of voltage gating of OmpF porin. *Biochem Cell Biol* **80**:517-23.
30. **Ruiz, N., D. Kahne, and T. J. Silhavy.** 2006. Advances in understanding bacterial outer-membrane biogenesis. *Nat Rev Microbiol* **4**:57-66.
31. **Schirmer, T., T. A. Keller, Y. F. Wang, and J. P. Rosenbusch.** 1995. Structural basis for sugar translocation through maltoporin channels at 3.1 Å resolution. *Science* **267**:512-4.
32. **Sen, K., J. Hellman, and H. Nikaido.** 1988. Porin channels in intact cells of *Escherichia coli* are not affected by Donnan potentials across the outer membrane. *J. Biol. Chem.* **263**:1182-7.
33. **Song, L., M. R. Hobaugh, C. Shustak, S. Cheley, H. Bayley, and J. E. Gouaux.** 1996. Structure of staphylococcal alpha-hemolysin, a heptameric transmembrane pore. *Science* **274**:1859-66.
34. **Stahl, C., S. Kubetzko, I. Kaps, S. Seeber, H. Engelhardt, and M. Niederweis.** 2001. MspA provides the main hydrophilic pathway through the cell wall of *Mycobacterium smegmatis*. *Mol. Microbiol.* **40**:451-464 (Authors' correction appeared in *Mol. Microbiol.* **57**, 1509).
35. **Stahl, C., S. Kubetzko, I. Kaps, S. Seeber, H. Engelhardt, and M. Niederweis.** 2005. MspA provides the main hydrophilic pathway through the cell wall of *Mycobacterium smegmatis*. *Mol Microbiol* **57**:1509.
36. **Stephan, J., J. Bender, F. Wolschendorf, C. Hoffmann, E. Roth, C. Mailänder, H. Engelhardt, and M. Niederweis.** 2005. The growth rate of *Mycobacterium smegmatis* depends on sufficient porin-mediated influx of nutrients. *Mol. Microbiol.* **58**:714-730.

37. **van Gelder, P., N. Saint, P. Phale, E. F. Eppens, A. Prilipov, R. van Boxtel, J. P. Rosenbusch, and J. Tommassen.** 1997. Voltage sensing in the PhoE and OmpF outer membrane porins of *Escherichia coli*: role of charged residues. *J Mol Biol* **269**:468-72.
38. **van Gelder, P., N. Saint, R. van Boxtel, J. P. Rosenbusch, and J. Tommassen.** 1997. Pore functioning of outer membrane protein PhoE of *Escherichia coli*: mutagenesis of the constriction loop L3. *Protein Eng* **10**:699-706.
39. **Weiss, M. S., T. Wacker, J. Weckesser, W. Welte, and G. E. Schulz.** 1990. The three-dimensional structure of porin from *Rhodobacter capsulatus* at 3 Å resolution. *FEBS Lett.* **267**:268-72.
40. **Wörner, M., O. Lioubashevski, M. T. Basel, S. Niebler, E. Gogritchiani, N. Egner, C. Heinz, J. Hoferer, M. Cipolloni, K. Janik, E. Katz, A. M. Braun, I. Willner, M. Niederweis, and S. H. Bossmann.** 2007. Characterization of nanostructured surfaces generated by reconstitution of the porin MspA from *Mycobacterium smegmatis*. *Small* **3**:1084-1097.

OPEN PORES IN THE OUTER MEMBRANE DRASTICALLY REDUCE
VIRULENCE OF *MYCOBACTERIUM TUBERCULOSIS*

by

JASON HUFF, KERSTIN WALTER, CHRISTIAN HOFFMANN, HOUHUI SONG,
FRANK WOLSCHENDORF, STEFAN EHLERS, AND MICHAEL NIEDERWEIS

In preparation for *PLoS Pathogen*

Format adapted for dissertation

ABSTRACT

The outer membrane of *Mycobacterium tuberculosis* forms an efficient permeability barrier that resists passage by toxic compounds but must be functionalized by proteins for uptake of nutrients. To date, porins that provide a pathway for small and hydrophilic compounds across the outer membrane of *M. tuberculosis* have not been identified. Conversely, the porin pathway in *Mycobacterium smegmatis* and its primary porin MspA have been well studied. In this study, we examined whether the virulence of *M. tuberculosis* in mice would be enhanced by increased nutrient uptake or compromised due to toxic solute exposure when MspA porins were used to permeabilize the outer membrane. While porin expression is required for virulence by most Gram-negative bacterial pathogens, permeabilization of the outer membrane by MspA expression drastically reduced the virulence of *M. tuberculosis* and was strongly selected against during infection in mice. However, only a modest reduction in virulence was observed when a transport-impaired MspA pore was expressed, indicating that both hydrophilic and hydrophobic solutes contribute to the attenuation of *M. tuberculosis*. These results indicate that *M. tuberculosis* has adapted to slow nutrient uptake and growth to acquire resistance to toxic solutes encountered during infection.

INTRODUCTION

Mycobacterium tuberculosis, the causative agent of tuberculosis, remains a global health burden infecting nearly a third of the world's population (19). After inhalation into the lung, *M. tuberculosis* is phagocytosed by resident alveolar macrophages.

M. tuberculosis can survive in these macrophages because it inhibits the maturation of the phagosome and prevents fusion with bactericidal lysosomes (38). However, with the onset of the adaptive immune response, stimulation of macrophages via IFN- γ overrides the blockade of phagosome maturation and enables them to destroy the bacteria in lysosomal compartments by delivery of bactericidal compounds including reactive nitrogen and oxygen intermediates (RNIs and ROIs), protons, defensins and cathelicidins. In order to establish a persistent infection under those adverse conditions, *M. tuberculosis* needs to replicate and hence faces the challenge to acquire nutrients while minimizing the influx of toxic compounds. This balancing act of meeting apparently opposing requirements is achieved by most Gram-negative bacterial pathogens by combining specific inner membrane uptake proteins with rather non-specific outer membrane pores that impose an exclusion limit for solutes exceeding approximately 600 Da (35). This allows small, hydrophilic sugar molecules to enter cells, but does not allow entry of macromolecules and considerably slows the uptake of toxic solutes such as bile (46) and hydrophilic antibiotics (18). Recently, cryo-electron micrographs showed the existence of an outer membrane in the mycobacterial cell envelope (23, 55). Mutations in the biosynthesis of lipids that constitute the outer membrane are detrimental to the virulence of *M. tuberculosis* (2), causing an increase in permeability (8) and/or loss of immunomodulatory lipids (42).

Many nutrient molecules such as inorganic ions and sugars are hydrophilic and hence cannot diffuse through lipid membranes at a physiologically relevant rate. As a consequence, the mycobacterial outer membrane must be functionalized by proteins for transport of these nutrients. To date, only very few proteins have been identified in the outer membrane of *M. tuberculosis*. OmpATb was discovered as an outer membrane protein with channel-forming activity and was proposed to be a porin of *M. tuberculosis* (41). However, its function as a porin has been questioned (33). Rv1698 was also identified as an outer membrane protein with channel activity (47), but its physiological function in *M. tuberculosis* is yet unknown.

In contrast to the lack of identified outer membrane proteins in *M. tuberculosis*, the porin pathway has been well examined in *Mycobacterium smegmatis*. The primary porin of *M. smegmatis*, MspA, is a large, octameric β -barrel protein forming a single pore of 1 nm internal diameter (15). It allows the diffusion of small and hydrophilic compounds across the outer membrane. Its deletion reduces glucose uptake by four-fold (48) and decreases sensitivity to a wide array of antibiotics (10, 50). Conversely, the expression of MspA in *M. tuberculosis* and the almost genetically identical *Mycobacterium bovis* BCG increases growth rate and susceptibility to antibiotics (30). Interestingly, deletion of porins renders *M. smegmatis* more resistant to NO-mediated killing by macrophages (14).

Our aim was to examine the role of the porin pathway in the virulence of *M. tuberculosis*. Because *M. tuberculosis* must balance the uptake of nutrients while resisting toxic compounds, we sought to answer how tipping this balance would affect virulence. As no porins are yet identified in *M. tuberculosis*, we utilized MspA as a tool

to permeabilize the outer membrane of *M. tuberculosis*. To distinguish between virulence defects resulting from direct channel activity and non-specific membrane permeabilization stemming from heterologous outer membrane protein expression, we constructed a transport-impaired MspA mutant. The mutant protein did not form stable channels and was deficient in glucose and *p*-nitrophenylphosphate (*p*NPP) permeability. We compared the virulence defects of *M. tuberculosis* expressing both wt and impaired forms of the MspA porin during mouse infections.

MATERIALS AND METHODS

Bacterial strains and growth conditions. *M. smegmatis* strains were grown at 37°C in Middlebrook 7H9 liquid medium (Difco Laboratories) supplemented with 0.2% glycerol and 0.05% Tween 80 or on Middlebrook 7H10 agar (Difco Laboratories) supplemented with 0.2% glycerol, unless indicated otherwise. Addition of 10% oleic acid-albumin-dextrose-catalase (OADC; Remel) to both solid and liquid media was required for culturing *M. tuberculosis* H37Rv. *M. tuberculosis* mc²6230 is an unmarked derivative of *M. tuberculosis* mc²6030 (43) and was grown in Middlebrook 7H9 liquid medium supplemented with 0.2% glycerol, 10% OADC, 0.025% Tyloxapol, 0.2% casamino acids, and 24 µg/mL pantothenate or on Middlebrook 7H10 agar supplemented with 0.2% glycerol, 10% OADC, 0.2% casamino acids, and 24 µg/mL pantothenate. *Escherichia coli* DH5α was used for all cloning experiments and was routinely grown in Luria-Bertani (LB) medium at 37°C. Antibiotics were used when required at the following concentrations: ampicillin (100 µg/ml for *E. coli*), kanamycin (30 µg/ml for *E. coli* and mycobacteria), hygromycin (200 µg/ml for *E. coli*, 50 µg/ml for mycobacteria).

Construction of *mspA* mutants. The end primers 5'-CGACCAGCACGGCATAACATC-3' and 5'-CGTTCTCGGCTCGATGATCC-3' and a specific mutagenesis primer were used in a combined-chain reaction (CCR) (6) to amplify mutated *mspA* genes from pMN016 (Table 1). The mutagenesis primers 5'-CATCCTGATCCTGGACGGTGAC-3' and 5'-CCCCGAACATCCTGATCCTGCTGGGTGACATCACCGCTCC-3' generated the mutated *mspA* genes encoding *mspA* D90L and *mspA* D90L/D91L, respectively. The

mutated *mspA* genes were digested with *Hind*III and *Sph*I and ligated into the 5,476 bp *Hind*III and *Sph*I-restricted fragment of pMN035 (Table 1) and transformed into *E. coli* DH5 α . This generated the expression plasmids pML170 and pML172 encoding *mspA* D90L and *mspA* D90L/D91L, respectively.

The 879 bp fragment containing wt *mspA* under *p_{imyc}* promoter control was cut out from pMN013 using *Xba*I and *Cla*I and ligated with the 8,221 bp *Xba*I and *Cla*I-restricted fragment of pCV125 to generate the integrative vector pML757 (Table 1) that integrates at the attachment site of mycobacteriophage L5. This plasmid was transformed into virulent *M. tuberculosis* H37Rv and selected for on kanamycin to generate the MspA-expressing mutant ML169. Integration of undigested pCV125 resulted in the strain ML159 (Table 1).

Construction of *ompA_{his}* expression vector. The C-terminal his-tagged *ompA* expression vector pML589 was derived from the plasmid pML588 (will be published elsewhere). The construct *p_{imyc}-ompA* was amplified by PCR from pML588 with the primers 5'-

TTATTTAAATTTAGTGGTGGTGGTGGTGGTGGTTGACCACGATCTCGACGCGA
CGA-3' and 5'-GCTTAATTAACAGAAAGGAGGTTAATGT-3', generating a 1,035 bp fragment flanked by *Pac*I and *Swa*I restriction sites. The plasmid pML588 and the PCR product were both digested with *Pac*I and *Swa*I, generating 5,216 bp and 1,024 bp fragments, respectively. The *Pac*I/*Swa*I digested *p_{imyc}-ompA_{his}* PCR fragment was then ligated into *Pac*I/*Swa*I digested pML588 to generate pML589.

Preparation of detergent extracts from mycobacteria and analysis by gel electrophoresis. MspA proteins were constitutively expressed and selectively extracted

from whole cells of *M. smegmatis* as described (21) as well as from *M. tuberculosis*. Briefly, *M. smegmatis* cells were washed with phosphate-buffered saline (PBS), centrifuged and resuspended in POP05 buffer (300 mM NaH₂PO₄/Na₂HPO₄, 0.3 mM Na₂EDTA, 150 mM NaCl, 0.5% (w/v) OPOE (Alexis Biochemicals) to a cell density of 100 µl/10 mg cells (wet weight) and heated to 100°C under stirring for 30 min. *M. tuberculosis* cultures were first treated with a 1:1 ratio of 10% formalin, then washed in PBS, resuspended in 100 µl/10 mg cells (wet weight) POPO5, and extracted as described above. Cell suspensions from *M. smegmatis* and from *M. tuberculosis* were then cooled on ice for 10 min and centrifuged at 11,200 x g at 4°C for 15 min. Protein extracts were separated on a denaturing 10% polyacrylamide gel and stained with Coomassie Blue. Quantitative image analysis of protein gel bands by pixel densitometry was performed using Labworks 4.6 software (UVP, Inc.).

Enzyme-linked immunosorbent assay (ELISA) on whole cells. To examine the localization and surface exposure of MspA proteins and, as a control, OmpA in *M. tuberculosis*, an enzyme-linked immunosorbent assay (ELISA) using whole cells was employed. To this end, the vectors pMN013, pML170, pML589, and pMS2 encoding MspA, MspA D90L, his-tagged OmpA, and empty, respectively, were transformed into avirulent *M. tuberculosis* mc²6230. This strain is an unmarked derivative of *M. tuberculosis* mc²6030, which is highly attenuated due to pantothenate auxotrophy and deletion of the virulence locus RD1 (43). Strains were grown to an OD₆₀₀ of about 0.8 - 1.0 and 10 ml of culture were harvested by centrifugation and washed in 10 ml TBST (50 mM Tris-HCl pH 8, 150 mM NaCl, 1 mM MgCl₂, 0.05% Tween 20). Cells were concentrated by resuspension in 1 ml TBST and 200 µl were transferred to a U-bottom

96-well microtiter plate. The plate was centrifuged at 3200 x *g* for 5 min at 4°C and cells were blocked with 3% skim milk (Difco) in TBST for 1 hour at 37°C. Cells were then washed twice with TBST and incubated for 1 hour at 37°C with 1:2,000 dilutions of either anti-OmpA antiserum (41) or anti-MspA antiserum pAK813 (34). Following three wash steps with 200 µl TBST (3200 x *g*, 5 min, 4°C), the cells were then incubated with a 1:5,000 dilution of anti-rabbit IgG secondary antibody conjugated to alkaline phosphatase and incubated for 1 hour at 37°C. Cells were then washed three times in TBST (3200 x *g*, 5 min, 4°C) and resuspended in 100 µl substrate buffer (0.1 M glycine, 1 mM ZnCl₂, 1 mM MgCl₂, 1% 4-nitrophenyl phosphate (*p*NPP)). After incubation for 3 hours at 37°C, the reaction was stopped with the addition of 100 µl 2 M NaOH. The plate was then centrifuged and 100 µl of the supernatant was transferred to a flat-bottom 96-well microtiter plate. Phosphatase activity was quantified by reading the absorption at 405 nm using a microplate reader (Synergy HT, Bio-TEK Instrument Inc, USA) and was normalized to the starting OD₆₀₀ of the cultures.

Purification of MspA and reconstitution into artificial lipid bilayers. Wild-type and mutant MspA proteins were purified as previously described (20). Briefly, protein extracts were precipitated in acetone and resuspended in AOPO5 buffer (25 mM HEPES/NaOH, 10 mM NaCl, 0.5% OPOE, pH 7.5). Proteins were then loaded onto a 1.7 mL POROS 20HQ anion-exchange column (Perceptive Biosystems), washed in AOPO5, and eluted in a salt concentration range of 0.76 M to 1.02 M NaCl. Buffers were then standardized by gel filtration in NaPOP (25 mM NaH₂PO₄/Na₂HPO₄, 0.5% n-OPOE, pH 7.5).

Channel activity of proteins was measured in lipid bilayer experiments as described elsewhere (20). In all single channel conductance experiments, 1 M KCl was used as the electrolyte. The single channel conductances of at least 100 pores reconstituted from a freshly diluted solution of purified proteins were analyzed in several diphytanoyl phosphatidylcholine (Avanti Polar Lipids) membranes with an applied direct-current voltage of -10 mV. Using Ag/AgCl electrodes, the membrane current was measured with a current amplifier (Keithley 428 current amplifier) and digitized by a desktop computer equipped with Keithley Metrabyte STA 1800U interface. Data acquisition was performed using Test Point 4.0 software (Keithley). Analysis of the current traces was carried out using a macro based on the Igor Pro 5.03 software (written by Dr. Harald Engelhardt, MPI of Biochemistry, Germany). The steps recorded in four to six membranes were pooled to generate the final distribution plots (SigmaPlot 9.0). The noise suppression factor was constant for all measurements.

Liposome Swelling Assay. 300 μ L of lipids (7.2 μ mol phosphatidylcholine type XVI-E (Sigma) and 0.4 μ mol dicetyl phosphate (MP) dissolved in chloroform were dried down to a uniform lipid film in a round bottom flask under a stream of argon. 200 μ L of a solution containing 10 μ g MspA in 0.5% (w/v) OPOE were added to the dried lipid film. Resuspension and homogenization of the proteolipid film was performed by gentle vortexing followed by bath sonication for 3 minutes. The resulting proteolipid solution was flushed with argon gas and dried down via a rotary vacuum evaporator in a 42°C water bath. The proteolipid film was then dissolved in 600 μ l of 15% (w/v) dextran T40 in 5 mM Tris-HCl, pH 8.0 by gentle shaking. Homogenization of the resulting proteoliposomes was achieved by incubation at room temperature for 1 hour.

The isoosmotic concentration of the proteoliposomes was determined by dilution in a buffer (5 mM Tris-HCl, pH 8.0) containing 15, 20, 25, 30 and 35 mM raffinose, which is too large to diffuse through the MspA pore. 30 μ L of proteoliposome suspension were added to 2 mL of the raffinose solutions under constant stirring at 25°C in a UV-spectrophotometer (Lambda 35, Perkin Elmer). Isoosmolarity was determined to be the concentration at which no change in OD₄₀₀ occurred after mixing. 2 mL of an isoosmotic solution of glucose were then mixed with 30 μ L of the proteoliposome solution and, under constant stirring at 25°C, changes in the OD₄₀₀ were recorded over time.

Phosphatase Assay. The PhoA activity of *M. smegmatis* ML42 (Δ mspA and Δ mspC, L5 attB::phoA) was measured as described previously (53). Strains were grown in Middlebrook 7H9 medium to an OD₆₀₀ of about 1.0. Cells were harvested by centrifugation at 4°C and resuspended in an equal volume of ice-cold 1 M Tris-buffer (pH 8.0). The OD₆₀₀ of the cell suspension was determined. Cells were kept on ice during all steps. A portion of each cell suspension was lysed by sonication using a microtip (Branson). PhoA activity was measured in both whole and lysed cells by adding 0.15 ml of samples (V_s) to 1 ml of detection buffer (1 M Tris-HCl, pH 8.0, 4 mM *p*-nitrophenylphosphate [*p*NPP]). After 30 min of incubation at 37°C, 100 μ l of 1 M K₂HPO₄ were added to stop the reaction. The sample was centrifuged and the A₄₀₅ of 1 ml of the supernatant was determined in a spectrophotometer (SmartSpec Plus; Bio Rad). The PhoA activity of whole and lysed cells was calculated using the following formula (26): activity (units) = (1,000 x A₄₀₅)/(t_i x OD₆₀₀ x V_s), where t_i is the incubation time in minutes and V_s is the volume of sample.

Bacterial culturing for infection experiments. For infection experiments, *M. tuberculosis* cultures were grown in Middlebrook 7H9 broth (Difco, Detroit, IM) supplemented with 10% OADC (Life Technologies, Gaithersburg, MD), 0.05% Tween 80 and 0.2% glycerol (VWR International GmbH, Darmstadt, Germany) at 37°C in aerated cultures. All strains transformed with a plasmid coding for hygromycin resistance were grown in hygromycin containing medium. Midexponential phase cultures were harvested, aliquoted, and frozen at -80°C. After thawing, viable cell counts were determined by plating serial dilutions on Middlebrook 7H10 agar supplemented with 10% bovine serum (Biowest, Nuaille, France). To ensure proper dispersion of *M. tuberculosis*, the bacterial suspension was drawn through a nonpyrogenic needle (Microlance3, BD, Drogheda, Ireland) prior to every infection experiment.

***In vivo* infection experiments.** Female, 6- to 8-week-old specific pathogen-free C57BL/6 mice, maintained in individually ventilated cages (IVC, Ebeco, Castrop-Rauxel, Germany) under biosafety level III conditions, were aerogenically infected (Glas-Col, Terre-Haute, IN) with approximately 100 or 1,000 cfu of the respective *M. tuberculosis* strains. Inoculum size was confirmed 24 h after infection by determining the bacterial burden in the lung. In order to follow the course of infection, bacterial replication in the lung was evaluated at different time points after infection with the different *M. tuberculosis* strains. Organs from five to six animals per time point were aseptically removed, weighed and homogenized in distilled sterile water containing 0.05% Tween 80. Tenfold serial dilutions of organ homogenates were plated on Middlebrook 7H10 agar supplemented with 10% bovine serum and incubated at 37°C for 21 days. Colonies on plates were enumerated and results expressed as log₁₀ cfu per organ. In accordance

with the Animal Research Ethics Board of the Ministry of Environment, Nature, Protection and Agriculture (Kiel, Germany) mice that lost 25% of their original weight during the course of infection were scored as moribund and had to be sacrificed.

Statistical analysis. All quantifiable data were expressed as means \pm SD and subjected to statistical analysis using either Mann-Whitney tests or, in the case of multiple comparisons, a one-way ANOVA combined with a Dunnett's post-test. Levels of statistical significance are expressed as follows: *: $P < 0.05$, **: $P < 0.01$; ***: $P < 0.001$. Where appropriate, growth in lungs was normalized to inoculum size by dividing growth post-infection by growth determined on day 1 after infection.

RESULTS

Very low level expression of MspA reduces *M. tuberculosis* virulence. In the absence of a bona fide porin of *M. tuberculosis*, the primary porin gene *mspA* of *M. smegmatis* was expressed in *M. tuberculosis* H37Rv to examine the role of the porin pathway in virulence. To this end, we integrated the vector pML757 which carries the *mspA* gene under the control of the constitutive *p_{myc}* promoter into the chromosomal attachment site for the mycobacteriophage L5, generating the strain *M. tuberculosis* ML169 (Table 1). However, no MspA was detected after extraction of ML169 cells with *n*-octylpolyethylene oxide (OPOE) using an established protocol in a western blot with the polyclonal anti-MspA antibody pAK813 (30, 34) (Fig. 1). Only upon over-exposure of a blot, a band corresponding to octameric MspA was observed (Fig. S1), indicating very low expression of *mspA* from the chromosome of *M. tuberculosis*.

C57BL/6 mice were infected with wild-type (wt) *M. tuberculosis* H37Rv and the *mspA*-expressing strain ML169 by the aerosol route, and virulence was determined by plating lung homogenates for colony forming units (cfu) on plates at the indicated time points. Although mice infected with ML169 had received a slightly higher inoculum during aerosol infection (1,077 cfu) than mice infected with wt *M. tuberculosis* (490 cfu), replication of ML169 was significantly lower in the lungs of mice at both 35 and 60 days after infection (Fig. 2). These results demonstrate that even very low expression of MspA protein (Fig. S1) significantly reduced virulence and persistence of *M. tuberculosis in vivo*.

	Relevant Genotype or Description	Source or Reference
Strains		
<i>E. coli</i> DH5 α	<i>recA1</i> ; <i>endA1</i> ; <i>gyrA96</i> ; <i>thi</i> ; <i>relA1</i> ; <i>hsdR17</i> (<i>rK-;mK+</i>); <i>supE44</i> ; ϕ 80 Δ <i>lacZ</i> Δ <i>M15</i> ; Δ <i>lacZYA-argF</i> ; <i>UE169</i>	(44)
<i>M. smegmatis</i> ML42	SMR5 derivative, Δ <i>mspA</i> / Δ <i>mspC</i> , L5 <i>attB</i> :: <i>p_{imyc}-phoA</i> , Δ <i>hyg</i>	(53)
<i>M. tuberculosis</i> H37Rv	wild-type <i>M. tuberculosis</i>	from Dr. Steyn
<i>M. tuberculosis</i> ML159	H37Rv derivative, L5 <i>attB</i> :: <i>pCV125</i>	This study
<i>M. tuberculosis</i> ML169	H37Rv derivative, L5 <i>attB</i> :: <i>pML757</i>	This study
<i>M. tuberculosis</i> mc ² 6230	<i>M. tuberculosis</i> mc ² 6030 derivative, Δ <i>panCD</i> , Δ <i>RD1</i>	(43)
Plasmids		
pCV125	ColE1 origin, L5 <i>int</i> , L5 <i>attP</i> , <i>aph</i>	(7)
pMS2	PAL5000 origin, ColE1 origin, <i>hyg</i>	(24)
pMN006	Promoterless- <i>mspA</i> , PAL5000 origin, ColE1 origin, <i>hyg</i>	(48)
pMN013	<i>p_{imyc}-mspA</i> , PAL5000 origin, ColE1 origin, <i>hyg</i>	(30)
pMN016	<i>p_{smyc}-mspA</i> , PAL5000 origin, ColE1 origin, <i>hyg</i>	(49)
pML170	<i>p_{smyc}-mspA</i> D90L, PAL5000 origin, ColE1 origin, <i>hyg</i>	This study
pML172	<i>p_{smyc}-mspA</i> D90L/D91L, PAL5000 origin, ColE1 origin, <i>hyg</i>	This study
pML589	<i>p_{imyc}-ompAhis</i> , PAL5000 origin, ColE1 origin, <i>hyg</i>	This study
pML757	<i>p_{imyc}-mspA</i> , ColE1 origin, L5 <i>int</i> , L5 <i>attP</i> , <i>aph</i>	This study

Table 1: Bacterial strains and plasmids used in this study. ColE1: *E. coli* replication of origin; PAL5000 origin: mycobacterial replication of origin; L5 *int*: mycobacteriophage L5 integrase; L5 *attP*: mycobacteriophage L5 attachment site; *hyg*: hygromycin resistance gene; *aph*: kanamycin resistance gene.

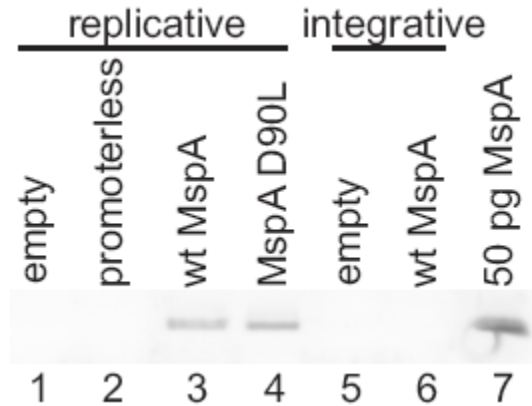


Figure 1. Expression of *mspA* in *M. tuberculosis*. Comparison of detergent-soluble raw extracts of *M. tuberculosis* by SDS-PAGE. MspA was expressed from either replicative or integrative vectors as noted above the lanes. The replicative vectors pMS2 (empty, lane 1), pMN006 (promoterless-*mspA*, lane 2), pMN013 (wt *mspA*, lane 3), pML170 (*mspA* D90L, lane 4), and the integrative vectors pCV125 (empty, lane 5; strain ML159) and pML757 (wt *mspA*, lane 6; strain ML169) were constitutively expressed in *M. tuberculosis* H37Rv. MspA proteins were selectively extracted with the detergent OPOE, separated on a 10% polyacrylamide gel, transferred to a nitrocellulose membrane, and detected with an MspA antiserum. Only octameric MspA bands were observed. Expression levels were quantified by pixel densitometry, normalized to pMN013, and were 0.1, 0.2, 101, 0.2, 0.2% of pMN013 for empty, promoterless, D90L, ML159, and ML169, respectively.

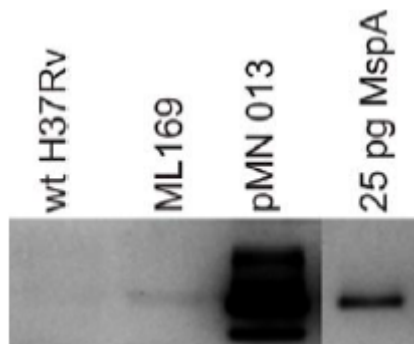


Figure S1. Detection of MspA expression in *M. tuberculosis* by blot over-exposure. MspA was selectively extracted from wt *M. tuberculosis*, *M. tuberculosis* ML169 (integrated *mspA*), or *M. tuberculosis* with pMN013 (replicative *mspA* plasmid). Proteins were separated, transferred, and detected with MspA antiserum. The blot was exposed at high sensitivity for 20 minutes.

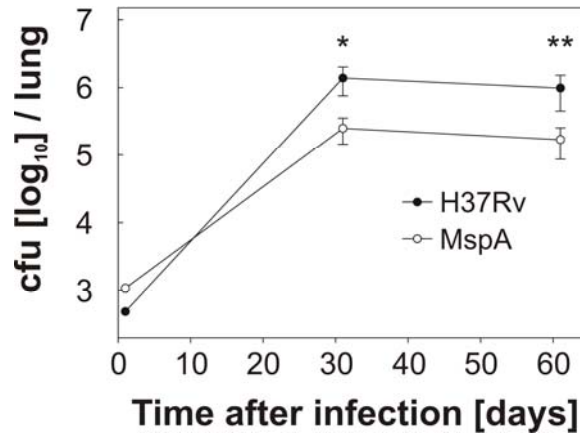


Figure 2. Virulence of *M. tuberculosis* chromosomally expressing *mspA* during mouse infections. C57BL/6 mice were infected by the aerosol route with an intended inoculum of 1,000 cfu of ML169 (integrated *mspA*) and virulent *M. tuberculosis* H37Rv. Bacterial replication in the lung was determined on days 31 and 61 after infection by plating lung homogenates on Middlebrook 7H10 plates supplemented with 10% bovine serum.

Episomal expression of MspA drastically reduces virulence of *M.*

tuberculosis. As only very little MspA was expressed from the integrated cassette in the chromosome of *M. tuberculosis*, we considered whether expression from episomal plasmids would exacerbate the virulence defect obtained with an integrated plasmid. For this purpose, we transformed into *M. tuberculosis* the episomal plasmids pMN013, which expresses *mspA* under the control of the *p_{myc}* promoter, and pMN006, which contains a promoterless-*mspA* cassette (Table 1). As can be seen in Figure 1, MspA was clearly detected in *M. tuberculosis* carrying pMN013 whereas the strain carrying pMN006 contained no detectable MspA. Therefore, *M. tuberculosis* carrying pMN006 served as a negative control for infection studies. C57BL/6 mice were infected by the aerosol route with 100 cfu of virulent *M. tuberculosis* H37Rv, H37Rv/pMN013, or H37Rv/pMN006. Five weeks after infection, bacterial growth in the lungs of mice having received the

mspA-expressing strain was approx. 300-fold lower than growth in the two groups of mice infected with either wt *M. tuberculosis* or *M. tuberculosis* with the promoterless-*mspA* construct (Fig. 3A). Growth of wt *M. tuberculosis* and *M. tuberculosis* with the promoterless construct was identical, demonstrating that expression of *mspA* caused the observed virulence defect.

In order to verify whether decreased initial replication *in vivo* translated into a lower rate of persistence over time, C57BL/6 mice were infected by the aerosol route with approx. 100 cfu of *M. tuberculosis* carrying either pMN006 or pMN013, and bacterial growth in the lungs was determined on days 61 and 90 after infection. Based on the results of our first infection experiment, we considered the possibility that *M. tuberculosis* with pMN013 might lose the *mspA* expression plasmid due to counterselection *in vivo*. Therefore, we determined the bacterial load in lung homogenates on Middlebrook 7H10 agar plates in the presence or absence of hygromycin. Compared to the control strain, bacterial loads in the lungs of mice infected with *mspA*-expressing *M. tuberculosis* were significantly lower on day 61 and beyond (Fig. 3B). This was particularly evident when lung homogenates were plated on hygromycin-containing 7H10 plates where growth of the *mspA*-expressing strain fell below the detection limit of 30 cfu/lung on days 61 and 90 post-infection, demonstrating that almost all cultivatable *M. tuberculosis* in this group of mice had lost the *mspA* expression plasmid pMN013. This indicated a selection pressure against maintaining the

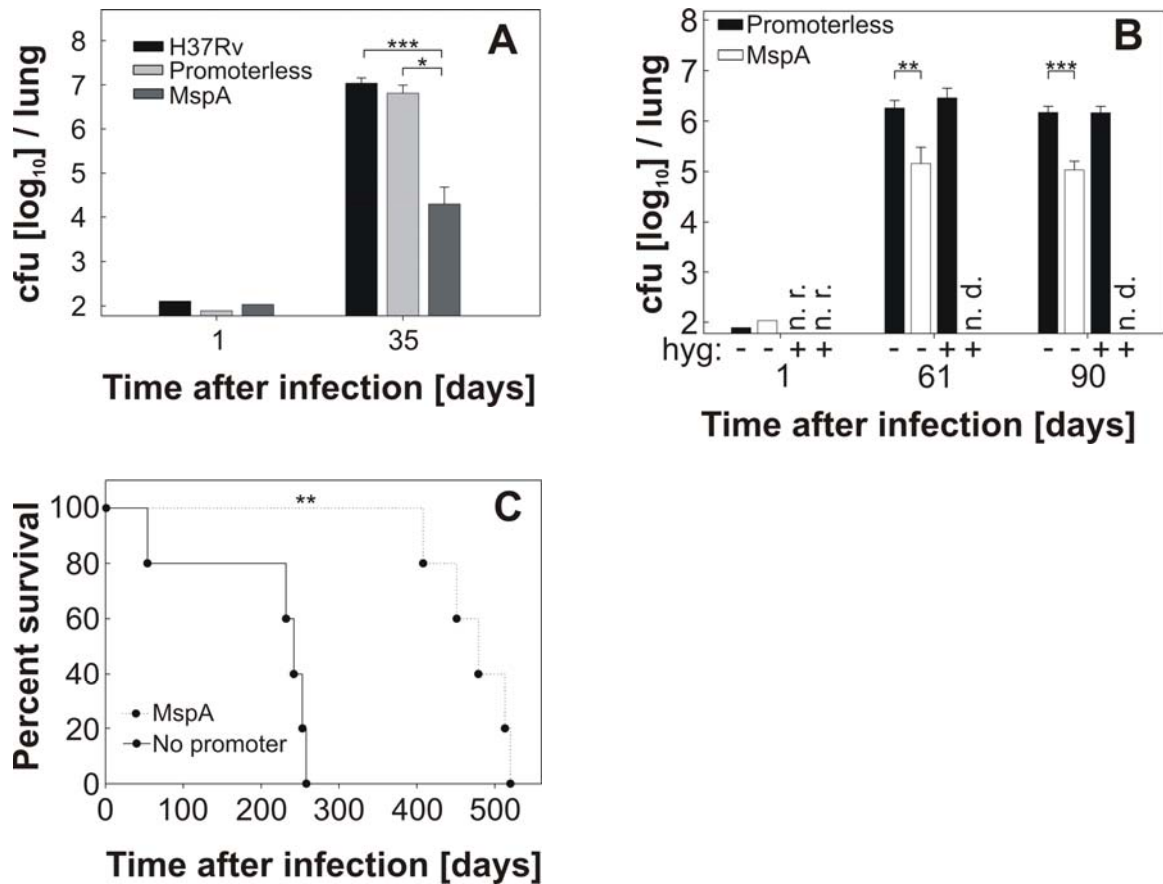


Figure 3. Virulence of *M. tuberculosis* episomally expressing *mspA* during mouse infections. (A) C57BL/6 mice were infected by the aerosol route with 100 cfu of virulent *M. tuberculosis* H37Rv, *M. tuberculosis* with pMN013 (wt *mspA*), or *M. tuberculosis* with pMN006 (promoterless-*mspA*). Five weeks after infection, the bacterial burden of the lung was determined on solid media without hygromycin. (B) C57BL/6 mice were infected by the aerosol route with 100 cfu of *M. tuberculosis* with either pMN013 or pMN006 and bacterial replication in the lung was evaluated on days 61 and 90 post-infection. Organ homogenates were plated on solid media in the presence (+ hyg) or absence (- hyg) of hygromycin. n. r. = not recorded. n.d. = not detected. (C) C57BL/6 mice were infected by the aerosol route with 100 cfu of *M. tuberculosis* carrying either pMN013 or pMN006 and the survival time of mice after infection was monitored.

mspA plasmid in mice. The significantly different bacterial loads between the two experimental groups also translated into differential survival of infected mice (Fig. 3C): mice infected with the *mspA*-expressing strain lived twice as long (mean time to death:

approx. 480 days) compared to mice infected with the promoterless-*mspA* control strain (mean time to death: approx. 240 days). Taken together, these results show that *mspA* expression is detrimental to the survival of *M. tuberculosis* in mice.

Screening for an MspA mutant with an impaired channel. Previously, it was shown that integration of MspA pores in the outer membrane increased permeability to both hydrophilic and hydrophobic solutes in *M. smegmatis* (48, 50) and in *M. tuberculosis* (30). This surprising result was attributed to direct (diffusion through the pore) and indirect (permeabilization due to i.e. lipid packing defects) effects of MspA insertion into mycobacterial outer membranes (50). To distinguish between these effects and to examine whether the virulence defect of *mspA* expression in *M. tuberculosis* was due to channel activity, we searched for mutants of MspA that reconstituted normally into membranes but were defective in channel activity. Candidates for such a mutant would likely include mutations in the aspartic acid residues located at positions 90 and 91 in the constriction zone (15). We hypothesized that mutations of D90 and/or D91 may alter porin properties and reduce or eliminate channel function without affecting localization or insertion into the outer membrane. We created and tested approximately 50 MspA mutants with altered constriction zones (will be published elsewhere). The plasmids pML170 and pML172 encode MspA D90L and MspA D90L/D91L, respectively (Table 1). Wt MspA and the two leucine mutants were extracted in similar amounts from whole cells of *M. smegmatis* using 0.5% OPOE as a detergent as described previously (20) indicating that the mutations in the constriction zone did not change expression levels of MspA (Fig. 4). No background expression of MspB was detectable in Commassie-stained gels (Fig. 4). All proteins were purified to apparent homogeneity as described (20) and

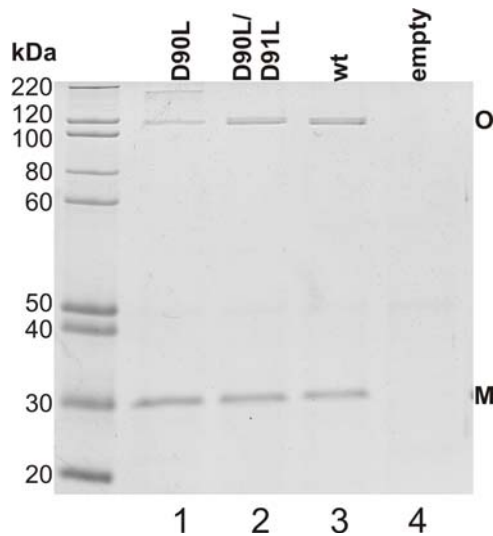


Figure 4. Expression of Leucine mutants in *M. smegmatis*. Comparison of detergent-soluble raw extracts of *M. smegmatis* by SDS-PAGE. The mutated *mspA* expression vectors pML170 (lane 1, MspA D90L) and pML172 (lane 2, MspA D90L/D91L) as well as pMN016 (lane 3, wt MspA) and pMS2 (lane 4, no MspA) were constitutively expressed in *M. smegmatis* ML42 ($\Delta mspA$, $\Delta mspC$, L5 *attB::phoA*) (53). MspA proteins were selectively extracted from ML42 at 100°C in a buffer containing 0.5% OPOE, separated on a 10% polyacrylamide gel, and stained with Coomassie Blue. Lane M contains the protein mass marker (Mark12, Invitrogen). The positions of the MspA octamer and monomer on the gel are notated by an O and an M, respectively. Expression was quantified by pixel densitometry of all MspA bands in each lane and normalized to wt MspA. Both D90L and D90L/D91L were 106% of wt MspA expression while the empty vector was 2% of wt MspA.

their channel-forming activity was examined in lipid bilayer experiments. The single amino acid substitution D90L resulted in an MspA mutant that does not form stable channels when the purified protein was reconstituted in artificial lipid bilayers (Fig. 5A). By contrast, mutation of both aspartates at positions 90 and 91 to leucine resulted in a functional pore forming stable channels in artificial bilayers (Fig. 5B). The average single channel conductance of the D90L/D91L double mutant was 2.4 nS (Fig. 5C), approximately half that of wt MspA (34). Importantly, the restoration of a wt-like

channel activity by introducing the leucine at position 91 indicated that the loss of stable channel formation by the D90L mutant was not due to a general folding or membrane insertion defect, but rather caused by a specific change of the constriction zone.

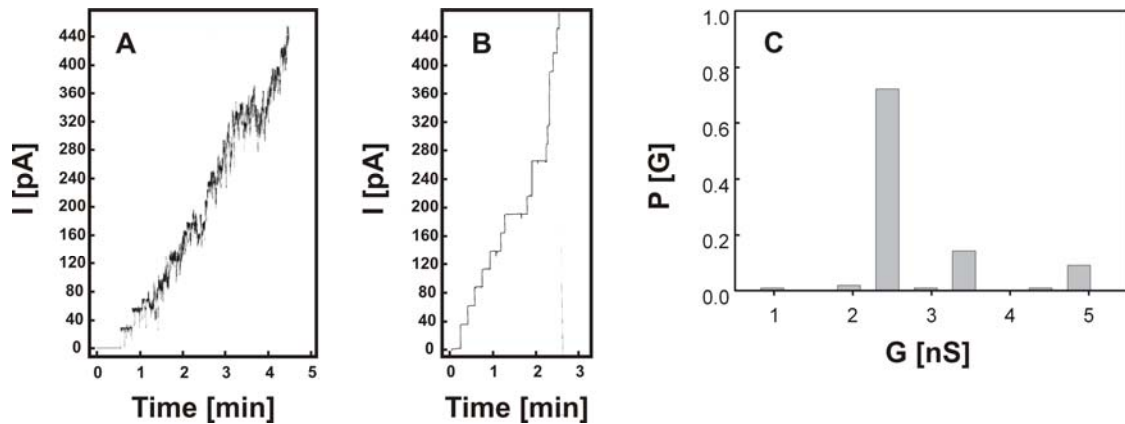


Figure 5. Single channel analysis of MspA D90L and D90L/D91L. (A) Single channel recording of MspA D90L in artificial lipid bilayers. Single-channel recordings of a diphytanoyl phosphatidylcholine membrane were obtained in the presence of diluted protein purified from *M. smegmatis* ML10 ($\Delta mspA$, $\Delta mspC$) (49) expressing MspA D90L from pML170. Protein solutions were added to both sides of the membrane and data were collected from at least four different membranes. Membrane current was measured in an aqueous solution of 1 M KCl with an applied transmembrane potential of -10 mV. (B) Single channel recording of MspA D90L/D91L in artificial lipid bilayers. Conditions and parameters of the recordings were obtained from purified MspA D90L/D91L in the same manner as MspA D90L. (C) Analysis of single channel conductances of purified MspA D90L/D91L. Analysis of the probability P of a conductance step G for single channel events. The average single channel conductance was approximately 2.4 nS. Single channel conductance analysis was not performed for MspA D90L as this protein did not form stable pores.

Glucose permeability through MspA D90L is drastically reduced. To assess whether MspA mutants were permeable to larger, physiologically more relevant substrates, we reconstituted purified MspA proteins into liposomes and tested their permeability towards glucose by liposome swelling experiments. In these experiments,

non-permeable dextran is encapsulated inside liposomes while protein is reconstituted into the liposomal membrane, and the optical density at 400 nm is recorded in an isoosmotic solution of solute. In an isoosmotic solution of glucose, diffusion of glucose into liposomes through porins is followed by an influx of water, which causes liposomes to swell, dilutes dextran, and reduces the optical density. Liposomes reconstituted with purified wt MspA rapidly lost optical density demonstrating that MspA is permeable to glucose (Fig. 6).

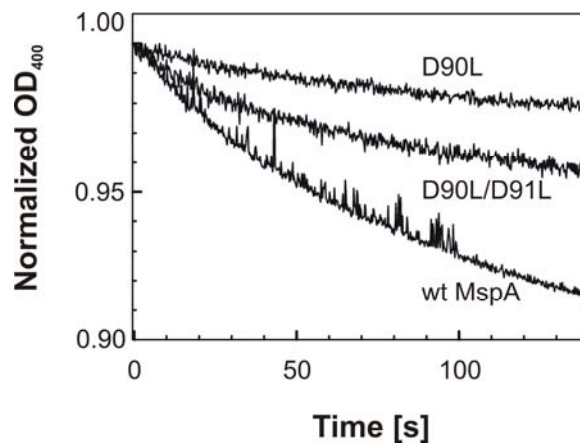


Figure 6. Diffusion of glucose through MspA D90L and D90L/D91L into liposomes. Phosphatidylcholine/dicetyl phosphate liposomes were reconstituted with purified MspA wt, D90L, or D90L/D91L and calibrated in an isoosmotic solution of raffinose. Addition of liposomes to an isoosmotic solution of glucose resulted in glucose diffusion through MspA channels, which was followed by water influx and swelling of the liposomes. Dilution of encapsulated, non-permeable dextran due to swelling was monitored by absorbance at 400 nm.

Conversely, reconstitution of MspA D90L in liposomes reduced optical density much slower indicating that diffusion of glucose through the pore of MspA D90L is not inefficient. Interestingly, liposomes reconstituted with the double mutant MspA D90L/D91L showed an intermediate rate of glucose diffusion. This finding is consistent

with the more hydrophobic constriction zone of the double mutant. These results demonstrate that MspA D90L has very limited permeability to glucose while the MspA D90L/D91L double mutation partially restores this permeability.

MspA D90L is not permeable to *p*-nitrophenylphosphate *in vivo*. To examine the channel activity of the D90L mutant in mycobacteria, a permeability assay was employed based upon the activity of the periplasmic alkaline phosphatase PhoA as recently established (53). For this assay, the *M. smegmatis* mutant strain ML42 (Table 1) was chosen because of two key attributes: (i) it has reduced outer membrane permeability due to deletion of two porin genes ($\Delta mspA$ and $\Delta mspC$) and (ii) it expresses *phoA* from an integrated cassette (*L5 attB::phoA*). The hydrophilic PhoA-substrate *p*-nitrophenylphosphate (*p*NPP) permeates the outer membrane primarily through porins. It is catalytically cleaved in the periplasm by PhoA, resulting in an increased absorption at 405 nm (53). The plasmids pMS2 (no *mspA*), pMN016 (wt *mspA*), and pML170 (*mspA* D90L) were analyzed in *M. smegmatis* ML42 to determine the permeability of MspA D90L to *p*NPP. Selective extraction of MspA proteins by boiling cells in the presence of the detergent OPOE (20) showed that both wt MspA and MspA D90L were expressed at similar levels in *M. smegmatis* ML42, whereas only a very low background of other Msp porins was observed in the strain containing the empty vector (Fig. 4). The phosphatase activity of whole cells of ML42 carrying the empty vector was low (Fig. 7) consistent with the low number of porins in this strain (53). However, expression of *mspA* increased the number of porins and concomitantly the phosphatase activity of ML42 (Fig. 7). Importantly, no increase in phosphatase activity above background was observed for ML42 expressing MspA D90L (Fig. 7). This was not due to differential expression of

phoA as lysates of all three strains did not show significantly different phosphatase activity (Fig. 7). These results demonstrate that MspA D90L is not permeable to the small and hydrophilic compound *pNPP in vivo*. As MspA D90L also did not form stable channels in artificial lipid bilayers (Fig. 5B) or efficiently transport glucose (Fig. 6), it is concluded that the MspA D90L mutant constitutes an impaired channel both *in vitro* as well as *in vivo* and can therefore serve as a tool to distinguish between direct and indirect effects of MspA insertion in the outer membrane of *M. tuberculosis*.

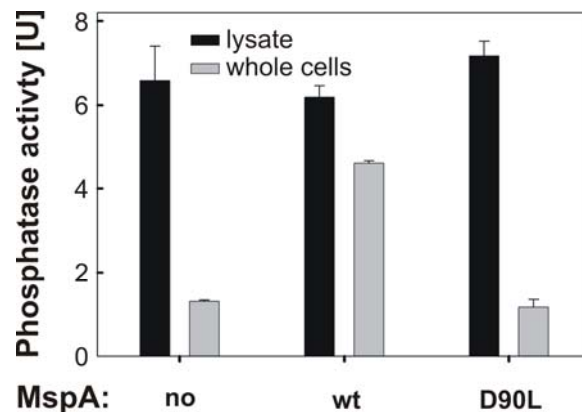


Figure 7. Activity of MspA D90L and D90L/D91L *in vivo*. The phosphatase activity of *M. smegmatis* ML42 ($\Delta mspA$ and $\Delta mspC$, L5 *attB::phoA*) was determined by absorbance at 405 nm after incubation with *para*-nitrophenylphosphate (*pNPP*). Gray and black bars indicate phosphatase activity in whole and lysed cells, respectively. Error bars indicate standard deviations.

Reduced virulence of MspA-expressing *M. tuberculosis* is due to porin function. It is possible that *M. tuberculosis* strains transgenic for *mspA* might be attenuated for virulence because of altered outer membrane properties resulting from heterologous protein insertion. In order to examine whether the channel activity of MspA

caused the decreased virulence of *mspA*-expressing *M. tuberculosis*, infection studies with strains expressing either wt MspA or MspA D90L were undertaken. To rule out differences in virulence due to differential expression in the outer membrane, the surface accessibility of both wt MspA and MspA D90L were determined in the avirulent strain *M. tuberculosis* mc²6230 ($\Delta panCD$, ΔRDI) (Table 1) by a whole cell enzyme-linked immunosorbent assay (ELISA). As a control, we detected surface exposure of a native outer membrane protein of *M. tuberculosis*, OmpA, using an antiserum against OmpA (41). To determine the sensitivity of the assay, the *ompA* expression vector pML589 (Table 1) was transformed into *M. tuberculosis* mc²6230 and detection of overexpressed levels was compared to endogenous levels (Fig. 8). These results show that our assay can detect and discriminate between protein levels on the surface of *M. tuberculosis*. The *mspA* expression vector pMN013 and the *mspA* D90L expression vector pML170 were transformed into *M. tuberculosis* mc²6230 and the surface accessibility of MspA was determined. Both forms of MspA were equally detectable by an antiserum against MspA (34) on the surface of *M. tuberculosis* (Fig. 8), in agreement with similar levels of extractable MspA from these two plasmids (Fig. 1).

M. tuberculosis strains carrying plasmids with either (i) promoterless-*mspA* (pMN006), (ii) wt *mspA* (pMN013), or (iii) *mspA* D90L (pML170) were infected in mice by aerosol with a high inoculum. In order to specifically determine the growth of plasmid-containing *M. tuberculosis* strains, lung homogenates were plated on Middlebrook 7H10 agar containing hygromycin. Figure 9 shows that replication of *M. tuberculosis* encoding the wt *mspA* gene was drastically impaired consistent with our previous results. By contrast, *M. tuberculosis* expressing the transport-impaired MspA

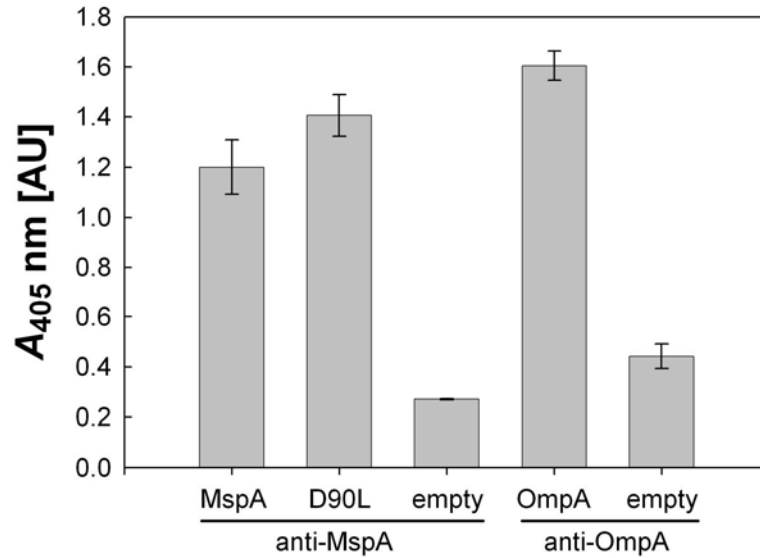


Figure 8. Surface accessibility of MspA, MspA D90L, and OmpA in *M. tuberculosis* by whole cell ELISA. The expression vectors pMN013, pML170, and pML589 were transformed into avirulent *M. tuberculosis* mc²6230 ($\Delta panCD$, $\Delta RD1$) to express MspA, MspA D90L, and OmpA, respectively. Surface exposed proteins were bound with either an MspA antiserum or an OmpA antiserum. Binding of secondary alkaline phosphatase conjugate antibody was followed by absorbance readings at 405 nm to measure phosphatase activity in the presence of *p*NPP. Absorption at 405 nm is proportional to protein detection levels. Detection on *M. tuberculosis* mc²6230 carrying the empty vector pMS2 by the MspA antiserum provided experimental background for MspA detection, while detection by the OmpA antiserum on the same strain determined endogenous OmpA expression levels.

D90L mutant grew at an intermediate rate in mouse lungs. However, the three groups of mice received different inocula (promoterless-*mspA*: 104; wt *mspA*: 1,155; *mspA* D90L: 2,381 cfu), making statistical evaluation difficult. To compare the net growth of each strain, cfu counts in the lungs of the three groups of infected mice were normalized for inoculum size (Figure 9). It is evident that *M. tuberculosis* expressing MspA D90L replicated 10-100 fold more efficiently than the strain containing wt *mspA*.

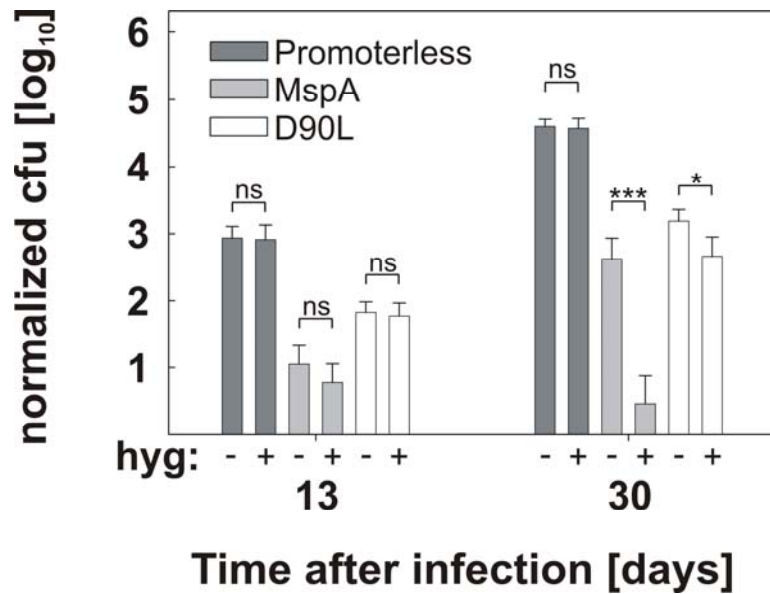


Figure 9. Virulence of *M. tuberculosis* expressing functional or transport-impaired MspA channels. C57BL/6 mice were infected by the aerosol route with an intended inoculum of 1,000 cfu of *M. tuberculosis* carrying either pMN006 (promoterless-*mspA*), pMN013 (wt *mspA*), or pML170 (*mspA* D90L). Replication in the lung was determined on days 13 and 30 after infection by plating lung homogenates on selective solid media with or without hygromycin. The net growth for the indicated strains was calculated by dividing the cfu counts on days 13 and 30 by the cfu counts determined on day 1 after infection.

However, the strain carrying the promoterless-*mspA* construct replicated 10-100 fold better than the strain expressing MspA D90L. While *M. tuberculosis* carrying the *mspA* D90L plasmid showed an intermediate level of virulence attenuation, this plasmid was retained during infection, in contrast to the wt *mspA* expression vector. These results indicate that both insertion of the MspA pore into the outer membrane of *M. tuberculosis* via a concomitant indirect change of the membrane permeability, and the channel activity of MspA contribute to the marked attenuation of *mspA* expressing *M. tuberculosis*.

DISCUSSION

Increased outer membrane permeability reduces the virulence of

M. tuberculosis. In this study, we examined whether survival of *M. tuberculosis* in mice would be enhanced by increased nutrient uptake or compromised due to elevated toxic solute exposure when the porin MspA (34) of *M. smegmatis* was used as a tool to permeabilize the outer membrane towards hydrophilic solutes. Both outcomes were previously observed for the nearly genetically identical *Mycobacterium bovis* BCG *in vitro* (30). However, it was not clear which of those counteracting effects would dominate in an *in vivo* model of tuberculosis. The results presented here clearly show that functional MspA pores in the outer membrane drastically reduced the virulence of *M. tuberculosis*.

While MspA promotes the growth of slowly growing mycobacteria in culture (30, 39), *M. tuberculosis* strongly selected against the *mspA* expression cassette during experimental murine infections as no replicative plasmid was detected in cells recovered from mouse lungs after 61 days post-infection. Despite this strong negative selection, a dramatic attenuation of *M. tuberculosis* virulence was still observed. Integration into the chromosome stabilized the *mspA* cassette at the expense of expression levels. Importantly, barely detectable expression of *mspA* from the chromosome still reduced virulence, demonstrating that even minute amounts of MspA pores still generated a significant virulence defect. These results show that MspA pores in the outer membrane are absolutely detrimental to the virulence of *M. tuberculosis*.

These results are in apparent contrast to Gram-negative bacterial pathogens which typically show reduced virulence of mutants having lost porins (9, 31, 37) and a better

survival of bacteria in infection models after increased expression of porins (27). For example, loss of porins compromised adherence to host cells (17, 51), epithelial cell invasion (4), antigenic variation (1, 12), phagosome maturation (32) and, in general, reduced nutrient uptake (13, 54). While it is not known whether MspA plays a role in adherence or invasion, it was shown that Msp porins do not alter phagocytic uptake into macrophages (14). Further, neither *mspA* expression in *M. tuberculosis* (39) nor deletion of *msp* genes in *M. smegmatis* (14) caused aberrant trafficking compared to wild-type organisms. It is also not expected that antigenic variation would contribute greatly to *M. tuberculosis* virulence as it is an intracellular pathogen not primarily controlled by antibody-dependent responses (36). Porins enhance the virulence of intracellular pathogens such as *Shigella flexneri* (5) which escapes to the nutrient-rich, low toxin environment of the host cytosol. Porins also appear to be beneficial for the intracellular survival of *Legionella pneumophila* (27) which resides in phagosomes similar to *M. tuberculosis*. The opposing role of porins for these two phagosome-residing pathogens might be due to different phagosomal compositions and the very small single channel conductance of the Legionella porin compared to MspA (100 pS versus 4.8 nS) (16, 34).

It has been known for a long time that loss of porins often results in drug resistant strains of Gram-negative bacteria (35). Similar observations were also made for mycobacteria. Deletion of Msp pores from *M. smegmatis* enhanced antibiotic resistance (11, 50). Conversely, expression of *mspA* increased the drug susceptibility of *M. tuberculosis* (30). The results of this study indicate that *M. tuberculosis* is particularly vulnerable to a porin-mediated increased susceptibility to toxic compounds *in vivo*, in

contrast to other Gram-negative bacterial pathogens, which appear to benefit more from efficient nutrient uptake and/or other functions of porins.

Both channel activity and nonspecific effects account for the virulence attenuation of recombinant *M. tuberculosis*. An important control in the mouse

experiments was the construction of the transport-impaired MspA D90L mutant.

Aspartate 90 lies within the constriction zone in the interior of the barrel (15) and is likely to alter channel properties of MspA. The observation that a second mutation at position 91 in the constriction zone (D91L) restored channel activity demonstrated that the D90L mutation indeed directly impaired the channel function of MspA rather than affecting the localization or incorporation of MspA into the outer membrane. This is most likely due to the close proximity of the hydrophobic leucine at position 90 and the anionic aspartate at position 91 which may destabilize the constriction zone, as indicated by lipid bilayer experiments. The MspA D90L mutant reveals a novel mechanism of how to impair translocation of solutes through a narrow channel constriction zone.

The transport-impaired MspA D90L mutant partially reduced the virulence of *M. tuberculosis* in mice. This indicates that indirect changes in the outer membrane by insertion of MspA, such as disruption of local lipid packing, permeabilize the outer membrane towards toxic hydrophobic solutes, as suggested previously (50). Additionally, putative unknown effects of expression of MspA on other proteins in the outer membrane may also partially explain the attenuated phenotype of *mspA*-expressing *M. tuberculosis*. Purdy *et. al.* recently identified a ubiquitin-derived peptide present in lysosomal extracts that efficiently kills *M. tuberculosis* (40). Expression of MspA increased susceptibility of both fast and slow growing mycobacteria to this peptide. However, this susceptibility did

not require the MspA channel as the transport-impaired D90L mutant caused a similar susceptibility as wt MspA (39). These results demonstrate that MspA has an indirect effect on susceptibility to ubiquitin-derived peptide *in vitro* and in macrophages, possibly by creating local perturbations in the outer membrane as suggested previously (50). Our *in vivo* experiments corroborate these data in that the indirect effect of MspA on the outer membrane and the ubiquitin peptide-mediated killing of *M. tuberculosis* as observed *in vitro* and in macrophages partially contribute to killing of *M. tuberculosis* in mice.

The channel function of MspA severely reduced the survival of *M. tuberculosis* in mice. Of the many antimicrobial compounds present in macrophages, nitric oxide (NO) was shown to be a potent molecule in killing mycobacteria (29). Indeed, loss of Msp porins from *M. smegmatis* increased survival both in macrophages and in the presence of NO *in vitro* (14). This was not due to an MspA-mediated reduction in the release of NO by macrophages as both wt *M. smegmatis* and a porin mutant elicited similar levels of NO production. Rather, these results indicated that MspA may facilitate diffusion of NO into *M. smegmatis* cells, a surprising finding considering that NO is soluble in both water and lipids (28) and hence, is generally thought to be able to diffuse through lipid membranes without the help of a protein (25). However, it may be that diffusion of NO across the notoriously impermeable mycobacterial outer membrane is much slower than across lipids bilayers containing C16 to C18 fatty acids. Molecular dynamics studies indeed indicated that increasing hydrocarbon length in lipid membranes creates larger and wider energy barriers to NO, implying reduced permeability (52). Considering that mycobacterial outer membranes contain mycolic acids, the longest known fatty acids (3), it is tempting to speculate that mycobacterial outer membranes constitute a much more

efficient permeability barrier to NO than other membranes. Therefore, a water-filled channel such as MspA might enhance NO diffusion into mycobacteria. Consistent with this hypothesis is the observation that other channel proteins such as aquaporins increase NO permeability in both liposomes and Chinese hamster ovary cells (22). Diffusion of very small toxic compounds may also account for the partial attenuation of *M. tuberculosis* expressing MspA D90L. The permeability of this MspA mutant was severely reduced, but residual glucose transport was evident along with permeability to ions, albeit through an unstable pore. It is possible that while MspA D90L did not create a diffusion pathway for larger toxic compounds, very small molecules such as NO may have some residual permeability through the MspA pore and, therefore, could also attenuate virulence in a direct manner. Similar arguments can be made for small and hydrophilic toxic solutes other than NO that might utilize the MspA channel as an entry mechanism into *M. tuberculosis* cells. Further experiments are required to identify solutes transported through the MspA channel that contribute to killing of *M. tuberculosis* in mice.

In apparent contrast to our results and those of others (40) with *M. tuberculosis*, expression of MspA in *M. bovis* BCG increased survival in macrophages (45). This may possibly be due to differences in the composition of the phagosome elicited by these two organisms and is not due to differences in MspA expression levels, which are similar in both organisms (not shown).

Conclusions. Our data suggest that *M. tuberculosis* has adapted to growth in the harsh environment of macrophage phagosomes by maintaining low outer membrane permeability to reduce the influx of toxic solutes at the expense of nutrient uptake. These

adjustments may have ultimately resulted in the slow growth of *M. tuberculosis* as suggested previously (49) and may play a crucial role in the survival of *M. tuberculosis* in the human host.

ACKNOWLEDGEMENTS

We thank Dr. Claudia Mailaender for help with the initial experiments, Stefanie Pfau and Silvia Maass for expert technical assistance, Drs. Sahar Aly and Christian Heinz for help with the data analysis and the characterization of the MspA D90L mutant, respectively. The strain *M. tuberculosis* mc²6230 was a kind gift from Dr. Bill Jacobs. JH was supported by a fellowship from the NIH training grant “Basic Mechanisms of Lung Diseases” (T32 HL07553). This work was supported by grants of the Deutsche Forschungsgemeinschaft to SE (EXC 306 Inflammation at Interfaces) and MN (NI412), by grant 0315220D of the German Ministry of Education and Research to SE, and by grant AI063432 of the National Institutes of Health to MN.

REFERENCES

1. **Alcala, B., C. Salcedo, L. Arreaza, R. Abad, R. Enriquez, L. De La Fuente, M. J. Uria, and J. A. Vazquez.** 2004. Antigenic and/or phase variation of PorA protein in non-subtypable *Neisseria meningitidis* strains isolated in Spain. *J Med Microbiol* **53**:515-8.
2. **Barry, C. E.** 2001. Interpreting cell wall 'virulence factors' of *Mycobacterium tuberculosis*. *Trends Microbiol* **9**:237-41.
3. **Barry, C. E., 3rd, R. E. Lee, K. Mdluli, A. E. Sampson, B. G. Schroeder, R. A. Slayden, and Y. Yuan.** 1998. Mycolic acids: structure, biosynthesis and physiological functions. *Prog. Lipid Res.* **37**:143-79.
4. **Bauer, F. J., T. Rudel, M. Stein, and T. F. Meyer.** 1999. Mutagenesis of the *Neisseria gonorrhoeae* porin reduces invasion in epithelial cells and enhances phagocyte responsiveness. *Mol Microbiol* **31**:903-13.
5. **Bernardini, M. L., M. G. Sanna, A. Fontaine, and P. J. Sansonetti.** 1993. OmpC is involved in invasion of epithelial cells by *Shigella flexneri*. *Infect Immun* **61**:3625-35.
6. **Bi, W., and P. J. Stambrook.** 1997. CCR: a rapid and simple approach for mutation detection. *Nucleic Acids Res* **25**:2949-51.
7. **Buchmeier, N., A. Blanc-Potard, S. Ehrt, D. Piddington, L. Riley, and E. A. Groisman.** 2000. A parallel intraphagosomal survival strategy shared by *Mycobacterium tuberculosis* and *Salmonella enterica*. *Mol Microbiol* **35**:1375-82.
8. **Camacho, L. R., P. Constant, C. Raynaud, M. A. Laneelle, J. A. Triccas, B. Gicquel, M. Daffé, and C. Guilhot.** 2001. Analysis of the phthiocerol dimycocerosate locus of *Mycobacterium tuberculosis*. Evidence that this lipid is involved in the cell wall permeability barrier. *J. Biol. Chem.* **276**:19845-54.
9. **Chatfield, S. N., C. J. Dorman, C. Hayward, and G. Dougan.** 1991. Role of ompR-dependent genes in *Salmonella typhimurium* virulence: mutants deficient in both ompC and ompF are attenuated in vivo. *Infect. Immun.* **59**:449-52.
10. **Danilchanka, O., C. Mailaender, and M. Niederweis.** 2008. Identification of a novel multidrug efflux pump of *Mycobacterium tuberculosis*. *Antimicrob Agents Chemother* **52**:2503-11.
11. **Danilchanka, O., M. Pavlenok, and M. Niederweis.** 2008. Role of porins for uptake of antibiotics by *Mycobacterium smegmatis*. *Antimicrob Agents Chemother* **52**:3127-34.
12. **de Filippis, I., C. F. de Andrade, L. Silva, D. R. Prevots, and A. C. Vicente.** 2007. PorA variable antigenic regions VR1, VR2, and VR3 of *Neisseria meningitidis* serogroups B and C isolated in Brazil from 1999 to 2004. *Infect Immun* **75**:3683-5.
13. **Easton, D. M., E. Maier, R. Benz, A. R. Foxwell, A. W. Cripps, and J. M. Kyd.** 2008. *Moraxella catarrhalis* M35 is a general porin that is important for growth under nutrient-limiting conditions and in the nasopharynxes of mice. *J Bacteriol* **190**:7994-8002.
14. **Fabrino, D. L., C. K. Bleck, E. Anes, A. Hasilik, R. C. Melo, M. Niederweis, G. Griffiths, and M. G. Gutierrez.** 2009. Porins facilitate nitric oxide-mediated killing of mycobacteria. *Microbes Infect* **11**:868-75.
15. **Faller, M., M. Niederweis, and G. E. Schulz.** 2004. The structure of a mycobacterial outer-membrane channel. *Science* **303**:1189-92.
16. **Gabay, J. E., M. Blake, W. D. Niles, and M. A. Horwitz.** 1985. Purification of *Legionella pneumophila* major outer membrane protein and demonstration that it is a porin. *J. Bacteriol.* **162**:85-91.

17. **Hara-Kaonga, B., and T. G. Pistole.** 2004. OmpD but not OmpC is involved in adherence of *Salmonella enterica* serovar Typhimurium to human cells. *Can J Microbiol* **50**:719-27.
18. **Harder, K. J., H. Nikaido, and M. Matsuhashi.** 1981. Mutants of *Escherichia coli* that are resistant to certain beta-lactam compounds lack the OmpF porin. *Antimicrob. Agents Chemother.* **20**:549-52.
19. **Harries, A. D., and C. Dye.** 2006. Tuberculosis. *Ann. Trop. Med. Parasitol.* **100**:415-31.
20. **Heinz, C., and M. Niederweis.** 2000. Selective extraction and purification of a mycobacterial outer membrane protein. *Anal. Biochem.* **285**:113-120.
21. **Heinz, C., E. Roth, and M. Niederweis.** 2003. Purification of porins from *Mycobacterium smegmatis*. *Methods Mol Biol* **228**:139-50.
22. **Herrera, M., N. J. Hong, and J. L. Garvin.** 2006. Aquaporin-1 transports NO across cell membranes. *Hypertension* **48**:157-64.
23. **Hoffmann, C., A. Leis, M. Niederweis, J. M. Plitzko, and H. Engelhardt.** 2008. Disclosure of the mycobacterial outer membrane: Cryo-electron tomography and vitreous sections reveal the lipid bilayer structure. *Proc. Natl. Acad. Sci. U S A* **105**:3963-3967.
24. **Kaps, I., S. Ehrt, S. Seeber, D. Schnappinger, C. Martin, L. W. Riley, and M. Niederweis.** 2001. Energy transfer between fluorescent proteins using a co-expression system in *Mycobacterium smegmatis*. *Gene* **278**:115-24.
25. **Kone, B. C.** 2006. NO break-ins at water gate. *Hypertension* **48**:29-30.
26. **Kriakov, J., S. Lee, and W. R. Jacobs, Jr.** 2003. Identification of a regulated alkaline phosphatase, a cell surface-associated lipoprotein, in *Mycobacterium smegmatis*. *J Bacteriol* **185**:4983-91.
27. **Krinos, C., A. S. High, and F. G. Rodgers.** 1999. Role of the 25 kDa major outer membrane protein of *Legionella pneumophila* in attachment to U-937 cells and its potential as a virulence factor for chick embryos. *J Appl Microbiol* **86**:237-44.
28. **MacMicking, J., Q. W. Xie, and C. Nathan.** 1997. Nitric oxide and macrophage function. *Annu Rev Immunol* **15**:323-50.
29. **MacMicking, J. D., R. J. North, R. LaCourse, J. S. Mudgett, S. K. Shah, and C. F. Nathan.** 1997. Identification of nitric oxide synthase as a protective locus against tuberculosis. *Proc Natl Acad Sci USA* **94**:5243-8.
30. **Mailaender, C., N. Reiling, H. Engelhardt, S. Bossmann, S. Ehlers, and M. Niederweis.** 2004. The MspA porin promotes growth and increases antibiotic susceptibility of both *Mycobacterium bovis* BCG and *Mycobacterium tuberculosis*. *Microbiology* **150**:853-864.
31. **Mildiner-Earley, S., and V. L. Miller.** 2006. Characterization of a novel porin involved in systemic *Yersinia enterocolitica* infection. *Infect Immun* **74**:4361-5.
32. **Mosleh, I. M., L. A. Huber, P. Steinlein, C. Pasquali, D. Gunther, and T. F. Meyer.** 1998. *Neisseria gonorrhoeae* porin modulates phagosome maturation. *J Biol Chem* **273**:35332-8.
33. **Niederweis, M.** 2003. Mycobacterial porins - new channel proteins in unique outer membranes. *Mol. Microbiol.* **49**:1167-77.
34. **Niederweis, M., S. Ehrt, C. Heinz, U. Klöcker, S. Karosi, K. M. Swiderek, L. W. Riley, and R. Benz.** 1999. Cloning of the *mspA* gene encoding a porin from *Mycobacterium smegmatis*. *Mol. Microbiol.* **33**:933-945.
35. **Nikaido, H.** 2003. Molecular basis of bacterial outer membrane permeability revisited. *Microbiol. Mol. Biol. Rev.* **67**:593-656.
36. **North, R. J., and Y. J. Jung.** 2004. Immunity to tuberculosis. *Annu Rev Immunol* **22**:599-623.
37. **Osorio, C. G., H. Martinez-Wilson, and A. Camilli.** 2004. The *ompU* paralogue *vca1008* is required for virulence of *Vibrio cholerae*. *J Bacteriol* **186**:5167-71.

38. **Pieters, J.** 2008. *Mycobacterium tuberculosis* and the macrophage: maintaining a balance. *Cell Host Microbe* **3**:399-407.
39. **Purdy, G. E., M. Niederweis, and D. G. Russell.** 2009. Decreased outer membrane permeability protects mycobacteria from killing by ubiquitin-derived peptides. *Mol Microbiol* **73**:844-57.
40. **Purdy, G. E., and D. G. Russell.** 2007. Lysosomal ubiquitin and the demise of *Mycobacterium tuberculosis*. *Cell Microbiol* **9**:2768-74.
41. **Raynaud, C., K. G. Papavinasundaram, R. A. Speight, B. Springer, P. Sander, E. C. Böttger, M. J. Colston, and P. Draper.** 2002. The functions of OmpATb, a pore-forming protein of *Mycobacterium tuberculosis*. *Mol. Microbiol.* **46**:191-201.
42. **Rousseau, C., N. Winter, E. Pivert, Y. Bordat, O. Neyrolles, P. Ave, M. Huerre, B. Gicquel, and M. Jackson.** 2004. Production of phthiocerol dimycocerosates protects *Mycobacterium tuberculosis* from the cidal activity of reactive nitrogen intermediates produced by macrophages and modulates the early immune response to infection. *Cell Microbiol* **6**:277-87.
43. **Sambandamurthy, V. K., S. C. Derrick, T. Hsu, B. Chen, M. H. Larsen, K. V. Jalapathy, M. Chen, J. Kim, S. A. Porcelli, J. Chan, S. L. Morris, and W. R. Jacobs, Jr.** 2006. *Mycobacterium tuberculosis* delta*RD1* delta*panCD*: a safe and limited replicating mutant strain that protects immunocompetent and immunocompromised mice against experimental tuberculosis. *Vaccine* **24**:6309-20.
44. **Sambrook, J., E. F. Fritsch, and T. Maniatis.** 1989. Molecular cloning: a laboratory manual, 2nd ed. Cold Spring Harbor Laboratory Press, Cold Spring Harbor, N. Y.
45. **Sharbati-Tehrani, S., B. Meister, B. Appel, and A. Lewin.** 2004. The porin MspA from *Mycobacterium smegmatis* improves growth of *Mycobacterium bovis* BCG. *Int J Med Microbiol* **294**:235-45.
46. **Simonet, V. C., A. Basle, K. E. Klose, and A. H. Delcour.** 2003. The *Vibrio cholerae* porins OmpU and OmpT have distinct channel properties. *J Biol Chem* **278**:17539-45.
47. **Siroy, A., C. Mailaender, D. Harder, S. Koerber, F. Wolschendorf, O. Danilchanka, Y. Wang, C. Heinz, and M. Niederweis.** 2008. Rv1698 of *Mycobacterium tuberculosis* represents a new class of channel-forming outer membrane proteins. *J. Biol. Chem.* **283**:17827-37.
48. **Stahl, C., S. Kubetzko, I. Kaps, S. Seeber, H. Engelhardt, and M. Niederweis.** 2001. MspA provides the main hydrophilic pathway through the cell wall of *Mycobacterium smegmatis*. *Mol. Microbiol.* **40**:451-464 (Authors' correction appeared in *Mol. Microbiol.* **57**, 1509).
49. **Stephan, J., J. Bender, F. Wolschendorf, C. Hoffmann, E. Roth, C. Mailänder, H. Engelhardt, and M. Niederweis.** 2005. The growth rate of *Mycobacterium smegmatis* depends on sufficient porin-mediated influx of nutrients. *Mol. Microbiol.* **58**:714-730.
50. **Stephan, J., C. Mailaender, G. Etienne, M. Daffe, and M. Niederweis.** 2004. Multidrug resistance of a porin deletion mutant of *Mycobacterium smegmatis*. *Antimicrob. Agents Chemother.* **48**:4163-70.
51. **Subramanian, K., R. B. Shankar, S. Meenakshisundaram, B. S. Lakshmi, P. H. Williams, and A. Balakrishnan.** 2008. LamB-mediated adherence of enteropathogenic *Escherichia coli* to HEp-2 cells. *J Appl Microbiol* **105**:715-22.
52. **Sugii, T., S. Takagi, and Y. Matsumoto.** 2005. A molecular-dynamics study of lipid bilayers: effects of the hydrocarbon chain length on permeability. *J Chem Phys* **123**:184714.

53. **Wolschendorf, F., M. Mahfoud, and M. Niederweis.** 2007. Porins are required for uptake of phosphates by *Mycobacterium smegmatis*. J Bacteriol **189**:2435-2442.
54. **Wylie, J. L., and E. A. Worobec.** 1995. The OprB porin plays a central role in carbohydrate uptake in *Pseudomonas aeruginosa*. J. Bacteriol. **177**:3021-6.
55. **Zuber, B., M. Chami, C. Houssin, J. Dubochet, G. Griffiths, and M. Daffe.** 2008. Direct visualization of the outer membrane of native mycobacteria and corynebacteria. J Bacteriol **190**:5672-5680.

TAKING PHAGE INTEGRATION TO THE NEXT LEVEL AS A GENETIC TOOL
FOR MYCOBACTERIA

by

JASON HUFF AND MICHAEL NIEDERWEIS

In preparation for *Gene*

Format adapted for dissertation

ABSTRACT

Genes must be stably integrated into bacterial chromosomes for complementation of gene deletion mutants in animal infection experiments or to express antigens in vaccine strains. However, it is difficult to create multiple, stable, unmarked chromosomal integrations in mycobacteria with currently available vectors. Here, we have constructed a novel integration vector for mycobacteria that enables expression of genes from a cassette protected by bi-directional transcriptional terminators to prevent transcriptional interference and/or polar effects. Removal of the integrase gene by a site-specific recombinase, easily identifiable by loss of a backbone reporter gene, stabilizes the integration cassette and makes this vector ideally suitable for virulence experiments.

This integration vector can be easily adapted to different mycobacteriophage integration sites due to its modular design. This feature was exploited to integrate a *gfp* expression cassette at three different locations in the chromosome of *Mycobacterium smegmatis* and *Mycobacterium tuberculosis*. Identical *gfp* expression levels were obtained from the *attB* sites of the mycobacteriophages L5, Giles and Ms6, indicating that none of these sites are compromised for gene expression. Reduced expression levels from all integrated constructs compared to *gfp* on an episomal vector were consistent with the difference in copy numbers. Further, we generated strains of *M. smegmatis* and *M. tuberculosis* with multiple integrations of a protected *gfp* expression cassette. Gfp fluorescence increased concomitantly with the chromosomal copy number demonstrating that these vectors can be used to generate stronger phenotypes by increased gene expression levels and/or to analyze several genes simultaneously *in vivo*.

INTRODUCTION

Genetic constructs can be integrated into mycobacterial chromosomes using plasmids carrying a mycobacteriophage integrase gene (*int*) and an appropriate phage attachment site (*attP*) (8, 12, 14, 18, 20). Commonly used integration vectors based upon mycobacteriophage L5, henceforth referred to as L5, contain the L5 *int* gene and the L5 *attP* sequence, which is homologous to the bacterial attachment site *attB* residing within the *glyV* tRNA gene (12) (Fig. 1). The phage integrase along with the mycobacterial integration host factor mIHF (15) catalyze site-specific recombination resulting in the integration of the plasmid at the *attB* site. Integration vectors are genetic tools required to maintain stable gene expression during animal infection studies. However, several caveats exist to generating stable, high-level integrated expression cassettes. For instance, the excisionase activity of L5 integrase destabilizes the integrated plasmid (25). Additionally, expression problems have been reported for genes integrated at the L5 *attB* site, often with disproportionately lower expression in comparison to the copy number of pAL5000-based episomal plasmids ((28) and Mailaender and Niederweis, unpublished results). Further, the number of genes that can be expressed from a single integration vector is limited (22).

Several approaches have been developed to circumvent these obstacles. For example, co-electroporation of an *attP*-containing integration vector and a nonreplicating *int*-containing vector provides integrase activity *in trans* which is then subsequently lost, thus stabilizing the integrated vector (25). Alternatively, the *int* gene can be removed from the chromosome via subsequent expression of site-specific recombinases such as

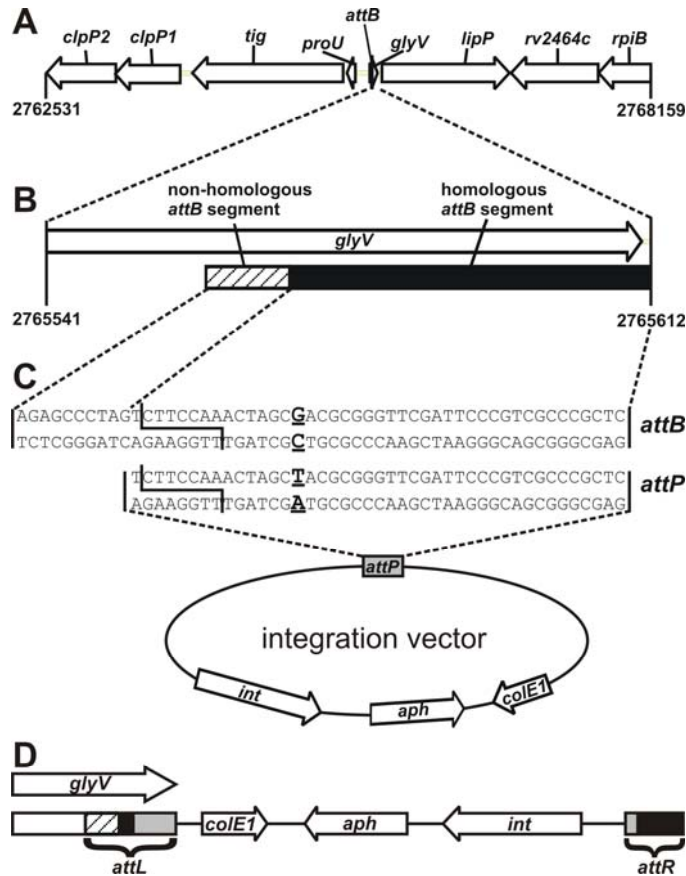


Figure 1. Genomic organization of the mycobacteriophage L5 bacterial attachment site and crossover with the phage attachment site. A) A 5.6 kbp fragment of the *M. tuberculosis* genome encompassing the mycobacteriophage L5 attachment site *attB*. The *attB* site overlaps the *glyV* tRNA gene and is composed of a nearly identical sequence to the phage attachment site *attP* as well as an essential but non-homologous 10 bp upstream sequence. Numbers flanking the genomic map correspond to coordinates in the *M. tuberculosis* H37Rv genome as noted in the Institute of Pasteur's Tuberculist website <http://genolist.pasteur.fr/TubercuList/>. Annotations of surrounding genes are listed above. B) Position of overlap between *attB* and *glyV*. The zoomed-in view of the 72 bp fragment encompassing *glyV* and *attB* shows that 52 of the 53 bp in *attB* overlap with *glyV* between coordinates 2765560-2765611. The non-homologous region of *attB* refers to an essential sequence of *attB* that is not present in the core region of mycobacteriophage L5 *attP*. C) Sequence and position of strand exchange. The DNA sequence of the *attB* site is overlaid with the *attP* sequence, which is cloned into a generic integration vector. Positions of strand exchange between the bacterial chromosome and the integrating plasmid as determined by (17) are noted by the jagged lines in the sequences. The base pairs in bold and underlined are the only mismatching base pairs between *attB* of *M. tuberculosis* and *attP*. Reconstitution of the *glyV* gene after integration in *M. tuberculosis* therefore contains a single point mutation. *int*, L5 integrase gene; *aph*, kanamycin resistance gene; *colE1*, *E. coli* origin of replication. D) Chromosomal arrangement of

genes resulting from a generic plasmid integration. Site-specific recombination of *attB* (hatched bar, non-homologous region; black bar, homologous region) and *attP* (grey bar) creates the flanking *attL* and *attR* sites. The color scheme shows the hybrid portions of *attL* and *attR* originating from *attB* and *attP* (note: figure is not to scale). The *glyV* gene is reconstituted at the *attL* site.

the bacteriophage P1 Cre recombinase (24) or the *Saccharomyces cerevisiae* Flp recombinase (27). The presence of an *attB* site on an integration vector reintroduces a new bacterial attachment site and enables for serial integrations (22). Another option is to transform separate plasmids containing the integration machinery from different mycobacteriophages, which allows genes to be integrated at different sites within the same bacterial chromosome (8). To date, it has not been determined whether integration of a plasmid at other locations in the chromosome leads to higher expression levels in mycobacteria compared to the L5 *attB* site.

The ability to create multiple, stable, unmarked integrations to express several genes simultaneously or to simply increase overall expression by increasing their copy number would be advantageous. However, no tools for genetic manipulation of mycobacteria exist that satisfy all these requirements. In this study, a new integrative plasmid was designed with a multiple cloning site flanked by bi-directional intrinsic transcriptional terminators. A backbone excisable by Cre recombinase enables the removal of the L5 *int* gene, resistance cassette, and remaining plasmid backbone. This can be monitored by the *xylE* reporter gene for strain identification. As all genetic components are flanked by single restriction sites, this plasmid can be easily adapted to alternative integration machineries from other mycobacteriophages. A series of plasmids for integration at the mycobacteriophages L5, Giles, and Ms6 attachment sites was

constructed and expression levels were compared in both fast and slow growing mycobacteria. The relationship between chromosomal copy number and expression levels was examined by performing multiple integrations at different chromosomal sites of the same strain. These plasmids will aid in the examination of mycobacterial genes in mouse infection experiments and/or in vaccine strain development where stable gene expression is required.

MATERIALS AND METHODS

Chemicals, enzymes and DNA. Hygromycin B was purchased from Calbiochem. All other chemicals were purchased from Merck, Roche or Sigma at the highest purity available. Enzymes for DNA restriction and modification were purchased from New England Biolabs. Isolation and modification of DNA was performed as described (3). Oligonucleotides were obtained from Integrated DNA Technologies.

Bacterial strains and growth conditions. *Escherichia coli* DH5 α was used for cloning experiments and was routinely grown in Luria-Bertani broth at 37°C. *M. smegmatis* strains were grown at 37°C in Middlebrook 7H9 medium (Difco) supplemented with 0.2% glycerol and 0.025% tyloxapol or on Middlebrook 7H10 agar (Difco) supplemented with 0.2% glycerol. *M. tuberculosis* mc²6230 is an unmarked derivative of *M. tuberculosis* mc²6030 (21) and was grown at 37°C in Middlebrook 7H9 liquid medium supplemented with 0.2% glycerol, 10% oleic acid-albumin-dextrose-catalase enrichment (OADC, Remel), 0.025% tyloxapol, 0.2% casamino acids, and 24 μ g/mL pantothenate or on Middlebrook 7H10 agar supplemented with 0.2% glycerol, 10% OADC, 0.2% casamino acids, and 24 μ g/mL pantothenate. Antibiotics were used when required at the following concentrations: hygromycin (200 μ g/ml for *E. coli*; 50 μ g/ml for mycobacteria) and kanamycin (50 μ g/ml for *E. coli*; 30 μ g/ml for mycobacteria).

Synthesis of *xylE_m*, attachment sites, polylinker, *loxP* sites, and bi-directional terminators. The 1,820 bp fragment between *SspI* and *XmaI* of pML1342 was synthesized by Geneart (Burlingame, CA) and cloned into the plasmid pML1320. The sequence of the *xylE* gene from *Pseudomonas putida* (NCBI accession: V01161.1) was

codon-optimized for efficient expression in *Mycobacterium tuberculosis* H37Rv. The *xyIE* gene sequence (*xyIE_m*) was optimized using a preferred codon usage chart (<http://www.kazusa.or.jp.codon/>) as previously described (24). The codon usage was further optimized by removing all rare codons that occur in the *M. tuberculosis* genome with a frequency of less than 10 per 1,000 codons. The sequence of *xyIE_m* was submitted to Genbank (accession #: GU128960). The *xyIE_m* gene sequence was fused to the *p_{wmyc}* promoter (10) and a transcription terminator based on the intrinsic terminator *trpt* downstream of the *E. coli* tryptophan operon (31) known as *tt_{trpA}*+ (AGCCCGCCTAATGGCGGGCTTTTTTTT) was added 15 bp downstream of the *xyIE_m* stop codon. Two *loxP* sites (ATAACTTCGTATAATGTATGCTATACGAAGTTAT) were positioned to flank the L5 *attP* and *attB* attachment sites (12), two bi-directional terminator sequences, and a multiple cloning site polylinker. The synthetic bi-directional terminators *tt_{sbiA}* and *tt_{sbiB}* were designed for efficient transcription termination by inclusion of ten leading adenosine residues, seven G/C base pairs in the hairpin stem, 4 unpaired bases in the hairpin loop, and ten thymidine residues downstream of the hairpin (6).

Construction of plasmids. The *E. coli* origin of replication was amplified from pML113 (30) by PCR using the primers 99 and 967 (Table S1) and digested with *ClaI* and *SspI*. The resulting 954 bp fragment was cloned into the 2,541 bp fragment of *ClaI/SspI* digested pML113 in order to remove the *bla* gene and to correctly position a required *SspI* restriction site downstream of the *E. coli* replication origin, generating the plasmid pML603. The gene encoding the mycobacteriophage L5 integrase was obtained from pML102 (30) via a one-step combined chain reaction (CCR) to remove the internal

SphI restriction site using the end primers 1147 and 1376 and the internal *SphI* mutagenesis primer 1377. The *L5 int* gene was ligated as a blunt-end fragment with the 3,421 bp fragment of *HpaI/ClaI* digested and filled-in pML603 to generate the plasmid pML1321. Digestion of pML1321 with *XmaI* and *SspI* resulted in a fragment containing the hygromycin resistance gene, the *L5* integrase gene, and the *E. coli* origin of replication. This 3,642 bp fragment was ligated with the 1,812 bp fragment of *XmaI/SspI* digested pML1320 to generate the plasmid pML1330. Because recombination of this plasmid occurred during passage through *E. coli*, the *L5 attB* site was removed by digestion with *XhoI* and *SpeI*, the overhangs were filled-in, and the resulting 5,404 bp fragment was ligated to generate the new *L5* integration vector pML1342.

The gfp_m^{2+} gene encodes green fluorescence protein (Gfp) that was previously mutated for enhanced fluorescence and stability and codon optimized for expression in mycobacteria (26). In order to clone the gfp_m^{2+} gene into pML1342, the gfp_m^{2+} gene was cut out from pMN437 (Steinhauer *et al.*, in press) via digestion with *ClaI* and *PmeI*, and the resulting 1,122 bp fragment was ligated into the polylinker of similarly digested pML1342 to generate the integrative, Gfp-expressing plasmid pML1335. The same gfp_m^{2+} digestion fragment was also ligated into *ClaI/HpaI* digested pMV306kan (28), a standard mycobacterial integration vector containing *L5 int* and *attP* to create pML1337.

To adapt pML1335 to the mycobacteriophage Giles integration system, the *MluI* restriction site in gfp_m^{2+} had to first be removed. This was accomplished by CCR with the end primers 145 and 131 and the mutagenesis primer 1598. This 851 bp CCR product was digested with *PacI* and *HindIII* and ligated into similarly digested pML1335, replacing gfp_m^{2+} with a gfp_m^{2+} carrying a silent mutation of the *MluI* site, generating

pML1347. The mycobacteriophage Giles *int* gene was amplified from pGH1000A (14) by PCR using the end primers 1605 and 1606. The resulting 1,344 bp product was digested with *KpnI* and ligated into the 5,043 bp fragment of *KpnI/HpaI* digested pML1347 to generate pML1355. The Giles *attP* site was then amplified from pGH1000A by PCR with the end primers 1603 and 1604. The resulting 338 bp product was digested with *MluI* and *AscI* and ligated into the similarly digested 6,127 bp fragment of pML1355 to generate the mycobacteriophage Giles integration vector pML1357.

To adapt pML1347 to the mycobacteriophage Ms6 integration system, the Ms6 *attP* site was amplified from pNIP40b (kindly provided by Dr. Nathalie Winter) by PCR with the end primers 1686 and 1687. The resulting 543 bp product was digested with *MluI* and *AscI* and ligated into the 6,231 bp fragment of similarly digested pML1347 to generate pML1360. The Ms6 *int* gene was then amplified from pNIP40b by PCR using the end primers 1688 and 1689. The resulting 1,278 bp product was digested with *KpnI* and ligated with the 5,323 bp fragment of *HpaI/KpnI* digested pML1360 to generate the mycobacteriophage Ms6 integration vector pML1361. Exchange of the *hyg* gene with the *aph* gene in pML1361 generated pML2300. This was done by amplification of *aph* from pMS2kan (10) by PCR using the primers 1749 and 1750, digestion of the resulting 1,421 bp product with *NruI* and *NsiI*, and ligation of the resulting 1,327 bp fragment into the 5,494 bp fragment of *NruI/NsiI* digested pML1361.

Construction of bacterial strains. Integrative vectors were electroporated into electro-competent *M. smegmatis* mc²155 or *M. tuberculosis* mc²6230 and positive clones were selected for by plating on Middlebrook 7H10 agar containing appropriate antibiotics. Strains constructed from plasmids containing the *gfp_m²⁺* gene were confirmed

primer	nucleotide sequence (5'-3')
99	GGCTCGCGTAGGAATCATCC
131	CTCTAGGGTCCCAATTAATTAGC
145	CGACCAGCACGGCATAATC
622 (P1)	ACAGGATTTGAACCTGCGGC
967	CGAATATTGGTAACTGTCAGACCAAGTTTACTC
1116 (P2)	CAGGTTGACGACAAGATCCCCGTCTGA
1147	AACATTATGGGCCGGTCAAGATAGG
1376	GGTACCGGGAACGGCAATGCTCCTG
1377	ACGTTGTAGGCATGGCGGCGGGCAGTCGGGTGCTT
1479 (P4 & P8)	AACGAGGTGTTCTGCGGCGGGGACTACAA
1598 (P5 & P9)	GACGGTAACTACAAGACCCGTGCC
1603	TTACGCGTCGCCGACCTACACGTATTTCGAG
1604	TTGGCGCGCCCTCGACGGACGCGGACGGAC
1605	AACGGAATGATGATCGCCGCGGTGAC
1606	TAGGTACCCTAAGACTGTCCGCTGCCGTCCGCGATCCGCAGTCGCGCCG
1678 (P3)	GACGGTAGTTCGTCGACAAGGCGTAGG
1679 (P6)	GTGGAAGGTCTCAGCGGTGCTCTGG
1680 (P7)	GACCCGATCTTCACGCACCTGGAGAGC
1681 (P10)	GCTGCCGATGGCTACTGATTAGATGG
1686	GTACGCGTCCACCAATTTCTCGTTACGTCG
1687	TGGCGCGCCTTTGCGATTGTCGAAGGTGAGTG
1688	AACCGAATCGCCCAGAATCTGACAGC
1689	GGTCATAGTCCAGGTTCCGCAGGGTACCAT
1749	AACGTTTCATCCATAGTTGCCTGACTCCC
1750	TCTATGCATGATCGAGGATGCCAGGG

Table S1: Primers used in this study.

via observation of Gfp fluorescence. Strains constructed from plasmids containing the *xyIE_m* gene were confirmed by dropping 50 µl of 1% catechol (Sigma) on top of the colonies and incubating at room temperature for approximately 5 to 10 minutes until a distinct yellow color appeared.

Strains destined for plasmid backbone removal were transformed with the plasmid pCreSacB and selected for on kanamycin. This allowed for expression of the Cre recombinase and concomitant removal of integrated backbone DNA between flanking

loxP sites, thus generating an unmarked strain. Plating on 7H10 agar containing either 10% or 2% sucrose for *M. smegmatis* or *M. tuberculosis* strains, respectively, counter-selected against pCreSacB. The absence of the chromosomal *hyg* cassette and the pCreSacB-encoded *aph* cassette was confirmed by growth on 7H10 agar but no growth on 7H10 agar containing either hygromycin or kanamycin. The genomic organization of all strains was examined by colony PCR using PuReTaq™ Ready-To-Go™ PCR beads (GE Healthcare) according to the manufacturer's protocol with appropriate primers.

Quantification of Gfp fluorescence. Bacterial strains were incubated in Middlebrook 7H9 liquid medium on a shaker at 37°C to an OD₆₀₀ of 0.8-1.0. Triplicate cultures were diluted in 7H9 medium to the same optical density and 200 µl were transferred to wells of a black, 96-well microtiter plate with flat, transparent bottoms (Costar #3631 from Corning). Fluorescence was measured via a Synergy HT plate reader (Bio-Tek) by excitation at 485 nm and emission at 528 nm. The absorbance at 600 nm was measured, and fluorescence of each culture sample was normalized to A₆₀₀.

Visualization of Xyle and Gfp reporter activity. Bacterial cultures were incubated in 7H9 medium on a shaker at 37°C and then standardized to an OD₆₀₀ of 1.0. Cultures were serially diluted and plated onto 7H10 agar plates. After incubation at 37°C, pictures of individual colonies were taken under standard white light with 1 ms exposure times using an AxioCam MRc camera (Zeiss) mounted on a Stemi 2000-C compound light microscope (Zeiss). To visualize Xyle activity, 50 µl of 1% catechol were dropped on the tops of colonies and incubated at room temperature for approximately 5 to 10 minutes until a distinct yellow color appeared (5). Pictures were taken under the same conditions as white light pictures. To visualize Gfp fluorescence, the white light was

turned off and an excitation wavelength of 485 nm was applied while emission was filtered at 528 nm and exposed for 15 seconds via the camera.

RESULTS AND DISCUSSION

Improvements to the mycobacteriophage L5 integration system. Our aim was to design a new plasmid for integration into mycobacterial chromosomes that would (i) be easily adaptable to multiple integration sites, (ii) prevent polar effects, (iii) simplify genetic modifications, (iv) allow for stable integration of expression cassettes, and (v) contain a reporter gene for easy identification of the backbone. To achieve these goals, a cassette containing two bi-directional intrinsic transcriptional terminators (*tt_{sbi}A* and *tt_{sbi}B*) flanking a polylinker was synthesized (Fig. 2). The L5 *attP* site was positioned adjacent to the protected polylinker cassette. Flanking these components are two *loxP* sites for backbone removal, which can be monitored via the *xylE* gene of *Pseudomonas putida* (5) that was codon-optimized for expression in mycobacteria (*xylE_m*). The entire *xylE_m-loxP-attP-tt_{sbi}A-polylinker-tt_{sbi}B-loxP* cassette was synthesized and cloned into a backbone containing the hygromycin resistance gene, the L5 integrase gene, and the *E. coli* origin of replication, generating the plasmid pML1342 (Table 1 and Fig. 2).

Previous reports have shown disproportionately reduced expression when genes were integrated at the L5 attachment site ((28) and Mailaender and Niederweis, unpublished results). Promoter occlusion from RNA polymerases extending from proximal promoters such as the *glyV* promoter may cause such reduced expression of genes integrated at the L5 *attB* site (1). To protect the expression cassette as well the surrounding genome from polar effects, we designed the intrinsic synthetic bi-directional transcriptional terminators A and B (*tt_{sbi}A* and *tt_{sbi}B*) (Fig. 2). These terminators were optimized for bi-directional function and high termination efficiency by incorporating ten

upstream adenine nucleotides, seven G-C base pairs in the stem, four unpaired nucleotides in the hairpin loop, and ten downstream thymine nucleotides (6).

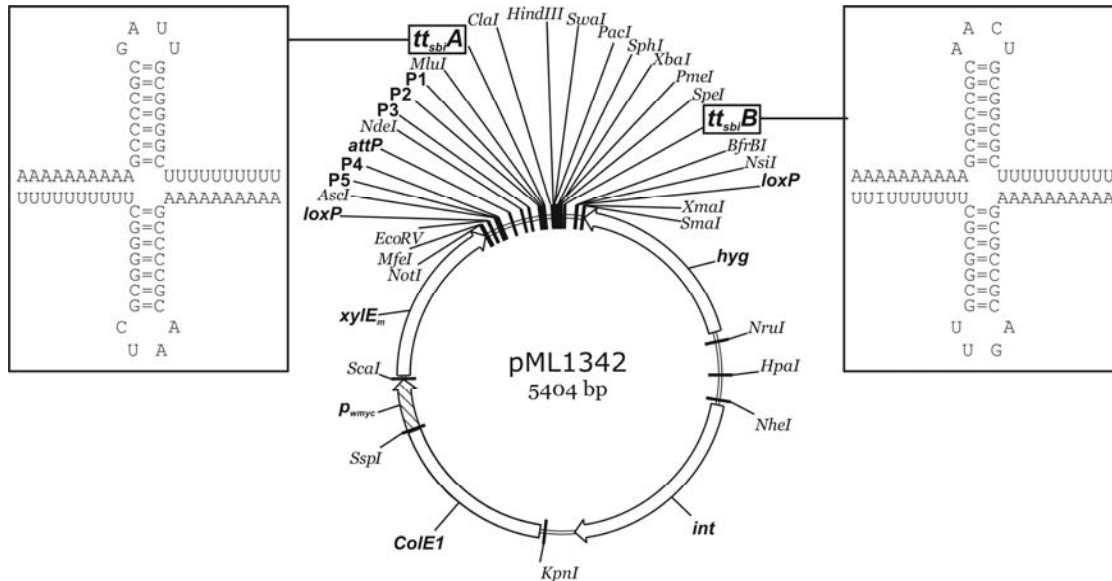


Figure 2. Plasmid map of integration vector pML1342. The integration vector pML1342 carries mycobacteriophage L5 integrase gene and the L5 phage attachment site *attP*. The synthesized *xylE_m* gene was adapted to preferred codons used by *M. tuberculosis*. *LoxP* sites flank an excisable backbone, leaving behind a stably integrated polylinker flanked by two bi-directional intrinsic terminators named *tt_{sbiA}* and *tt_{sbiB}*. The protected polylinker includes the restriction sites *PacI*, *SmaI* and *PmeI* which occur rarely or not at all in the *M. tuberculosis* genome. Five additional restriction sites are also included in the polylinker for cloning convenience. The assumed secondary structures of the bi-directional terminators are shown to the sides. Each component of the plasmid is flanked by single-cutting restriction endonuclease sites. Flanking P sites in the *attP* region are required for intasome formation, a complex comprising L5 *attP*, L5 Int, and mIHF (16).

It has been shown that continued expression of the L5 *int* gene causes plasmid instability due to the excisionase activity of the L5 integrase (25). One solution to this problem is to encode integrase on a second nonreplicating vector and co-transform both plasmids simultaneously. However, reduced transformation efficiencies using this

approach were reported (25). Therefore, we sought to remove the integrase gene without reducing transformation efficiency by encoding *int* on an excisable backbone. By positioning two *loxP* sites flanking the *hyg-int-colE1-xyIE_m* backbone, excision of the backbone upon expression of the Cre recombinase gene leaves behind a stably integrated and terminator-protected expression cassette. Integration of pML1342 and removal of the backbone can be monitored by the backbone reporter gene *xyIE_m*. In summary, the modular design of pML1342 contains a polylinker of single restriction endonuclease sites flanked by protective bi-directional terminators, a removable backbone for stable integrations equipped with a codon-optimized reporter gene (*xyIE_m*), and single restriction sites flanking all genetic components to enable easy replacement of each module.

Strains	Genotype	Relevant Description	Reference
<i>M. smegmatis</i> mc ² 155	Ept	competent wild-type <i>M. smegmatis</i>	(23)
<i>M. smegmatis</i> ML261	mc ² 155 derivative; L5 <i>attB</i> ::pML1335	new integration vector; <i>gfp_m</i> ²⁺	this study
<i>M. smegmatis</i> ML262	ML261 derivative; L5 <i>attB</i> :: <i>gfp_m</i> ²⁺	pML1335 backbone removed; <i>gfp_m</i> ²⁺	this study
<i>M. smegmatis</i> ML263	mc ² 155 derivative; L5 <i>attB</i> ::pML1337	standard integration vector; <i>gfp_m</i> ²⁺	this study
<i>M. smegmatis</i> ML264	mc ² 155 derivative; L5 <i>attB</i> ::pML1342	new integration vector; empty	this study
<i>M. smegmatis</i> ML444	mc ² 155 derivative; Giles <i>attB</i> ::pML1357	new integration vector; Giles <i>int/attP</i> , <i>gfp_m</i> ²⁺	this study
<i>M. smegmatis</i> ML446	mc ² 155 derivative; Ms6 <i>attB</i> ::pML1361	new integration vector, Ms6 <i>int/attP</i> , <i>gfp_m</i> ²⁺	this study
<i>M. smegmatis</i> ML451	ML262 derivative; Ms6 <i>attB</i> ::pML2300	<i>gfp_m</i> ²⁺ ; integrated at both L5 and Ms6 <i>attBs</i>	this study
<i>M. smegmatis</i> ML452	ML262 derivative; Giles <i>attB</i> ::pML1357	<i>gfp_m</i> ²⁺ ; integrated at both L5 and Giles <i>attBs</i>	this study
<i>M. smegmatis</i> ML453	ML262 derivative; Giles <i>attB</i> ::pML1357, Ms6 <i>attB</i> ::pML2300	<i>gfp_m</i> ²⁺ ; integrated at L5, Ms6 and Giles <i>attBs</i>	this study
<i>M. smegmatis</i> ML454	ML444 derivative; Giles <i>attB</i> :: <i>gfp_m</i> ²⁺	pML1357 backbone removed; <i>gfp_m</i> ²⁺	this study
<i>M. smegmatis</i> ML455	ML446 derivative; Ms6 <i>attB</i> :: <i>gfp_m</i> ²⁺	pML1361 backbone removed; <i>gfp_m</i> ²⁺	this study
<i>M. tuberculosis</i> mc ² 6230	<i>M. tuberculosis</i> H37Rv derivative; Δ <i>RD1</i> , Δ <i>panCD</i>	avirulent <i>M. tuberculosis</i> ; "wild-type"	(21)
<i>M. tuberculosis</i> ML440	mc ² 6230 derivative; L5 <i>attB</i> ::pML1335	new integration vector; <i>gfp_m</i> ²⁺	this study
<i>M. tuberculosis</i> ML442	ML440 derivative; L5 <i>attB</i> :: <i>gfp_m</i> ²⁺	pML1335 backbone removed; <i>gfp_m</i> ²⁺	this study
<i>M. tuberculosis</i> ML441	mc ² 6230 derivative; L5 <i>attB</i> ::pML1337	standard integration vector; <i>gfp_m</i> ²⁺	this study
<i>M. tuberculosis</i> ML268	mc ² 6230 derivative; L5 <i>attB</i> ::pML1342	new integration vector; empty	this study
<i>M. tuberculosis</i> ML448	mc ² 6230 derivative; Giles <i>attB</i> ::pML1357	new integration vector; Giles <i>int/attP</i> , <i>gfp_m</i> ²⁺	this study
<i>M. tuberculosis</i> ML450	mc ² 6230 derivative; Ms6 <i>attB</i> ::pML1361	new integration vector, Ms6 <i>int/attP</i> , <i>gfp_m</i> ²⁺	this study

<i>M. tuberculosis</i> ML456	ML442 derivative; Ms6 <i>attB</i> ::pML2300	<i>gfp_m²⁺</i> integrated at both L5 and Ms6 <i>attBs</i>	this study
<i>M. tuberculosis</i> ML457	ML442 derivative; Giles <i>attB</i> ::pML1357	<i>gfp_m²⁺</i> integrated at both L5 and Giles <i>attBs</i>	this study
<i>M. tuberculosis</i> ML458	ML442 derivative; Giles <i>attB</i> ::pML1357, Ms6 <i>attB</i> ::pML2300	<i>gfp_m²⁺</i> integrated at L5, Ms6 and Giles <i>attBs</i>	this study
<i>M. tuberculosis</i> ML459	ML448 derivative; Giles <i>attB</i> :: <i>gfp_m²⁺</i>	pML1357 backbone removed; <i>gfp_m²⁺</i>	this study
<i>M. tuberculosis</i> ML460	ML450 derivative; Ms6 <i>attB</i> :: <i>gfp_m²⁺</i>	pML1361 backbone removed; <i>gfp_m²⁺</i>	this study
Plasmids			
pMN437	<i>pAL5000, colE1, hyg, p_{smyc}-gfp_m²⁺</i>	episomal <i>gfp_m²⁺</i> plasmid; 6,236 bp	(Steinhauer <i>et. al.</i> , in press)
pML102	<i>pAL5000, colE1, aph, sacB, L5 int</i>	L5- <i>int</i> containing plasmid; 8,647 bp	(30)
pML113	<i>colE1, bla, FRT-hyg-FRT, L5 attP</i>	<i>colE1</i> containing plasmid; 4,365 bp	(30)
pML603	<i>colE1, hyg</i>	<i>colE1</i> and <i>hyg</i> containing backbone; 3,495 bp	this study
pML1321	<i>colE1, hyg, L5 int</i>	pML603 with L5 <i>int</i> ; 4,867 bp	this study
pML1320	<i>colE1, p_{wmyc}-xylE_m, loxP, L5 attP, tt_{sbi}A, L5 attB, tt_{sbi}B, loxP, aph</i>	synthetic <i>xylE_m</i> , protected <i>attB</i> /polylinker flanked by <i>loxP</i> ; 4,841 bp	Genart
pML1330	<i>colE1, hyg, L5 int, xylE_m, loxP, L5 attP, tt_{sbi}A, L5 attB, tt_{sbi}B, loxP</i>	pML603 backbone with synthetic construct; 5,459 bp	this study
pML1342	<i>colE1, L5 int, L5 attP, hyg, xylE_m, loxP, L5 attP, tt_{sbi}A, tt_{sbi}B, loxP</i>	new L5 integration vector (no <i>attB</i>); 5,404 bp	this study
pML1335	<i>colE1, L5 int, L5 attP, xylE_m, hyg, p_{smyc} - gfp_m²⁺</i>	pML1342 backbone, <i>p_{smyc} -gfp_m²⁺</i> ; 6,484 bp	this study
pMV306kan	<i>colE1, L5 int, L5 attP, aph</i>	standard L5 integration vector; 3,995 bp	(28)
pML1337	<i>colE1, L5 int, L5 attP, aph, p_{smyc} -gfp_m²⁺</i>	pMV306kan backbone, <i>p_{smyc} -gfp_m²⁺</i> ; 5,101 bp	this study
pGH1000A	<i>colE1, Giles int, Giles attP, hyg</i>	standard Giles integration vector; 5,226 bp	(14)
pML1357	<i>colE1, xylE_m, gfp_m²⁺, hyg, Giles int, Giles attP</i>	pML1335 backbone, Giles <i>int/attP</i> ; 6,454 bp	this study
pNIP40b	<i>colE1, Ms6 int, Ms6 attP, hyg</i>	standard Ms6 integration vector; 7,290 bp	Dr. N. Winter
pML1361	<i>colE1, xylE_m, gfp_m²⁺, hyg, Ms6 int, Ms6 attP</i>	pML1335 backbone, Ms6 <i>int/attP</i> ; 6,594 bp	this study
pML2300	<i>colE1, xylE_m, gfp_m²⁺, aph, Ms6 int, Ms6 attP</i>	kanamycin resistant derivative of pML1361; 6,821 bp	this study
pCreSacBI	<i>colE1, p_{groEL}-cre, p_{groEL}-sacRB, aph</i>	counter-selectable Cre-recombinase vector; 7,891 bp	Dr. A. Steyn

Table 1. Strains and plasmids used in this study. *pAL5000*: mycobacterial origin of replication, *colE1*: *E. coli* origin of replication, *hyg*: hygromycin resistance gene, *p_{smyc}*: strong mycobacterial promoter, *gfp_m²⁺*: *gfp* gene mutated for enhanced fluorescence and stability and codon optimized green fluorescence protein gene, *aph*: kanamycin resistance gene, *sacB*: sucrose resistance operon, *int*: integrase gene, *bla*: ampicillin resistance gene, *FRT*: Flp recombinase recognition site, *attP*: phage attachment site, *xylE_m*: codon optimized catechol 2,3 dioxygenase gene, *loxP*: Cre recombinase recognition site, *tt_{sbi}A/B*: synthetic bi-directional terminators, *p_{wmyc}*: weak mycobacterial promoter, *p_{groEL}*: *groEL* promoter.

Identification of clones via reporter gene activities. To complement mutants or introduce genes into vaccine strains, it is desirable to create stable integrations in the bacterial chromosome as extrachromosomally replicating plasmids cannot be selected for during infection experiments. To demonstrate that unmarked integrations can be created using pML1342, we used reporter genes to monitor both the integration of an expression cassette and excision of the destabilizing *int*-containing backbone. The transformation efficiency (Table 2) of pML1342 was reduced in comparison to the commonly used integration vector pMV306kan in *M. smegmatis* mc²155 (23) and in *M. tuberculosis* mc²6230 ($\Delta RD1$, $\Delta panCD$) (21) (Table 1), which may be attributed to the larger size of pML1342 and differences in the antibiotic resistance they confer. To visualize expression of pML1342 and pMV306kan transformants, we inserted at the polylinker of both plasmids *gfp_m²⁺*, a variant of the *gfp* gene encoding green fluorescent protein which was codon-optimized for expression in mycobacteria and carries mutations for enhanced fluorescence and stability (26). This generated the pML1342-derived plasmid pML1335 and the pMV306kan-derived plasmid pML1337. *M. smegmatis* transformants positive for pML1335 integration, referred to as *M. smegmatis* ML261 (Table 1), were easily identified by Gfp fluorescence and XylE activity (Fig. 3). Removal of the pML1335 backbone upon expression of Cre recombinase was visualized by loss of XylE activity in the resulting *M. smegmatis* ML262, a stable strain void of the *int* gene. Clones with pML1337 (*M. smegmatis* ML263) were identifiable by Gfp fluorescence alone. The *int*-containing backbone of pML1337 was not excisable as this pMV306-derived vector does not contain *loxP* sites. Though not quantitative, *M. smegmatis* mc²155 carrying the *gfp_m²⁺* replicative plasmid pMN437 (Table 1) displayed much higher Gfp fluorescence in

Organism	Strain	Plasmid	Efficiency
<i>M. smegmatis</i>	mc ² 155	pML1342	8.1 x 10 ³
<i>M. smegmatis</i>	mc ² 155	pML1335	4.9 x 10 ³
<i>M. smegmatis</i>	mc ² 155	pMV306kan	2.1 x 10 ⁴
<i>M. smegmatis</i>	mc ² 155	pML1337	3.2 x 10 ⁴
<i>M. smegmatis</i>	mc ² 155	pML1357	2.8 x 10 ⁴
<i>M. smegmatis</i>	mc ² 155	pML1361	4.0 x 10 ⁴
<i>M. smegmatis</i>	ML262	pML1357	1.7 x 10 ⁴
<i>M. smegmatis</i>	ML262	pML2300	1.4 x 10 ⁴
<i>M. smegmatis</i>	ML262	pML1357 + pML2300	2.2 x 10 ³
<i>M. tuberculosis</i>	mc ² 6230	pML1342	2.4 x 10 ³
<i>M. tuberculosis</i>	mc ² 6230	pML1335	2.7 x 10 ³
<i>M. tuberculosis</i>	mc ² 6230	pMV306kan	9.6 x 10 ⁴
<i>M. tuberculosis</i>	mc ² 6230	pML1337	9.2 x 10 ⁴
<i>M. tuberculosis</i>	mc ² 6230	pML1357	4.3 x 10 ⁴
<i>M. tuberculosis</i>	mc ² 6230	pML1361	1.3 x 10 ⁴
<i>M. tuberculosis</i>	ML442	pML1357	1.5 x 10 ⁴
<i>M. tuberculosis</i>	ML442	pML2300	5.2 x 10 ⁴
<i>M. tuberculosis</i>	ML442	pML1357 + pML2300	3.4 x 10 ³

Table 2. Transformation efficiencies. 500 ng of each plasmid were electroporated into competent *M. smegmatis* or *M. tuberculosis* strains and selected for on 7H10 solid media with appropriate antibiotics. Colony-forming units (cfu) were counted and used to calculate transformation efficiencies in cfu per μg DNA.

colonies (Fig. 3), consistent with the higher copy number of episomal pAL5000 plasmids (9, 19). Transformation with the empty pML1342 vector generated *M. smegmatis* ML264 and served as a negative control for Gfp fluorescence, but clones were still identifiable via catechol reactivity resulting from *xyIE_m* in the plasmid backbone.

Comparison of *gfp_m²⁺* expression from the L5 *attB* site in mycobacteria.

Episomal plasmids containing the pAL5000 origin of replication were estimated to have a copy number of three (19) to eight (9) in mycobacteria. Expression of genes from the L5

attB site has been reported to be disproportionately less than the episomal copy number (28). It is possible that polar effects from nearby promoters may inhibit expression of genes at the L5 *attB* site, and the positioning of bi-directional intrinsic transcriptional terminators flanking the expression cassette may prevent this. To quantitatively determine expression levels from unprotected versus terminator-protected gfp_m^{2+} expression cassettes integrated at the L5 *attB* site, the Gfp fluorescence of *M. smegmatis* ML261 (protected cassette present in pML1335) was compared to that of *M. smegmatis*

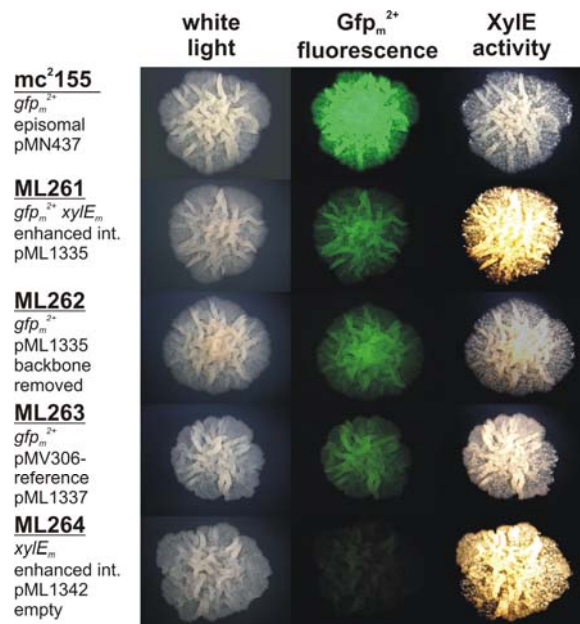


Figure 3. Identification of positive clones by visualization of plasmid-encoded reporter genes. Confocal micrographs of single colonies were taken at 20 x magnification. For comparison, micrographs of single colonies were taken under white light. Gfp fluorescence was visualized using an excitation wavelength of 490 nm and an emission filter at 512 nm. Yellow colony color indicative of XylE activity was visualized under white light after 10 min exposure to 1% catechol. The *M. smegmatis* strain for each colony is notated in bold and underlined. Presence of the genes gfp_m^{2+} and/or $xylE_m$ in each strain is listed beneath the strain name. The name and description of the plasmid carried by each strain is also included. enhanced int.: enhanced integration plasmid with gfp_m^{2+} (pML1335) or without gfp_m^{2+} (pML1342). pMV306-reference: standard integration vector pMV306kan with gfp_m^{2+} named pML1337.

ML263 (unprotected cassette present in pMV306-derived pML1337). No difference in fluorescence was observed between these two strains (Fig. 4). Excision of the pML1335 backbone in ML261 (generating ML262) had also no significant effect on fluorescence. The pAL5000-based plasmid pMN437 provided a 14-fold increased fluorescence in *M. smegmatis* compared to the control strain ML263, in agreement with estimates of pAL5000 copy numbers (9). These results indicate that gene expression levels are not strongly affected by site-specific effects at the L5 *attB* site in *M. smegmatis*. While

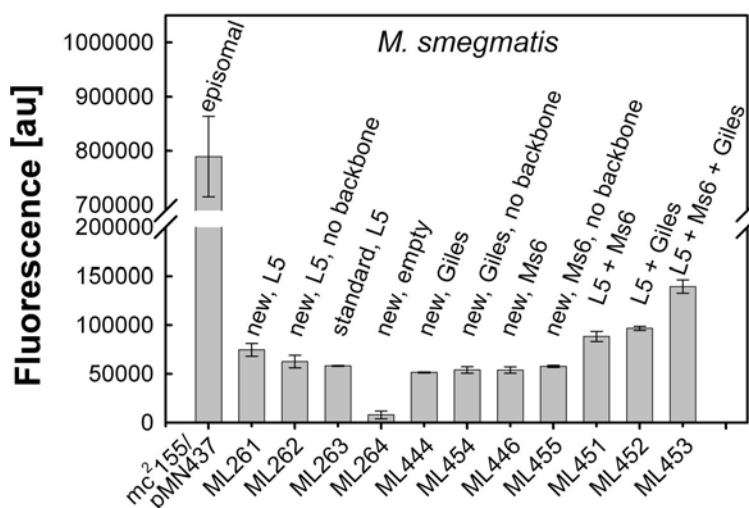


Figure 4. Expression of gfp_m^{2+} from episomal and integrative vectors in *M. smegmatis*. The fluorescence of cultures grown to an $OD_{600} \sim 0.8$ was measured and normalized to optical density. Measurements were performed in triplicate and results are representative of at least three independent experiments. Strain names are notated below the graph and descriptions of the plasmids used to generate each strain are notated above each bar. The plasmid names associated with each strain and description are: episomal: pMN437; new, L5: pML1335; standard, L5: pML1337; new, empty: pML1342; new, Giles: pML1357; new, Ms6: pML1361; L5, Ms6: pML2300 in ML262; L5, Giles: pML1357 in ML262; L5, Ms6, Giles: pML2300 co-transformed with pML1357 in ML262.

transcription termination efficiency of *tt_{sbiA}* and *tt_{sbiB}* in mycobacteria was not directly tested, similar consensus terminators were shown to be efficient in mycobacteria (29). de Hoon *et. al.* acknowledge that consensus intrinsic terminators are difficult to predict in mycobacteria, yet all bacterial RNA polymerases are highly homologous and are terminated by similar mechanisms (2).

Similar results were obtained for *M. tuberculosis* using the same vectors (Fig. 5).

Fluorescence of *M. tuberculosis* carrying the episomal *gfp_m²⁺* vector pMN437 was 9-fold

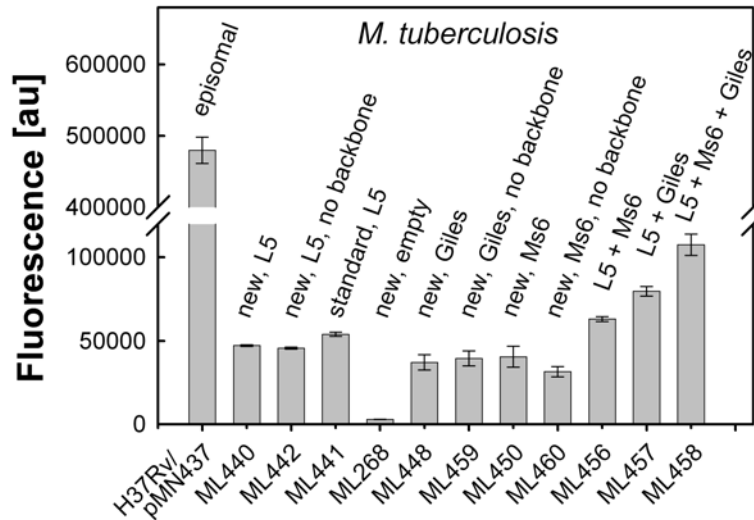


Figure 5. Expression of *gfp_m²⁺* from episomal and integrative vectors in *M. tuberculosis*. The fluorescence of avirulent *M. tuberculosis* mc²6230 cultures grown to an OD₆₀₀ ~ 0.8 was measured and normalized to optical density. Measurements were performed in triplicate and results are representative of at least three independent experiments. Strain names are notated below the graph and descriptions of the plasmids used to generate each strain are notated above each bar. The plasmid names associated with each strain and description are: episomal: pMN437; new, L5: pML1335; standard, L5: pML1337; new, empty: pML1342; new, Giles: pML1357; new, Ms6: pML1361; L5, Ms6: pML2300 in ML442; L5, Giles: pML1357 in ML442; L5, Ms6, Giles: pML2300 co-transformed with pML1357 in ML442.

higher than that of the strain integrated with the standard, unprotected gfp_m^{2+} cassette (*M. tuberculosis* ML441). Both the strain with integrated pML1335 containing the protected gfp_m^{2+} cassette (ML440) and the strain with the pML1335 backbone removed (ML442) did not show significantly increased fluorescence levels. These results indicate that transcriptional interference is not an important factor in determining expression levels at the L5 *attB* site. It may be that the intrinsic terminator within the L5 *attP* site upstream of the core already prevents readthrough transcription from the *glyV* gene (12). Addition of flanking bi-directional terminators, however, may prevent readthrough transcription from the integrated cassette into the surrounding genome and thereby avoid artificial phenotypes resulting from integration.

Adaptation of pML1335 to alternative integration sites. Due to its large size, the bacterial chromosome needs to be tightly compacted in order to fit within the constraints of the cell. The nonuniform bacterial nucleoid contains different topological domains of varying compaction which may influence transcriptional activity (13). It is conceivable that the L5 *attB* site resides within a tightly compacted region in mycobacterial chromosomes and accessibility to RNA polymerases is restricted, thus limiting gene expression. Alternative integration sites present in both *M. smegmatis* and *M. tuberculosis* exist in the *proT* and *alaV* tRNA genes for the mycobacteriophages Giles and Ms6 (Fig. 6). The modular design of pML1335 enabled us to easily replace the L5 *int* gene and *attP* region, generating the integrative plasmids pML1357 and pML1361 (Table 1) specific for the Giles and Ms6 *attB* sites, respectively.

To compare gene expression from different sites in mycobacterial chromosomes, pML1357 and pML1361 were transformed in *M. smegmatis* mc²155, generating the

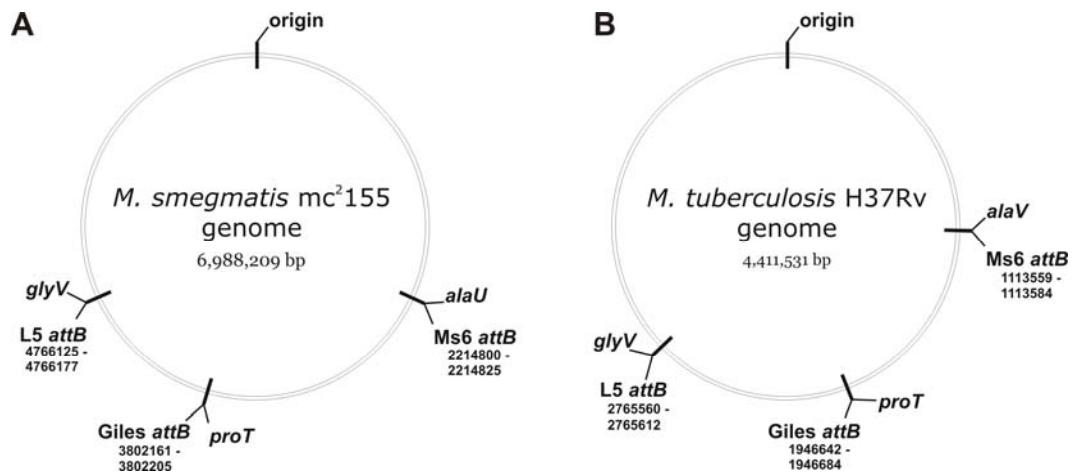


Figure 6. Mycobacteriophage attachment sites in *M. smegmatis* and *M. tuberculosis* chromosomes. The mycobacteriophage *attB* sites present in both species of mycobacteria are noted along with the tRNA genes in which they overlap. Coordinates are listed for each *attB* site. The origin is defined as the start of the *dnaA* gene and determines the first coordinate base pair.

strains *M. smegmatis* ML444 (Giles) and ML446 (Ms6), respectively (Table 1). These two plasmids transformed into *M. smegmatis* mc²155 with nearly ten-fold higher efficiency than the L5 *attB*-specific pML1335 (Table 2). This could be due to higher expression levels or greater efficiencies of their respective integrases. These strains were identifiable in large sized colonies by their XyleE activity (not shown). However, the XyleE activity of ML444 (Giles) and ML446 (Ms6) was much weaker than that of ML261 (L5), which readily reacted with catechol and produced a very prominent yellow color in culture smears (Fig. S1). These results indicated that genes in the unprotected backbone are not equally expressed at all integration sites in the *M. smegmatis* chromosome. In contrast, expression of *gfp_m*²⁺ was identical at the L5, Giles and Ms6 *attB* sites (Fig. 4). At all three integration sites, the presence or absence of the plasmid backbone did not affect expression of *gfp_m*²⁺ from the protected cassette (Fig. 4). These results show that

similar expression can be achieved *in vitro* at the L5, Giles, and Ms6 integration sites by using expression cassettes protected by intrinsic transcriptional terminators.

To determine whether the integration vectors pML1357 (Giles) and pML1361 (Ms6) function similarly in slowly growing mycobacteria, they were transformed into *M. tuberculosis* mc²6230, generating the strains ML448 and ML450, respectively (Table 1).

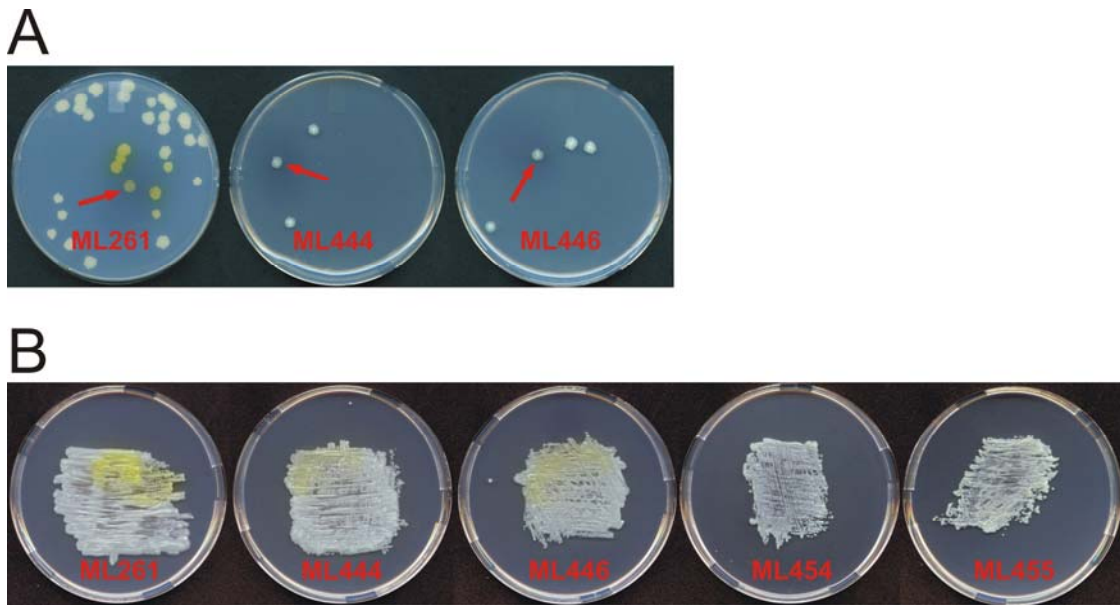


Figure S1. Activity of *xylE_m* integrated at *M. smegmatis* L5, Giles and Ms6 *attB* sites. A) Strains were diluted and plated for single colonies on Middlebrook 7H10 agar. 10 μ L of 1% catechol were dropped onto colonies indicated by arrows. After 5 minutes of incubation at room temperature, plates were scanned using an Epson Perfection V700 photo scanner. B) Strains were streaked onto 7H10 agar plates containing 0.5% Tyloxapol. 50 μ L of 1% catechol were dropped onto the upper half of each four day old culture smear, which were incubated and scanned as in A.

Similarly to *M. smegmatis*, transformation was more efficient for these two plasmids compared to the L5 *attB*-specific pML1335 (Table 2). In contrast to *M. smegmatis*, the backbone reporter *xylE_m* provided similar catechol reactivity when expressed from all

three integration sites (not shown). Figure 5 shows that expression of the protected gfp_m^{2+} cassette from the L5, Giles, and Ms6 integration sites of the *M. tuberculosis* chromosome was also identical at all three sites and is independent of the presence or absence of the plasmid backbones. These results indicate that the L5 *attB* site is as suitable as the other chromosomal sites tested in *M. smegmatis* and *M. tuberculosis* for the expression of a gene of interest. This study demonstrates the versatility of our basic integration vector pML1342 in being adaptable to multiple phage integration sites as well as efficient gene expression from the protected cassette at all chromosomal sites in both fast and slow growing mycobacteria. To our knowledge, this is the first study comparing gene expression levels at different chromosomal sites in mycobacteria.

Simultaneous integration of expression cassettes at different chromosomal sites. For some studies, high expression levels are required to generate a detectable phenotype. This may be difficult to achieve in virulence studies as episomal plasmids cannot be selected for during infection. An alternative approach to increasing expression from chromosomal constructs is to integrate multiple copies of the gene of interest. This approach also allows for the simultaneous examination of different integrated genes. After integration, the L5 *attB* sequence is reconstituted at the resulting *attL* site (12) (Fig. 1), but is not a functional reconstitution, perhaps due to steric blockade by tight integrase binding (Dr. Graham Hatfull, personal communication). To circumvent this, Saviola and Bishai integrated a vector carrying a new L5 *attB* site into the chromosome of *M. smegmatis*. The plasmid-born *attB* site could then serve as a second site for subsequent integration (22). Therefore, we positioned an L5 *attB* site within the protected polylinker of pML1342 to support serial integrations. However, a small fraction of the *attP/attB*-

carrying pML1330 recombined during passage through *E. coli* (Fig. S2), which made cloning in this vector difficult. Recombination may not have been previously observed as the *attB* sequence was mutated rather than tolerated (22), in contrast to our observations. Since the entire *glyV* gene was used in their construct, the authors acknowledge the possibility that mutation resulted from toxicity of the *glyV* gene product to *E. coli*. Likewise, an unmutated *attB* site may support recombination with *attP* in *E. coli*.

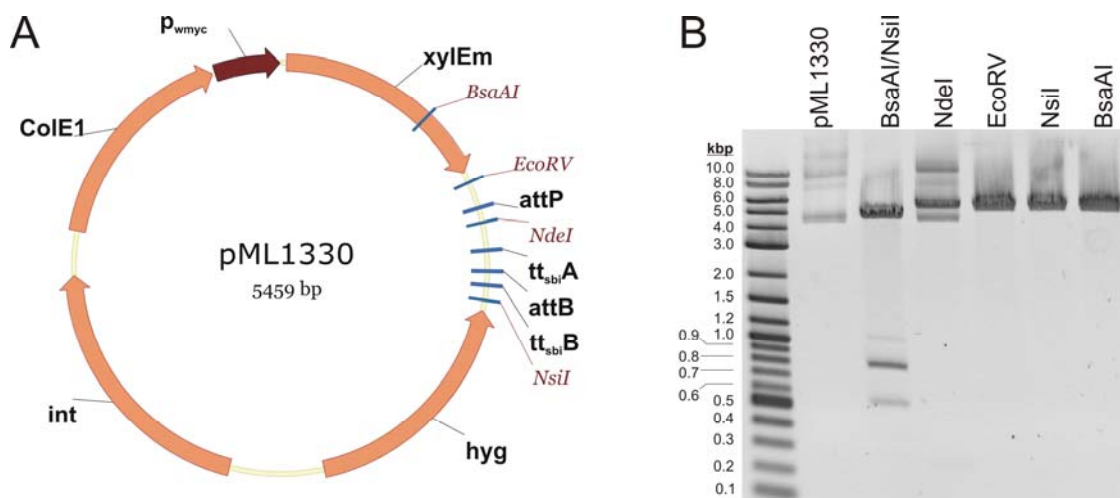


Figure S2. Recombination of a plasmid containing L5 *attP* and L5 *attB* in *E. coli*. A) plasmid map of pML1330. Restriction digest with *SpeI* and *XhoI*, fill-in, and blunt end relegation generated the *attB*-less plasmid pML1342 (Figure 2). B) DNA gel of restriction enzyme digested pML1330. The plasmid pML1330 was digested with the indicated restriction enzymes. Expected bands are *BsaAI/NsiI*: 838 bp; *NdeI*, *EcoRV*, *NsiI*, *BsaAI*: 5,459 bp. Should recombination occur, a putative band of 566 bp may be evident after double digestion with *BsaAI* and *NsiI*.

Interestingly, concentrated *E. coli* IHF promoted some L5 *attB/attP* recombination *in vitro*, despite the inability of *E. coli* crude extracts or purified but not concentrated *E. coli* IHF to do the same (11).

An alternative to reiterative, adjacent positioning of identical genes at the same attachment site is to integrate plasmids at different locations in the chromosome (8). To this end, the hygromycin resistance cassette of the Ms6 integration vector pML1361 was replaced by a kanamycin resistance cassette, generating the plasmid pML2300. This plasmid along with the Giles integration vector pML1357 carrying the *hyg* gene were co-transformed in *M. smegmatis* ML261 and *M. tuberculosis* ML442 (both strains containing L5 *attB*::*gfp_m²⁺*, unmarked), generating the *gfp_m²⁺* triple integration strains *M. smegmatis* ML453 and *M. tuberculosis* ML458, respectively (Table 1). Expectedly, the transformation efficiency (Table 2) of both the Giles (pML1357) and the Ms6 (pML2300) plasmids together in *M. smegmatis* ML261 was nearly ten-fold lower than pML1357 alone (generating the L5/Giles double *gfp_m²⁺* integrated ML451) and pML2300 alone (generating the L5/Ms6 double *gfp_m²⁺* integrated ML452). This was also the case when the same two plasmids were co-transformed into *M. tuberculosis* ML442 in comparison to pML1357 alone (generating the L5/Giles double *gfp_m²⁺* integrated ML454) and pML2300 alone (generating the L5/Ms6 double *gfp_m²⁺* integrated ML455).

The triple integrated strains *M. smegmatis* ML453 and *M. tuberculosis* ML458 were identified by colony PCR (Fig. 7). Figures 4 and 5 clearly show that for both *M. smegmatis* and *M. tuberculosis*, the triple integrated strains provide higher fluorescence than the double integrated strains, which in turn provide higher fluorescence levels than the single integrated strains. These results show that an increase in gene expression can be achieved by superintegration at multiple sites in the chromosome. However, the fluorescence intensity did not increase linearly with the chromosomal copy number. This may be due to self aggregation of Gfp (4) or by inner filter effects (7).

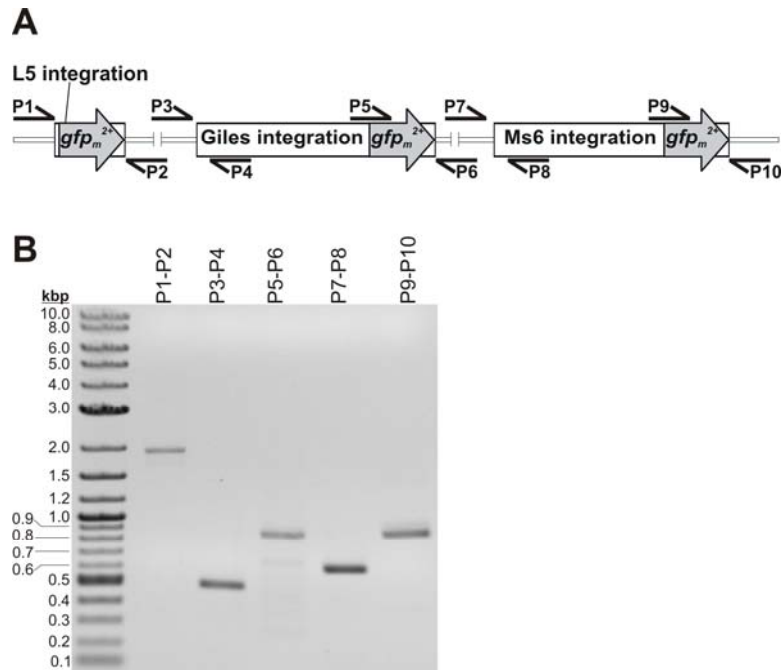


Fig. 7 Co-transformation and superintegration in *M. tuberculosis*. *M. tuberculosis* ML442 (*L5 attB::gfp_m²⁺*; backbone removed) was co-transformed with pML2300 and pML1357, generating the strain ML458. A) Genomic map of *M. tuberculosis* ML458 with *gfp_m²⁺* integrated at three positions in the chromosome. Integration of pML2300 and pML1357 in ML442 at the Ms6 and Giles *attB* sites, respectively, triples the number of *gfp_m²⁺* genes in the newly constructed strain ML448. Approximate positions of primers used for confirmation of ML458 are drawn. After PCR amplification using the following primer pairs, the expected bands on a DNA gel are: P1-P2: 1,991 bp; P3-P4: 497 bp; P5-P6: 868 bp; P7-P8: 622 bp; P9-P10: 883 bp. Refer to Fig. S1 for primer sequences. Note: figure is not to scale. B) Gel of PCR-amplified DNAs from ML458 using primer combinations listed in A.

CONCLUSIONS

It is often desirable to create multiple, stable chromosomal integrations of several genes with maximal expression levels. Our series of plasmids was designed to protect an expression cassette with bi-directional transcriptional terminators, contain convenient single cutting restriction sites flanking all genetic components, include a monitorable, excisable backbone, and be adaptable to alternative integration sites in the chromosomes of both fast and slow growing mycobacteria. The modular design of these plasmids makes them also useful for a new generation of episomal vectors for mycobacteria with different resistance markers.

The use of alternative integration machinery allows for separate integrations at various sites in mycobacterial chromosomes to integrate several different genes or to increase expression of a gene of interest. Additionally, our experiments show that equal expression levels are obtained from various sites within mycobacterial chromosomes, demonstrating that these phage attachment sites are equally suitable for chromosomal complementation experiments. Further, protection of the integrated expression cassette isolates the chromosomal modification from the surrounding genome. Thus, while transcriptional interference does not appear to reduce expression from integrated plasmids, flanking bi-directional transcriptional terminators reduce the influence of the integrated construct on nearby genes and prevent unwarranted secondary effects of gene integrations e. g. in complemented strains.

ACKNOWLEDGEMENTS

We thank Dr. Charles Turnbough for excellent advice on the design of efficient bi-directional transcriptional terminators. The strain *M. tuberculosis* mc²6230 was a kind gift from Dr. Bill Jacobs. The plasmid pML603 was kindly constructed by Dr. Olga Danilchanka. We thank Dr. Adrie Steyn for providing the Cre recombinase expression plasmid pCreSacB1.

REFERENCES

1. **Adhya, S., and M. Gottesman.** 1982. Promoter occlusion: transcription through a promoter may inhibit its activity. *Cell* **29**:939-44.
2. **Artsimovitch, I., V. Svetlov, L. Anthony, R. R. Burgess, and R. Landick.** 2000. RNA polymerases from *Bacillus subtilis* and *Escherichia coli* differ in recognition of regulatory signals in vitro. *J Bacteriol* **182**:6027-35.
3. **Ausubel, F. M., R. Brent, R. E. Kingston, D. D. Moore, J. G. Seidmann, J. A. Smith, and K. Struhl.** 1987. *Current Protocols in Molecular Biology*. John Wiley & Sons, New York.
4. **Crameri, A., E. A. Whitehorn, E. Tate, and W. P. Stemmer.** 1996. Improved green fluorescent protein by molecular evolution using DNA shuffling. *Nat. Biotechnol.* **14**:315-319.
5. **Curcic, R., S. Dhandayuthapani, and V. Deretic.** 1994. Gene expression in mycobacteria: transcriptional fusions based on *xylE* and analysis of the promoter region of the response regulator *mtrA* from *Mycobacterium tuberculosis*. *Mol Microbiol* **13**:1057-64.
6. **de Hoon, M. J., Y. Makita, K. Nakai, and S. Miyano.** 2005. Prediction of transcriptional terminators in *Bacillus subtilis* and related species. *PLoS Comput Biol* **1**:e25.
7. **Eftink, M. R.** 1997. Fluorescence methods for studying equilibrium macromolecule-ligand interactions. *Methods Enzymol* **278**:221-57.
8. **Freitas-Vieira, A., E. Anes, and J. Moniz-Pereira.** 1998. The site-specific recombination locus of mycobacteriophage Ms6 determines DNA integration at the tRNA(Ala) gene of *Mycobacterium* spp. *Microbiology* **144** (Pt 12):3397-406.
9. **Gavigan, J. A., J. A. Ainsa, E. Perez, I. Otal, and C. Martin.** 1997. Isolation by genetic labeling of a new mycobacterial plasmid, pJAZ38, from *Mycobacterium fortuitum*. *J Bacteriol* **179**:4115-22.
10. **Kaps, I., S. Ehrt, S. Seeber, D. Schnappinger, C. Martin, L. W. Riley, and M. Niederweis.** 2001. Energy transfer between fluorescent proteins using a co-expression system in *Mycobacterium smegmatis*. *Gene* **278**:115-24.
11. **Lee, M. H., and G. F. Hatfull.** 1993. Mycobacteriophage L5 integrase-mediated site-specific integration in vitro. *J. Bacteriol.* **175**:6836-41.
12. **Lee, M. H., L. Pascopella, W. R. Jacobs, Jr., and G. F. Hatfull.** 1991. Site-specific integration of mycobacteriophage L5: integration-proficient vectors for *Mycobacterium smegmatis*, *Mycobacterium tuberculosis*, and bacille Calmette-Guerin. *Proc Natl Acad Sci USA* **88**:3111-5.
13. **Luijsterburg, M. S., M. C. Noom, G. J. Wuite, and R. T. Dame.** 2006. The architectural role of nucleoid-associated proteins in the organization of bacterial chromatin: a molecular perspective. *J Struct Biol* **156**:262-72.
14. **Morris, P., L. J. Marinelli, D. Jacobs-Sera, R. W. Hendrix, and G. F. Hatfull.** 2008. Genomic characterization of mycobacteriophage giles: evidence for phage acquisition of host DNA by illegitimate recombination. *J Bacteriol* **190**:2172-82.
15. **Pedulla, M. L., M. H. Lee, D. C. Lever, and G. F. Hatfull.** 1996. A novel host factor for integration of mycobacteriophage L5. *Proc Natl Acad Sci USA* **93**:15411-6.
16. **Pena, C. E., J. M. Kahlenberg, and G. F. Hatfull.** 1999. Protein-DNA complexes in mycobacteriophage L5 integrative recombination. *J Bacteriol* **181**:454-61.
17. **Pena, C. E., J. E. Stoner, and G. F. Hatfull.** 1996. Positions of strand exchange in mycobacteriophage L5 integration and characterization of the attB site. *J Bacteriol* **178**:5533-6.

18. **Pham, T. T., D. Jacobs-Sera, M. L. Pedulla, R. W. Hendrix, and G. F. Hatfull.** 2007. Comparative genomic analysis of mycobacteriophage Tweety: evolutionary insights and construction of compatible site-specific integration vectors for mycobacteria. *Microbiology* **153**:2711-23.
19. **Ranes, M. G., J. Rauzier, M. Lagranderie, M. Gheorghiu, and B. Gicquel.** 1990. Functional analysis of pAL5000, a plasmid from *Mycobacterium fortuitum*: construction of a "mini" *mycobacterium-Escherichia coli* shuttle vector. *J Bacteriol* **172**:2793-7.
20. **Ribeiro, G., M. Viveiros, H. L. David, and J. V. Costa.** 1997. Mycobacteriophage D29 contains an integration system similar to that of the temperate mycobacteriophage L5. *Microbiology* **143 (Pt 8)**:2701-8.
21. **Sambandamurthy, V. K., S. C. Derrick, T. Hsu, B. Chen, M. H. Larsen, K. V. Jalapathy, M. Chen, J. Kim, S. A. Porcelli, J. Chan, S. L. Morris, and W. R. Jacobs, Jr.** 2006. *Mycobacterium tuberculosis* delta*RD1* delta*panCD*: a safe and limited replicating mutant strain that protects immunocompetent and immunocompromised mice against experimental tuberculosis. *Vaccine* **24**:6309-20.
22. **Saviola, B., and W. R. Bishai.** 2004. Method to integrate multiple plasmids into the mycobacterial chromosome. *Nucleic Acids Res* **32**:e11.
23. **Snapper, S. B., R. E. Melton, S. Mustafa, T. Kieser, and W. R. Jacobs, Jr.** 1990. Isolation and characterization of efficient plasmid transformation mutants of *Mycobacterium smegmatis*. *Mol Microbiol* **4**:1911-9.
24. **Song, H., and M. Niederweis.** 2007. Functional expression of the Flp recombinase in *Mycobacterium bovis* BCG. *Gene* **399**:112-9.
25. **Springer, B., P. Sander, L. Sedlacek, K. Ellrott, and E. C. Böttger.** 2001. Instability and site-specific excision of integration-proficient mycobacteriophage L5 plasmids: development of stably maintained integrative vectors. *Int J Med Microbiol* **290**:669-75.
26. **Steinhauer, K., I. Eschenbacher, N. Radischat, C. Detsch, M. Niederweis, and P. Goroncy-Bermes.** 2009. Rapid evaluation of the mycobactericidal efficacy of disinfectants in the quantitative carrier test EN 14563 using fluorescent *Mycobacterium terrae*. *Appl Environ Microbiol*.
27. **Stephan, J., V. Stemmer, and M. Niederweis.** 2004. Consecutive gene deletions in *Mycobacterium smegmatis* using the yeast FLP recombinase. *Gene* **343**:181-90.
28. **Stover, C. K., V. F. de la Cruz, T. R. Fuerst, J. E. Burlein, L. A. Benson, L. T. Bennett, G. P. Bansal, J. F. Young, M. H. Lee, G. F. Hatfull, and et al.** 1991. New use of BCG for recombinant vaccines. *Nature* **351**:456-60.
29. **Timm, J., E. M. Lim, and B. Gicquel.** 1994. *Escherichia coli*-mycobacteria shuttle vectors for operon and gene fusions to *lacZ*: the pJEM series. *J. Bacteriol.* **176**:6749-53.
30. **Wolschendorf, F., M. Mahfoud, and M. Niederweis.** 2007. Porins are required for uptake of phosphates by *Mycobacterium smegmatis*. *J Bacteriol* **189**:2435-2442.
31. **Wu, A. M., and T. Platt.** 1978. Transcription termination: nucleotide sequence at 3' end of tryptophan operon in *Escherichia coli*. *Proc Natl Acad Sci U S A* **75**:5442-6.

MYCOBACTERIAL OUTER MEMBRANES: IN SEARCH OF PROTEINS

by

MICHAEL NIEDERWEIS, OLGA DANILCHANKA, JASON HUFF, CHRISTIAN
HOFFMANN, AND HARALD ENGELHARDT

In press for *Trends in Microbiology*

Copyright

2010

by

American Society for Microbiology

Used by permission

Format adapted for dissertation

ABSTRACT

The cell wall is a major virulence factor of *Mycobacterium tuberculosis* and contributes to its intrinsic drug resistance. Recently, cryo-electron microscopy studies showed that the cell wall lipids form an unusual outer membrane in mycobacteria. However, the outer membrane components of most transport pathways in *M. tuberculosis* are unknown. Here, we summarize the current knowledge on the structure of the mycobacterial outer membrane and its few known proteins. Through comparison to transport processes in Gram-negative bacteria, we highlight several outer membrane proteins of *M. tuberculosis* awaiting discovery. The identification and characterization of these proteins are critical for understanding the physiology and pathogenicity of *M. tuberculosis*.

Mycobacteria have a complex cell envelope. Scientific interest in mycobacteria has been sparked by the medical importance of *Mycobacterium tuberculosis* and by properties that distinguish them from other microorganisms. In particular, mycobacteria possess a remarkably complex cell envelope consisting of a cytoplasmic membrane and a cell wall, which constitutes an efficient permeability barrier and plays a crucial role in the intrinsic drug resistance and in survival under harsh conditions (10). These microbes produce a fascinating diversity of lipids (10, 46) such as the mycolic acids, exceptionally long fatty acids that account for 30% to 40% of the cell envelope mass (2, 68). Mycolic acids are covalently linked to peptidoglycan via an arabinogalactan polymer, a polysaccharide composed of arabinose and galactose subunits. In a typical arrangement, the peptidoglycan network is substituted by linear galactan molecules, which bear several branched arabinose chains (10, 46). These branches end in four arabinose dimers, each forming the head group for two mycolic acid molecules. The mycolic acid-arabinogalactan-peptidoglycan polymer is arranged to form a hydrophobic layer with other lipids and the cytoplasmic membrane (47, 59). A model describing the complete primary structure of this complex cell wall has been published recently (5). The observation of pore proteins in the mycobacterial cell wall (56, 92) and their structural analysis (25) supported the model that the cell wall lipids are organized in an outer membrane despite the classification of mycobacteria as Gram-positive bacteria (40, 54). Recently, tremendous progress has been made to elucidate the organization of lipids in the mycobacterial cell wall and to identify pore proteins that functionalize this unique compartment. These results have far reaching implications for the physiology and virulence of *Mycobacterium tuberculosis* and are reviewed here.

The mycobacterial outer membrane. In 1982, Minnikin proposed that mycobacteria have a second lipid bilayer formed by an inner leaflet of mycolic acids (covalently bound to the peptidoglycan) and an outer leaflet of free lipids (46). This proposal was the basis for a variety of models, suggesting an asymmetric outer membrane-like lipid layer of exceptional thickness (≥ 10 nm) (10, 14, 23). Although freeze-fracture experiments supported the existence of this second membrane (66), electron microscopy of ultrathin sections failed to demonstrate the lipid bilayer structure, which was readily observed for the cytoplasmic membrane (24, 63). The breakthrough was achieved by cryo-electron tomography (CET) (28) and electron microscopy of ultrathin cryosections (28, 104), techniques that abstain from harsh chemical treatment of biological samples (Box 1). CET revealed the native three-dimensional organization of the cell envelope of *Mycobacterium smegmatis* and *Mycobacterium bovis* BCG and disclosed the bilayer structure of the outer membrane (Figure 1). While the lipopolysaccharide-containing outer membrane of Gram-negative bacteria consists of leaflets of different thicknesses (43), cryo-electron microscopy showed that the mycobacterial outer membrane is approximately 8 nm thick and is morphologically symmetrical. This finding, in combination with the observation that the mild detergent octyl β -glucoside permeabilizes the outer membrane of *M. smegmatis*, suggests that free lipids with heterogeneous head groups are distributed over both leaflets in the mycobacterial outer membrane and are not restricted to the outer leaflet alone (28), in contrast to all previous models.

Cryo-electron tomography (CET) provides close-to-life structure analysis of intact (native) cells in 3-D at macromolecular resolution. Samples are prepared in such a way (cryo-preparation) that preserves the distribution and interaction of macromolecular complexes and allows the visualization of biological structures *in situ*. The technique is applicable to isolated macromolecular assemblies, viruses, and microbial and eukaryotic cells [94].

For cryo-preparation, cells are mounted on electron microscope specimen supports (copper grids covered with a film containing small holes of 1-2 μm in diameter) during growth in liquid medium. Then, they are subjected to rapid freezing (vitrification) by plunging into a cryogen (e.g., liquid ethane) at about $-180\text{ }^{\circ}\text{C}$, without any dehydration, chemical fixation or staining. Thick biological samples (cells, tissues) are prepared by high pressure freezing to prevent crystallization of water and thinned by cryosectioning afterwards. Vitrified cells are structurally preserved down to the macromolecular level.

For cryosectioning, cell suspensions or small samples of tissue are transferred into small tubes which are mounted in a cryo-ultramicrotome under the atmosphere of liquid nitrogen following high pressure freezing. Cryosections of 30 to 300 nm thickness are collected and transferred to microscope grids. All samples are held frozen and are inspected in the electron microscope at liquid nitrogen temperature.

A series of projections (tomographic data) is automatically recorded by tilting the specimen around one axis (or two perpendicular axes) in the transmission electron microscope. Finally, the data are three-dimensionally reconstructed and visualized using specific algorithms and software (e.g. *TOM toolbox* (52)).

Box 1. The cryo-electron tomography (CET) technique.

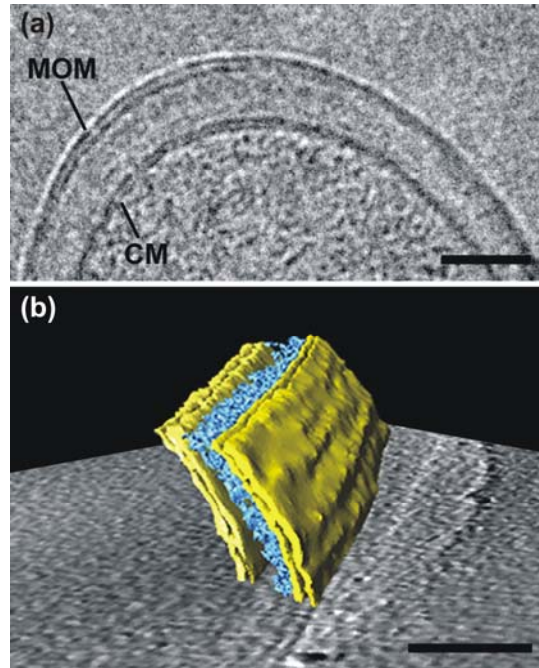


Figure 1. Cryo-electron microscopy of the mycobacterial cell envelope. Visualization of the mycobacterial outer membrane (MOM) from *Mycobacterium bovis* BCG by cryosectioning (a) and by cryo-electron tomography (b). The periplasmic space between the MOM and the cytoplasmic membrane (CM) contains the layers of the arabinogalactan-peptidoglycan polymer (indicated in blue in the 3-D representation). Scale bars: 50 nm. Figure adapted, with permission, from Ref. (28).

However, cryo-electron microscopy images do not give clues about the conformation of the mycolic acids in the outer membrane. Mycolic acids consist of up to 90 carbon atoms, forming a long branch called the meromycolate and a shorter α -branch (Figure 2a). The meromycolate contains cyclopropane rings, substitutions, or double bonds that are characteristic for the mycobacterial species (3). If the meromycolate had an elongated conformation (29, 59), it would span the complete hydrophobic matrix leaving space for free lipids to intercalate (Model I in Figure 2b). Results of monolayer experiments and simulation data are indeed consistent with a folded conformation for the

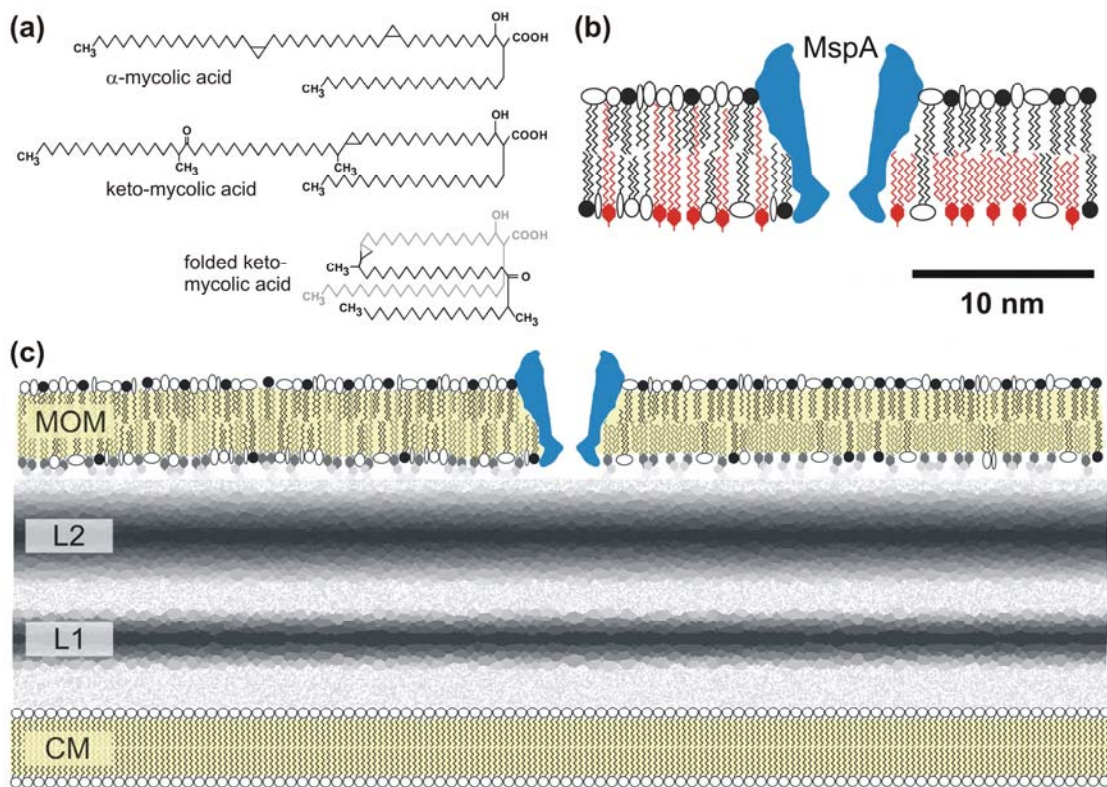


Figure 2. Models of the mycobacterial outer membrane and cell envelope. (a) Schematic structure of mycolic acids in the elongated and folded conformation (based on the major components found in *M. tuberculosis* (96, 99)). **(b)** Models of the mycobacterial outer membrane (adapted, with permission, from (28, 104)). Mycolic acids are drawn in red and inserted either in the elongated conformation (Model I, left side) or the folded conformation (Model II, right side). A porin, here MspA from *M. smegmatis*, is represented in blue. The symbols of lipid head groups indicate that different free lipids may occur in both leaflets of the outer membrane. Scale bar: 10 nm. **(c)** Model of the mycobacterial cell envelope. The dimensions of the membranes and the periplasmic layers are taken from (28). CM: cytoplasmic membrane (membrane proteins are not shown), L1, L2: periplasmic layers of still unknown identity. L2 represents at least part of the peptidoglycan-arabinogalactan polymer. MOM: mycobacterial outer membrane according to the representation in (b). The hydrophobic matrix of membranes is indicated in yellow color. The models in (b) and (c) are approximately drawn to scale.

meromycolate at moderate temperature and low lateral membrane pressure with kinks at positions of cis double bonds or trans cyclopropane rings (95, 96). This conformation might be stabilized by keto or methoxy groups that were recently proposed to interact with lipid head groups (104). A sketch of a folded keto-mycolic acid is depicted in Figure 2a and shown as part of the mycobacterial outer membrane (Model II, Figure 2b). However, direct experimental evidence how mycolic acids are folded *in situ* does not exist.

The outer membrane organization represented by these two models, as well as the structures of mycolic acids, are likely functionally important. Mutations in mycobacteria that either affect modifications (6, 27, 67) or length of the mycolic acids (38) result in phenotypes with altered colony morphology, persistence in host cells, or in a labile outer membrane structure with changed permeability properties (98). While mutations that lead to a complete loss of mycolic acids are lethal to mycobacteria, corresponding mutants of closely related corynebacteria are viable (64). Cryo-electron microscopy of a mycolic-acid deficient mutant of *Corynebacterium glutamicum* showed that the outer membrane bilayer is missing (28, 104). The cell envelope of this mutant is also more permeable to drugs (26), highlighting the significance of the outer membrane as a permeability barrier. These observations define the periplasmic space and the outer membrane as two new subcellular compartments (30, 49) in mycobacteria (Figure 2c). The arabinogalactan-peptidoglycan polymer resides within the periplasm and likely corresponds to the layered but still unidentified structures in the cryo-electron microscopy images (Figure 1). Of importance for the physiology of mycobacteria is how these two compartments are functionalized for uptake and secretion processes. For example, Gram-negative bacteria

such as *Escherichia coli* employ more than 60 outer membrane proteins (48), the majority of which form channels to enable transport across the outer membrane (57). The genome of *M. tuberculosis* appears to encode more than 140 putative outer membrane proteins (86). However, only very few have been identified and characterized thus far.

The porin pathway across mycobacterial outer membranes. While hydrophobic compounds can penetrate membranes by temporarily dissolving in the lipid bilayer, direct diffusion of water-soluble compounds across any lipid bilayer is too slow to support bacterial growth. Thus, uptake of most hydrophilic solutes across the mycobacterial outer membrane likely requires proteins. A strong argument in favor of this hypothesis is provided by the existence of porins in mycobacteria. Porins are defined as non-specific protein channels in bacterial outer membranes which enable the influx of hydrophilic solutes (57). MspA was discovered as the major porin (56) and the most abundant protein of *M. smegmatis* (61). Deletion of *mspA* reduced the outer membrane permeability of *M. smegmatis* towards glucose (87), phosphate (101), metal ions and amino acids (88) indicating that MspA represents the major general diffusion pathway in *M. smegmatis*. Not surprisingly, loss of Msp porins reduced the growth rate of *M. smegmatis* (88, 101) demonstrating that influx of hydrophilic nutrients limits the growth of porin mutants.

The requirement for fast nutrient uptake rates is likely not as stringent for *M. tuberculosis*, with a generation time of 24 hours compared to 3 hours for *M. smegmatis*. This might be the reason why *M. tuberculosis* does not have MspA homologues (54). However, other pore-forming proteins have been detected in *M. tuberculosis* and *M. bovis* BCG (34, 37, 81, 85), suggesting that diffusion across the lipid

bilayer of the outer membrane is too slow at least for some solutes. Further studies of pore-forming proteins of *M. tuberculosis* would provide important clues for its physiology by revealing which solutes utilize these pathways. In addition, porins play a major role in antibiotic uptake in *M. smegmatis* (18) and Gram-negative bacteria (57). Hence, functional and structural data might also indicate how these pores could be exploited to more efficiently transport drugs into the cell to improve tuberculosis chemotherapy.

The C-terminal domain of one of these pore-forming proteins, OmpATb (Rv0899), has weak similarity to outer membrane proteins of the OmpA family of Gram-negative bacteria. Purified recombinant OmpATb was shown to form channels in lipid membranes (1, 81). Uptake of serine but not of glycine was reduced in the mutant of *M. tuberculosis* lacking *ompATb* (71). Although transcription of *ompATb* was 30-fold induced at pH 5.5 *in vitro*, the permeability of *M. tuberculosis* to serine was decreased under those conditions (71). Considering these conflicting results, it appears doubtful that the primary function of OmpATb in *M. tuberculosis* is that of a major porin (54).

Rv1698 was identified as an outer membrane protein of *M. tuberculosis* with channel activity (85, 86). Expression of *rv1698* partially complemented the permeability defects of an *M. smegmatis* porin mutant. However, recent experiments suggest that the physiological function of Rv1698 is probably not that of a porin (Wolschendorf and Niederweis, unpublished). Thus, despite long-term efforts by several groups, a doubtless identification of *M. tuberculosis* porins that mediate uptake of small, hydrophilic solutes across the outer membrane has not yet been achieved.

The *mspA* gene of *M. smegmatis* was expressed in *M. bovis* BCG and *M. tuberculosis* to assess the role of the porin pathway in these species (41, 82). Even a very low number of MspA pores increased glucose uptake and accelerated growth of *M. bovis* BCG (41). Further, both *M. bovis* BCG and *M. tuberculosis* became more susceptible to β -lactam antibiotics, isoniazid, ethambutol and streptomycin. These results indicate that the very low efficiency and/or low number of endogenous pores contribute to the slow nutrient uptake and the intrinsic resistance of these organisms to drugs.

Structure of mycobacterial outer membrane proteins. The crystal structure of MspA is the only structure solved for any mycobacterial outer membrane protein (25). It has proven to be of immense value not only as a paradigm for a new class of proteins, but also for understanding the function of MspA (31), for elucidating its membrane topology (40), and for applications in nanotechnology (4, 11, 102). MspA has an octameric goblet-like conformation with a single central channel 10 nm in length (Figure 3). This structure

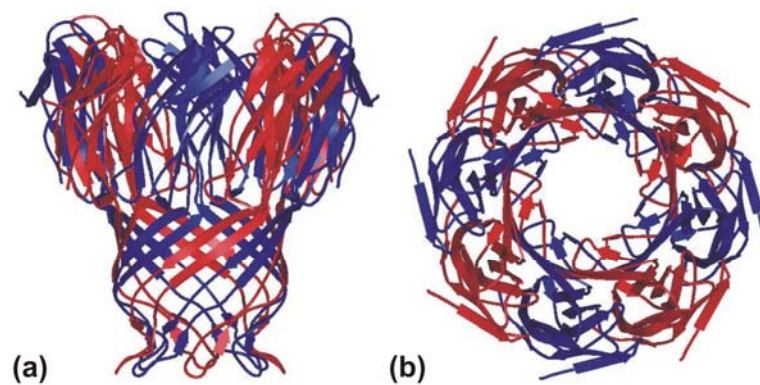


Figure 3. Structure of the porin MspA of *M. smegmatis*. (a) Side view, (b) top view. The atomic coordinates of MspA were taken from the crystal structure (PDB accession code: 1UUN, (25)). Alternating adjacent monomers are colored in red and blue.

is different from that of trimeric porins in Gram-negative bacteria which have one pore per monomer and are approximately 5 nm long (79). The constriction zone of the octameric MspA channel consists of 16 aspartate residues (D90/D91) creating a high density of negative charges (25) which likely explain the cation preference of MspA (56). Due to its novel protein architecture, MspA became the founding member of a new class of outer membrane proteins which has more than 30 homologous members in mycobacteria (53). More high-resolution structures are needed to identify unique characteristics of mycobacterial outer membrane proteins as well as features that are shared with proteins of Gram-negative bacteria.

Energy-dependent uptake of nutrients across outer membranes. The porin pathway is not efficient enough (i) for solutes of very low abundance (below 1 μM), such as iron, because small concentration gradients result in very low diffusion rates; and (ii) for large, hydrophilic solutes such as vitamin B₁₂ that most likely exceed the size exclusion limit of porins. These solutes require uptake by active transport across the outer membrane of Gram-negative bacteria (65). Substrates of energy-dependent transport systems bind with high affinity to surface receptors, many with dissociation constants in the sub-nanomolar range. In *E. coli*, energy is provided by the inner membrane complex ExbBD via the periplasmic protein TonB to multiple outer membrane receptors (65).

Iron is highly limited to bacterial pathogens due to sequestration by the host (45) and, therefore, needs to be acquired by active transport. This is achieved by high affinity siderophores which are specifically taken up by outer membrane receptor proteins in Gram-negative bacteria (8). *E. coli* contains three major independent siderophore receptors in the outer membrane: FhuA, FepA and FecA. Upon binding an iron-loaded

siderophore, energy transferred by TonB initiates structural rearrangements in the transporter, releasing the siderophore into the periplasm where a substrate binding protein shuttles it to a specific transporter of the ATP-binding cassette transporter family in the inner membrane (8, 65).

M. tuberculosis produces two salicylate-derived siderophores. The more polar carboxymycobactin is released into the medium whereas the less polar mycobactin remains cell-associated (69). In this bacterium, an ABC transporter composed of the proteins IrtA and IrtB is required for transport of siderophores across the inner membrane (73). Uptake of iron-loaded carboxymycobactin is not energy-dependent (89), leading to the hypothesis that siderophores might diffuse through porins (69). However, in other microbes such as *E. coli*, the concentration of extracellular iron-loaded siderophores is not high enough to support passive diffusion during infection (9). Computer models suggest that even the smaller siderophore exochelin of *M. smegmatis* (83) in its iron-bound form appears to be too large to pass through the MspA pore (Jones and Niederweis, unpublished). This argues for the existence of energy-dependent receptors in mycobacteria for active uptake of iron-loaded siderophores across the outer membrane. Uptake of vitamin B₁₂ (75) and other scarce or large solutes provides a similar challenge for *M. tuberculosis* and probably also requires outer membrane receptors.

Uptake of hydrophobic compounds across outer membranes. Nikaido and co-workers have shown that diffusion rates through the water-filled channels of porins drop drastically with increasing solute hydrophobicity (57). Both direct diffusion of anionic fatty acids through lipid membranes (77) and an alternative ‘flip-flop’ movement of protonated fatty acids through membranes (33) are slow. These findings explain why

bacteria and eukaryotes have evolved proteins for fatty acid uptake across membranes (76). For example, the outer membrane protein FadL mediates energy-independent uptake of fatty acids by *E. coli* (93).

Considerable circumstantial evidence suggests that *M. tuberculosis* uses lipids as a carbon source after the onset of the adaptive immune response in mice (44, 50, 51, 78). However, no FadL homologue is apparent in mycobacteria, and the mechanism by which fatty acids cross the mycobacterial outer membrane is unknown. Identification of an outer membrane fatty acid transporter will be important for understanding the physiology of *M. tuberculosis* in the human host and might shed light on the types of lipids used by this microbe. In addition to fatty acids, cholesterol is another hydrophobic compound which appears to be used by *M. tuberculosis* as a carbon source (32, 62, 94). The *mce4* operon is required for efficient uptake of cholesterol (62). Interestingly, Mce4A, Mce4B, Mce4C, Mce4D and Mce4F have been proposed to be outer membrane proteins based on secondary structure predictions and other characteristics common to outer membrane proteins (86). They might form an outer membrane channel to enable cholesterol to enter the cell.

Efflux processes. *M. tuberculosis* is intrinsically resistant to many antibiotics due to the formidable permeability barrier established by the outer membrane, in synergy with other resistance mechanisms such as multi-drug efflux (58). Considering that the *M. tuberculosis* genome encodes 69 putative drug efflux pumps (19), it is not surprising that all current tuberculosis drugs are substrates of efflux. In Gram-negative bacteria, only efflux across both membranes is an effective resistance mechanism (36). The major drug efflux system of *E. coli* is a tripartite pump consisting of an inner-membrane

transporter protein (AcrB), a periplasmic adapter protein (AcrA) and an outer membrane channel (TolC). *E. coli tolC* mutants are highly susceptible to a wide variety of toxic compounds (90).

TolC homologues are ubiquitous among Gram-negative bacteria; however, they do not seem to exist in mycobacteria. We hypothesize that *M. tuberculosis* might have an outer membrane channel protein that connects to inner membrane pumps, allowing for efficient efflux across the two membranes. This hypothesis is supported by the observation that over-expression of the *M. tuberculosis* inner membrane ABC transporter Rv0194 in *M. bovis* BCG increased resistance to ampicillin (17). Because targets of β -lactam antibiotics are located in the periplasm, increased resistance must result from efflux across the outer membrane. A connection of an outer membrane channel with an inner membrane efflux pump similar to the drug efflux systems in Gram-negative bacteria would also provide the energy required for efflux against the concentration gradient. Discovery of a TolC-like protein would represent a major breakthrough in our understanding of drug efflux in *M. tuberculosis*.

Other putative outer membrane proteins. A few transport processes requiring outer membrane proteins are highlighted above. Yet, many other functions as described in Gram-negative bacteria are completed by proteins embedded in the outer membrane (48). We propose that functionally equivalent proteins exist in mycobacteria.

For example, YaeT is required by *E. coli* to correctly insert proteins into the outer membrane (21, 100). Conditional depletion of the homologous Omp85 in *Neisseria gonorrhoeae* results in periplasmic accumulation of misfolded proteins (97).

Mycobacteria might possess a functional homologue of protein insertion machinery in the

outer membrane. Similarly, Gram-negative bacteria require an outer membrane protein, Imp, to insert lipopolysaccharide (LPS) into the outer leaflet of the outer membrane (103). Such membrane assembly proteins are likely also required for the many different lipids in the outer leaflet of mycobacterial outer membranes. One example is the phthiocerol dimycocerosates (PDIMs) whose transport requires the inner membrane transporter MmpL7 (12, 16) and the lipoprotein LppX (91), but it is unknown how PDIMs cross the outer membrane to reach the cell surface.

Mycobacteria produce capsules (35, 74) and biofilms (60, 72, 80), but it is unknown how the materials for these extracellular structures are secreted to the cell surface. In *E. coli*, capsular material is translocated across the outer membrane by the Wza protein (15, 22). Given the requirement of extracellular structures for the survival of *M. tuberculosis* during infection (74), we propose that a secretion machinery for biofilm and capsular materials in the outer membrane also exists.

An area of intense research involves the proteinaceous virulence factors in *M. tuberculosis* culture filtrates. Proteins are transported across the inner membrane via the general (Sec), twin-arginine (Tat), or Esx secretion pathways. Importantly, *esxI* is required for the release of the virulence factors Esat-6 and Cfp-10 (20, 84). Yet, the outer membrane components of these secretion pathways await identification. Additionally, lipases (70), esterases (39), attachment and invasion proteins, and multiple other proteins (86) such as those of the enigmatic PE family (13) perform functions on the surface of the cell and are likely anchored or integrated in the outer membrane.

Concluding remarks and future directions. Outer membrane proteins of *M. tuberculosis* are intriguing for several reasons. First, considering that many nutrient

molecules are hydrophilic and thus have inherently slow diffusion rates across lipid membranes, it is likely that proteins in the outer membrane are required for their uptake (55). Hence, their identification is essential for understanding the physiology and pathogenicity of this microorganism. Second, outer membrane proteins of *M. tuberculosis* reside in an unusual lipid membrane distinct from that of Gram-negative bacteria. Therefore, their structures are probably novel, as shown for the porin MspA of *M. smegmatis* (25). It is likely that they also function by novel mechanisms. Third, outer membrane proteins required for virulence such as OmpATb (71) represent attractive drug targets because inhibitors do not have to cross the notoriously impermeable outer membrane, a major determinant of intrinsic drug resistance (10). Fourth, many outer membrane proteins of pathogenic Gram-negative bacteria are involved in interactions with host cells (42). We assume that this will also be the case for *M. tuberculosis* and that these interactions are critical to the outcome of infection. In conclusion, the outer membrane represents a novel subcellular compartment in mycobacteria harboring proteins of unknown structures and functions. The visualization of mycobacterial outer membranes and the discovery and characterization of a few proteins that reside in this compartment have opened a new field in tuberculosis research of paramount scientific and medical importance.

However, considerable challenges remain to be overcome to fully understand the role of the outer membrane for the physiology and pathogenesis of *M. tuberculosis*. These challenges include: (i) a complete ultrastructural characterization of the cell envelope of *M. tuberculosis* whose capsule remains to be visualized (35). Recent mutants with defects in capsular glucan biosynthesis offer the possibility to visualize this delicate

structure (74). (ii) The arrangement and configuration of lipids in the mycobacterial outer membrane is unknown, but is very likely a primary determinant of its permeability properties. The machinery required to assemble this complex structure is still a mystery. (iii) The identification of the low abundance outer membrane proteins of *M. tuberculosis* represents a considerable experimental challenge. We have recently proposed the combinatorial protocol of simplified subcellular fractionation and whole-cell protease digestion to examine membrane association and surface accessibility as a novel approach to identify outer membrane proteins in mycobacteria (86). However, both methods are prone to experimental errors and require proper controls and careful execution to yield reliable results. (iv) The elucidation of the physiological function of novel proteins is difficult if the phenotype of a mutant is not apparent. This is likely the case for many outer membrane proteins, as was shown for porins with multiple functional orthologs (54). Microarrays for phenotypic characterization have been recently established for mycobacteria and should prove helpful to overcome this hurdle (7). The identification and characterization of outer membrane proteins of *M. tuberculosis* are critical for understanding the physiology and pathogenicity of this microorganism, and might lead to the development of new anti-tuberculosis drugs.

ACKNOWLEDGEMENTS

We thank all members of the Niederweis and Engelhardt labs for helpful discussions. This work was supported by the Network of Excellence for 3D-Electron Microscopy of the 6th framework of the European Union and by grants AI063432 and AI083632 of the National Institutes of Health to MN.

REFERENCES

1. **Alahari, A., N. Saint, S. Campagna, V. Molle, G. Molle, and L. Kremer.** 2007. The N-terminal domain of OmpATb is required for membrane translocation and pore-forming activity in mycobacteria. *J Bacteriol* **189**:6351-8.
2. **Barry, C. E.** 2001. Interpreting cell wall 'virulence factors' of *Mycobacterium tuberculosis*. *Trends Microbiol* **9**:237-41.
3. **Barry, C. E., 3rd, R. E. Lee, K. Mdluli, A. E. Sampson, B. G. Schroeder, R. A. Slayden, and Y. Yuan.** 1998. Mycolic acids: structure, biosynthesis and physiological functions. *Prog. Lipid Res.* **37**:143-79.
4. **Basel, M. T., R. K. Dani, M. Kang, M. Pavlenok, V. Chikan, P. E. Smith, M. Niederweis, and S. H. Bossmann.** 2009. Direct observation of gold nanoparticle assemblies with the porin MspA on mica. *ACS Nano* **3**:462-6.
5. **Bhamidi, S., M. S. Scherman, C. D. Rithner, J. E. Prenni, D. Chatterjee, K. H. Khoo, and M. R. McNeil.** 2008. The identification and location of succinyl residues and the characterization of the interior arabinan region allows for a model of the complete primary structure of *Mycobacterium tuberculosis* mycolyl arabinogalactan. *J Biol Chem* **283**:12992–13000.
6. **Bhatt, A., A. K. Brown, A. Singh, D. E. Minnikin, and G. S. Besra.** 2008. Loss of a mycobacterial gene encoding a reductase leads to an altered cell wall containing beta-oxo-mycolic acid analogs and accumulation of ketones. *Chem Biol* **15**:930-9.
7. **Bochner, B. R.** 2009. Global phenotypic characterization of bacteria. *FEMS Microbiol Rev* **33**:191-205.
8. **Braun, V.** 2003. Iron uptake by *Escherichia coli*. *Front Biosci* **8**:s1409-21.
9. **Braun, V., and H. Killmann.** 1999. Bacterial solutions to the iron-supply problem. *Trends Biochem Sci* **24**:104-9.
10. **Brennan, P. J., and H. Nikaido.** 1995. The envelope of mycobacteria. *Annu. Rev. Biochem.* **64**:29-63.
11. **Butler, T. Z., M. Pavlenok, I. M. Derrington, M. Niederweis, and J. H. Gundlach.** 2008. Single-molecule DNA detection with an engineered MspA protein nanopore. *Proc Natl Acad Sci U S A* **105**:20647-52.
12. **Camacho, L. R., D. Ensergueix, E. Perez, B. Gicquel, and C. Guilhot.** 1999. Identification of a virulence gene cluster of *Mycobacterium tuberculosis* by signature-tagged transposon mutagenesis. *Mol Microbiol* **34**:257-67.
13. **Cascioferro, A., G. Delogu, M. Colone, M. Sali, A. Stringaro, G. Arancia, G. Fadda, G. Palu, and R. Manganeli.** 2007. PE is a functional domain responsible for protein translocation and localization on mycobacterial cell wall. *Mol Microbiol* **66**:1536-47.
14. **Chatterjee, D.** 1997. The mycobacterial cell wall: structure, biosynthesis and sites of drug action. *Curr Opin Chem Biol* **1**:579-88.
15. **Collins, R. F., and J. P. Derrick.** 2007. Wza: a new structural paradigm for outer membrane secretory proteins? *Trends Microbiol* **15**:96-100.
16. **Cox, J. S., B. Chen, M. McNeil, and W. R. Jacobs, Jr.** 1999. Complex lipid determines tissue-specific replication of *Mycobacterium tuberculosis* in mice. *Nature* **402**:79-83.
17. **Danilchanka, O., C. Mailaender, and M. Niederweis.** 2008. Identification of a novel multidrug efflux pump of *Mycobacterium tuberculosis*. *Antimicrob Agents Chemother* **52**:2503-11.
18. **Danilchanka, O., M. Pavlenok, and M. Niederweis.** 2008. Role of porins for uptake of antibiotics by *Mycobacterium smegmatis*. *Antimicrob Agents Chemother* **52**:3127-34.

19. **De Rossi, E., J. A. Ainsa, and G. Riccardi.** 2006. Role of mycobacterial efflux transporters in drug resistance: an unresolved question. *FEMS Microbiol. Rev.* **30**:36-52.
20. **Digiuseppe Champion, P. A., and J. S. Cox.** 2007. Protein secretion systems in mycobacteria. *Cell Microbiol* **9**:1376-84.
21. **Doerrler, W. T., and C. R. Raetz.** 2005. Loss of outer membrane proteins without inhibition of lipid export in an *Escherichia coli* YaeT mutant. *J Biol Chem* **280**:27679-87.
22. **Dong, C., K. Beis, J. Nesper, A. L. Brunkan-Lamontagne, B. R. Clarke, C. Whitfield, and J. H. Naismith.** 2006. Wza the translocon for *E. coli* capsular polysaccharides defines a new class of membrane protein. *Nature* **444**:226-9.
23. **Dover, L. G., A. M. Cerdeno-Tarraga, M. J. Pallen, J. Parkhill, and G. S. Besra.** 2004. Comparative cell wall core biosynthesis in the mycolated pathogens, *Mycobacterium tuberculosis* and *Corynebacterium diphtheriae*. *FEMS Microbiol Rev* **28**:225-50.
24. **Etienne, G., F. Laval, C. Villeneuve, P. Dinadayala, A. Abouwarda, D. Zerbib, A. Galamba, and M. Daffe.** 2005. The cell envelope structure and properties of *Mycobacterium smegmatis* mc(2)155: is there a clue for the unique transformability of the strain? *Microbiology* **151**:2075-86.
25. **Faller, M., M. Niederweis, and G. E. Schulz.** 2004. The structure of a mycobacterial outer-membrane channel. *Science* **303**:1189-92.
26. **Gebhardt, H., X. Meniche, M. Tropis, R. Kramer, M. Daffe, and S. Morbach.** 2007. The key role of the mycolic acid content in the functionality of the cell wall permeability barrier in *Corynebacterineae*. *Microbiology* **153**:1424-34.
27. **Glickman, M. S., J. S. Cox, and W. R. Jacobs, Jr.** 2000. A novel mycolic acid cyclopropane synthetase is required for cording, persistence, and virulence of *Mycobacterium tuberculosis*. *Mol Cell* **5**:717-27.
28. **Hoffmann, C., A. Leis, M. Niederweis, J. M. Plitzko, and H. Engelhardt.** 2008. Disclosure of the mycobacterial outer membrane: Cryo-electron tomography and vitreous sections reveal the lipid bilayer structure. *Proc. Natl. Acad. Sci. U S A* **105**:3963-3967.
29. **Hong, X., and A. J. Hopfinger.** 2004. Construction, molecular modeling, and simulation of *Mycobacterium tuberculosis* cell walls. *Biomacromolecules* **5**:1052-65.
30. **Hoppert, M., and F. Mayer.** 1999. Principles of macromolecular organization and cell function in bacteria and archaea. *Cell Biochem Biophys* **31**:247-84.
31. **Huff, J., M. Pavlenok, S. Sukumaran, and M. Niederweis.** 2009. Functions of the periplasmic loop of the porin MspA from *Mycobacterium smegmatis*. *J Biol Chem* **284**:10223-31.
32. **Joshi, S. M., A. K. Pandey, N. Capite, S. M. Fortune, E. J. Rubin, and C. M. Sassetti.** 2006. Characterization of mycobacterial virulence genes through genetic interaction mapping. *Proc Natl Acad Sci USA* **103**:11760-5.
33. **Kampf, J. P., D. Cupp, and A. M. Kleinfeld.** 2006. Different mechanisms of free fatty acid flip-flop and dissociation revealed by temperature and molecular species dependence of transport across lipid vesicles. *J Biol Chem* **281**:21566-74.
34. **Kartmann, B., S. Stenger, and M. Niederweis.** 1999. Porins in the cell wall of *Mycobacterium tuberculosis*. *J. Bacteriol.* **181**:6543-6546. (Authors' correction appeared in *J. Bacteriol.* **181**, 7650).
35. **Lemassu, A., A. Ortalo-Magne, F. Bardou, G. Silve, M. A. Laneelle, and M. Daffé.** 1996. Extracellular and surface-exposed polysaccharides of non-tuberculous mycobacteria. *Microbiology* **142**:1513-20.
36. **Li, X. Z., and H. Nikaido.** 2004. Efflux-mediated drug resistance in bacteria. *Drugs* **64**:159-204.

37. **Lichtinger, T., A. Burkovski, M. Niederweis, R. Kramer, and R. Benz.** 1998. Biochemical and biophysical characterization of the cell wall porin of *Corynebacterium glutamicum*: the channel is formed by a low molecular mass polypeptide. *Biochemistry* **37**:15024-32.
38. **Liu, J., and H. Nikaido.** 1999. A mutant of *Mycobacterium smegmatis* defective in the biosynthesis of mycolic acids accumulates meromycolates. *Proc Natl Acad Sci USA* **96**:4011-6.
39. **Lun, S., and W. R. Bishai.** 2007. Characterization of a novel cell wall-anchored protein with carboxylesterase activity required for virulence in *Mycobacterium tuberculosis*. *J Biol Chem* **282**:18348-56.
40. **Mahfoud, M., S. Sukumaran, P. Hülsmann, K. Grieger, and M. Niederweis.** 2006. Topology of the porin MspA in the outer membrane of *Mycobacterium smegmatis*. *J Biol Chem* **281**:5908-15.
41. **Mailaender, C., N. Reiling, H. Engelhardt, S. Bossmann, S. Ehlers, and M. Niederweis.** 2004. The MspA porin promotes growth and increases antibiotic susceptibility of both *Mycobacterium bovis* BCG and *Mycobacterium tuberculosis*. *Microbiology* **150**:853-864.
42. **Massari, P., S. Ram, H. Macleod, and L. M. Wetzler.** 2003. The role of porins in neisserial pathogenesis and immunity. *Trends Microbiol* **11**:87-93.
43. **Matias, V. R., A. Al-Amoudi, J. Dubochet, and T. J. Beveridge.** 2003. Cryo-transmission electron microscopy of frozen-hydrated sections of *Escherichia coli* and *Pseudomonas aeruginosa*. *J Bacteriol* **185**:6112-8.
44. **McKinney, J. D., K. Honer zu Bentrup, E. J. Munoz-Elias, A. Miczak, B. Chen, W. T. Chan, D. Swenson, J. C. Sacchetti, W. R. Jacobs, Jr., and D. G. Russell.** 2000. Persistence of *Mycobacterium tuberculosis* in macrophages and mice requires the glyoxylate shunt enzyme isocitrate lyase. *Nature* **406**:735-8.
45. **Miethke, M., and M. A. Marahiel.** 2007. Siderophore-based iron acquisition and pathogen control. *Microbiol Mol Biol Rev* **71**:413-51.
46. **Minnikin, D. E.** 1982. Lipids: Complex lipids, their chemistry, biosynthesis and roles, p. 95-184. *In* C. Ratledge and J. Stanford (ed.), *The biology of the mycobacteria: Physiology, identification and classification*, vol. I. Academic Press, London.
47. **Minnikin, D. E., L. Kremer, L. G. Dover, and G. S. Besra.** 2002. The methyl-branched fortifications of *Mycobacterium tuberculosis*. *Chem. Biol.* **9**:545-53.
48. **Molloy, M. P., B. R. Herbert, M. B. Slade, T. Rabilloud, A. S. Nouwens, K. L. Williams, and A. A. Gooley.** 2000. Proteomic analysis of the *Escherichia coli* outer membrane. *Eur. J. Biochem.* **267**:2871-81.
49. **Morita, Y. S., R. Velasquez, E. Taig, R. F. Waller, J. H. Patterson, D. Tull, S. J. Williams, H. Billman-Jacobe, and M. J. McConville.** 2005. Compartmentalization of lipid biosynthesis in mycobacteria. *J. Biol. Chem.* **280**:21645-21652.
50. **Munoz-Elias, E. J., and J. D. McKinney.** 2005. *Mycobacterium tuberculosis* isocitrate lyases 1 and 2 are jointly required for *in vivo* growth and virulence. *Nat Med* **11**:638-44.
51. **Neyrolles, O., R. Hernandez-Pando, F. Pietri-Rouxel, P. Fornes, L. Tailleux, J. A. Payan, E. Pivert, Y. Bordat, D. Aguilar, M. C. Prevost, C. Petit, and B. Gicquel.** 2006. Is adipose tissue a place for *Mycobacterium tuberculosis* persistence? *PLoS ONE* **1**:e43.
52. **Nickell, S., F. Forster, A. Linaroudis, W. D. Net, F. Beck, R. Hegerl, W. Baumeister, and J. M. Plitzko.** 2005. TOM software toolbox: acquisition and analysis for electron tomography. *J Struct Biol* **149**:227-34.
53. **Niederweis, M.** 2008. Mycobacterial porins, p. 153-165. *In* M. Daffe and J.-M. Reyrat (ed.), *The mycobacterial cell envelope*. ASM Press, Washington, DC.

54. **Niederweis, M.** 2003. Mycobacterial porins - new channel proteins in unique outer membranes. *Mol. Microbiol.* **49**:1167-77.
55. **Niederweis, M.** 2008. Nutrient acquisition by mycobacteria. *Microbiology* **154**:679-692.
56. **Niederweis, M., S. Ehrt, C. Heinz, U. Klöcker, S. Karosi, K. M. Swiderek, L. W. Riley, and R. Benz.** 1999. Cloning of the *mspA* gene encoding a porin from *Mycobacterium smegmatis*. *Mol. Microbiol.* **33**:933-945.
57. **Nikaido, H.** 2003. Molecular basis of bacterial outer membrane permeability revisited. *Microbiol. Mol. Biol. Rev.* **67**:593-656.
58. **Nikaido, H.** 2001. Preventing drug access to targets: cell surface permeability barriers and active efflux in bacteria. *Semin. Cell. Dev. Biol.* **12**:215-23.
59. **Nikaido, H., S. H. Kim, and E. Y. Rosenberg.** 1993. Physical organization of lipids in the cell wall of *Mycobacterium chelonae*. *Mol. Microbiol.* **8**:1025-1030.
60. **Ojha, A., M. Anand, A. Bhatt, L. Kremer, W. R. Jacobs, Jr., and G. F. Hatfull.** 2005. GroEL1: a dedicated chaperone involved in mycolic acid biosynthesis during biofilm formation in mycobacteria. *Cell* **123**:861-73.
61. **Ojha, A., and G. F. Hatfull.** 2007. The role of iron in *Mycobacterium smegmatis* biofilm formation: the exochelin siderophore is essential in limiting iron conditions for biofilm formation but not for planktonic growth. *Mol Microbiol* **66**:468-83.
62. **Pandey, A. K., and C. M. Sasseti.** 2008. Mycobacterial persistence requires the utilization of host cholesterol. *Proc Natl Acad Sci USA* **105**:4376-80.
63. **Paul, T. R., and T. J. Beveridge.** 1992. Reevaluation of envelope profiles and cytoplasmic ultrastructure of mycobacteria processed by conventional embedding and freeze-substitution protocols. *J. Bacteriol.* **174**:6508-17.
64. **Portevin, D., C. De Sousa-D'Auria, C. Houssin, C. Grimaldi, M. Chami, M. Daffe, and C. Guilhot.** 2004. A polyketide synthase catalyzes the last condensation step of mycolic acid biosynthesis in mycobacteria and related organisms. *Proc. Natl. Acad. Sci. USA* **101**:314-9.
65. **Postle, K., and R. A. Larsen.** 2007. TonB-dependent energy transduction between outer and cytoplasmic membranes. *Biometals* **20**:453-65.
66. **Puech, V., M. Chami, A. Lemassu, M. A. Laneelle, B. Schiffler, P. Gounon, N. Bayan, R. Benz, and M. Daffé.** 2001. Structure of the cell envelope of corynebacteria: importance of the non-covalently bound lipids in the formation of the cell wall permeability barrier and fracture plane. *Microbiology* **147**:1365-82.
67. **Rao, V., F. Gao, B. Chen, W. R. Jacobs, Jr., and M. S. Glickman.** 2006. Trans-cyclopropanation of mycolic acids on trehalose dimycolate suppresses *Mycobacterium tuberculosis* -induced inflammation and virulence. *J Clin Invest* **116**:1660-7.
68. **Rastogi, N., E. Legrand, and C. Sola.** 2001. The mycobacteria: an introduction to nomenclature and pathogenesis. *Rev Sci Tech* **20**:21-54.
69. **Ratledge, C., and L. G. Dover.** 2000. Iron metabolism in pathogenic bacteria. *Annu Rev Microbiol* **54**:881-941.
70. **Raynaud, C., C. Guilhot, J. Rauzier, Y. Bordat, V. Pelicic, R. Manganeli, I. Smith, B. Gicquel, and M. Jackson.** 2002. Phospholipases C are involved in the virulence of *Mycobacterium tuberculosis*. *Mol Microbiol* **45**:203-17.
71. **Raynaud, C., K. G. Papavinasundaram, R. A. Speight, B. Springer, P. Sander, E. C. Böttger, M. J. Colston, and P. Draper.** 2002. The functions of OmpATb, a pore-forming protein of *Mycobacterium tuberculosis*. *Mol. Microbiol.* **46**:191-201.
72. **Recht, J., and R. Kolter.** 2001. Glycopeptidolipid acetylation affects sliding motility and biofilm formation in *Mycobacterium smegmatis*. *J Bacteriol* **183**:5718-24.

73. **Rodriguez, G. M., and I. Smith.** 2006. Identification of an ABC transporter required for iron acquisition and virulence in *Mycobacterium tuberculosis*. *J Bacteriol* **188**:424-30.
74. **Sambou, T., P. Dinadayala, G. Stadthagen, N. Barilone, Y. Bordat, P. Constant, F. Levillain, O. Neyrolles, B. Gicquel, A. Lemassu, M. Daffe, and M. Jackson.** 2008. Capsular glucan and intracellular glycogen of *Mycobacterium tuberculosis*: biosynthesis and impact on the persistence in mice. *Mol Microbiol* **70**:762-74.
75. **Savvi, S., D. F. Warner, B. D. Kana, J. D. McKinney, V. Mizrahi, and S. S. Dawes.** 2008. Functional characterization of a vitamin B12-dependent methylmalonyl pathway in *Mycobacterium tuberculosis*: implications for propionate metabolism during growth on fatty acids. *J Bacteriol* **190**:3886-95.
76. **Schaffer, J. E.** 2002. Fatty acid transport: the roads taken. *Am J Physiol Endocrinol Metab* **282**:E239-46.
77. **Schmider, W., A. Fahr, H. E. Blum, and G. Kurz.** 2000. Transport of heptafluorostearate across model membranes. Membrane transport of long-chain fatty acid anions I. *J Lipid Res* **41**:775-87.
78. **Schnappinger, D., S. Ehrt, M. I. Voskuil, Y. Liu, J. A. Mangan, I. M. Monahan, G. Dolganov, B. Efron, P. D. Butcher, C. Nathan, and G. K. Schoolnik.** 2003. Transcriptional adaptation of *Mycobacterium tuberculosis* within macrophages: Insights into the phagosomal environment. *J Exp Med* **198**:693-704.
79. **Schulz, G. E.** 2003. Transmembrane beta-barrel proteins. *Adv Protein Chem* **63**:47-70.
80. **Schulze-Röbbecke, R., and R. Fischeder.** 1989. Mycobacteria in biofilms. *Zentralbl Hyg Umweltmed* **188**:385-90.
81. **Senaratne, R. H., H. Mobasheri, K. G. Papavinasasundaram, P. Jenner, E. J. Lea, and P. Draper.** 1998. Expression of a gene for a porin-like protein of the OmpA family from *Mycobacterium tuberculosis* H37Rv. *J. Bacteriol.* **180**:3541-3547.
82. **Sharbati-Tehrani, S., B. Meister, B. Appel, and A. Lewin.** 2004. The porin MspA from *Mycobacterium smegmatis* improves growth of *Mycobacterium bovis* BCG. *Int J Med Microbiol* **294**:235-45.
83. **Sharman, G. J., D. H. Williams, D. F. Ewing, and C. Ratledge.** 1995. Isolation, purification and structure of exochelin MS, the extracellular siderophore from *Mycobacterium smegmatis*. *Biochem J* **305 (Pt 1)**:187-96.
84. **Simeone, R., D. Bottai, and R. Brosch.** 2009. ESX/type VII secretion systems and their role in host-pathogen interaction. *Curr Opin Microbiol* **12**:4-10.
85. **Siroy, A., C. Mailänder, D. Harder, S. Koerber, F. Wolschendorf, O. Danilchanka, Y. Wang, C. Heinz, and M. Niederweis.** 2008. Rv1698 of *Mycobacterium tuberculosis* represents a new class of channel-forming outer membrane proteins. *J. Biol. Chem.* **283**:17827-37.
86. **Song, H., R. Sandie, Y. Wang, M. A. Andrade-Navarro, and M. Niederweis.** 2008. Identification of outer membrane proteins of *Mycobacterium tuberculosis*. *Tuberculosis* **88**:526-44.
87. **Stahl, C., S. Kubetzko, I. Kaps, S. Seeber, H. Engelhardt, and M. Niederweis.** 2001. MspA provides the main hydrophilic pathway through the cell wall of *Mycobacterium smegmatis*. *Mol. Microbiol.* **40**:451-464 (Authors' correction appeared in *Mol. Microbiol.* **57**, 1509).
88. **Stephan, J., J. Bender, F. Wolschendorf, C. Hoffmann, E. Roth, C. Mailänder, H. Engelhardt, and M. Niederweis.** 2005. The growth rate of *Mycobacterium smegmatis* depends on sufficient porin-mediated influx of nutrients. *Mol. Microbiol.* **58**:714-730.

89. **Stephenson, M. C., and C. Ratledge.** 1980. Specificity of exochelins for iron transport in three species of mycobacteria. *J Gen Microbiol* **116**:521-3.
90. **Sulavik, M. C., C. Houseweart, C. Cramer, N. Jiwani, N. Murgolo, J. Greene, B. DiDomenico, K. J. Shaw, G. H. Miller, R. Hare, and G. Shimer.** 2001. Antibiotic susceptibility profiles of *Escherichia coli* strains lacking multidrug efflux pump genes. *Antimicrob Agents Chemother* **45**:1126-36.
91. **Sulzenbacher, G., S. Canaan, Y. Bordat, O. Neyrolles, G. Stadthagen, V. Roig-Zamboni, J. Rauzier, D. Maurin, F. Laval, M. Daffe, C. Cambillau, B. Gicquel, Y. Bourne, and M. Jackson.** 2006. LppX is a lipoprotein required for the translocation of phthiocerol dimycocerosates to the surface of *Mycobacterium tuberculosis*. *Embo J* **25**:1436-44.
92. **Trias, J., V. Jarlier, and R. Benz.** 1992. Porins in the cell wall of mycobacteria. *Science* **258**:1479-81.
93. **van den Berg, B.** 2005. The FadL family: unusual transporters for unusual substrates. *Curr Opin Struct Biol* **15**:401-7.
94. **Van der Geize, R., K. Yam, T. Heuser, M. H. Wilbrink, H. Hara, M. C. Anderton, E. Sim, L. Dijkhuizen, J. E. Davies, W. W. Mohn, and L. D. Eltis.** 2007. A gene cluster encoding cholesterol catabolism in a soil actinomycete provides insight into *Mycobacterium tuberculosis* survival in macrophages. *Proc Natl Acad Sci USA* **104**:1947-52.
95. **Villeneuve, M., M. Kawai, H. Kanashima, M. Watanabe, D. E. Minnikin, and H. Nakahara.** 2005. Temperature dependence of the Langmuir monolayer packing of mycolic acids from *Mycobacterium tuberculosis*. *Biochim Biophys Acta* **1715**:71 – 80.
96. **Villeneuve, M., M. Kawai, M. Watanabe, Y. Aoyagi, Y. Hitotsuyanagi, K. Takeya, H. Gouda, S. Hirono, D. E. Minnikin, and H. Nakahara.** 2007. Conformational behavior of oxygenated mycobacterial mycolic acids from *Mycobacterium bovis* BCG. *Biochim Biophys Acta* **1768**:1717-26.
97. **Voulhoux, R., M. P. Bos, J. Geurtsen, M. Mols, and J. Tommassen.** 2003. Role of a highly conserved bacterial protein in outer membrane protein assembly. *Science* **299**:262-5.
98. **Wang, L., R. A. Slayden, C. E. Barry, 3rd, and J. Liu.** 2000. Cell wall structure of a mutant of *Mycobacterium smegmatis* defective in the biosynthesis of mycolic acids. *J. Biol. Chem.* **275**:7224-7229.
99. **Watanabe, M., Y. Aoyagi, H. Mitome, T. Fujita, H. Naoki, M. Ridell, and D. E. Minnikin.** 2002. Location of functional groups in mycobacterial meromycolate chains; the recognition of new structural principles in mycolic acids. *Microbiology* **148**:1881-1902.
100. **Werner, J., and R. Misra.** 2005. YaeT (Omp85) affects the assembly of lipid-dependent and lipid-independent outer membrane proteins of *Escherichia coli*. *Mol Microbiol* **57**:1450-9.
101. **Wolschendorf, F., M. Mahfoud, and M. Niederweis.** 2007. Porins are required for uptake of phosphates by *Mycobacterium smegmatis*. *J Bacteriol* **189**:2435-2442.
102. **Wörner, M., O. Lioubashevski, M. T. Basel, S. Niebler, E. Gogritchiani, N. Egner, C. Heinz, J. Hoferer, M. Cipolloni, K. Janik, E. Katz, A. M. Braun, I. Willner, M. Niederweis, and S. H. Bossmann.** 2007. Characterization of nanostructured surfaces generated by reconstitution of the porin MspA from *Mycobacterium smegmatis*. *Small* **3**:1084-1097.
103. **Wu, T., A. C. McCandlish, L. S. Gronenberg, S. S. Chng, T. J. Silhavy, and D. Kahne.** 2006. Identification of a protein complex that assembles lipopolysaccharide in the outer membrane of *Escherichia coli*. *Proc Natl Acad Sci USA* **103**:11754-9.

104. **Zuber, B., M. Chami, C. Houssin, J. Dubochet, G. Griffiths, and M. Daffe.** 2008. Direct visualization of the outer membrane of native mycobacteria and corynebacteria. *J Bacteriol* **190**:5672-5680.

SUMMARY AND CONCLUSIONS

***M. TUBERCULOSIS* PATHOGENESIS AND THE MYCOBACTERIAL CELL ENVELOPE.**

***M. tuberculosis* resides in macrophage phagosomes.** Upon inhalation exposure to *M. tuberculosis*, bacilli are phagocytosed by resident alveolar macrophages where they are compartmentalized in phagosomes and early endosomes. Trafficking vesicles are designed to ultimately deliver pathogens to antimicrobial lysosomes in a process that reduces the pH of the phagosome. However, *M. tuberculosis*-containing vacuoles do not readily acidify and fusion of phagosomes with lysosomes is blocked (81). Entry into host cells is followed by tissue invasion and induction of an immune response, which ultimately remodels the site of infection to a cellular mass called the granuloma designed to isolate, contain, and kill the bacteria (91). Microenvironments inside granulomas differ significantly between granulomas, even within the same infected host (11). Despite structural and compositional differences between granulomas, intra- and extracellular microenvironments encountered by *M. tuberculosis* are primarily restrictive for mycobacterial growth at least partly due to proton exposure, hypoxia, the presence of reactive nitrogen and oxygen intermediates (RNIs and ROIs), and limited nutrient supply (91, 113). However, *M. tuberculosis* has evolved a wide array of defensive mechanisms to cope with the harsh environment of the phagosome. Additionally, *M. tuberculosis* must also have evolved strategies for acquiring nutrients in order to establish persistent infections under these conditions. While the outer membrane presents a barrier between the pathogen and its environment, very little is known about how the outer membrane of

M. tuberculosis contributes to toxic solute defense or how/which proteins functionalize this membrane for the selective uptake of nutrients.

Requirement of surface lipids and proteins. A thick, waxy coating is characteristic of the *Mycobacteriaceae* and is responsible for the hydrophobic nature of these cells and their acid-fastness. Despite very slow growth of many pathogenic species, mycobacteria must take up compounds and extrude waste products as the interchange of molecules with the environment is essential to all cellular life. However, the outer membrane is an efficient permeability barrier (13) across which the diffusion of hydrophilic molecules is too slow to be biologically relevant (78). Functionalization of the outer membrane by proteinaceous effectors is therefore required for the transport of hydrophilic compounds. This is supported by the identification of channel forming proteins in the outer membrane of both fast (77, 112) and slow (98, 101) growing mycobacteria.

Rationale for thesis project. The porin MspA represents the primary mediator of the hydrophilic pathway across the outer membrane of *M. smegmatis* (106). MspA is functionally similar but structurally unique compared to porins of Gram negative bacteria. As a result, the components of MspA which contribute to porin function were unknown. Identification of MspA translocation determinants would be important for our understanding of one of the most fundamental processes of bacterial growth and adaptation to varying environments. Consistent with this, Gram negative bacteria have developed multiple mechanisms of porin regulation at genetic and functional levels (78). Of equal intrigue is that Msp homologues do not exist in pathogenic mycobacteria such as *M. tuberculosis*, nor have general porins been identified in this species. It is therefore

unknown how the hydrophilic pathway is functionalized or regulated in *M. tuberculosis*. To the contrary, MspA serves as a model for transport of small and hydrophilic compounds across mycobacterial outer membranes. Because recombinant proteins from *M. smegmatis* provide the most simplistic approach to examine the hydrophilic pathway in *M. tuberculosis* during infection, high-level, stable expression of integrated genes is required. Therefore, the aims of this dissertation were to A) identify and characterize molecular determinants of translocation through the MspA pore, B) to examine the role of the hydrophilic pathway in *M. tuberculosis* during infection and to determine whether an increase in the efficiency of this pathway would be beneficial or detrimental to virulence, and C) to enhance genomic integration strategies for efficient, stable expression from mycobacterial chromosomes via the generation of a new series of integration vectors.

TRANSLOCATION DETERMINANTS OF MSPA.

This work provides the first identification of MspA translocation determinants and characterizes their influence on the function of the porin. Both the periplasmic loop L6 and specific residues within the constriction zone are required for normal channel function of MspA. Our understanding of how MspA functions for transport of small and hydrophilic compounds is critical to investigations into nutrient, antibiotic, and toxic solute uptake, generation of models for transport across mycobacterial outer membranes, and developing MspA for technological applications.

MspA loop L6 is a molecular determinant of translocation. Because the L6 loop likely does not have a stable structure, is positioned beneath the constriction zone (32), and is accessible to the biotinylation reagent MPB in whole cells (62), it was

proposed that it may influence the translocation properties of MspA. Indeed, deletions in the L6 loop altered translocation of ions and small molecules, pore stability, voltage gating, and expression in the outer membrane. Interestingly, deletion of nearly the entire L6 loop resulted in channels that were still functional *in vitro* and *in vivo* and fully complemented the growth defect of an *M. smegmatis* triple porin mutant. These results identified the L6 loop as a molecular determinant for substrate translocation through the MspA pore. However, it is not essential for channel activity and is dispensable for pore function.

Role of the L6 loop in voltage-dependent gating. The finding that MspA undergoes voltage gating (29) supports the suggestion that voltage-dependent gating may be an intrinsic property of all β -barrel membrane proteins (6). However, the physiological relevance of this phenomenon has not been established (29, 97). Multiple studies have attributed gating to electrostatics of charged residues within the rigid barrel lumen (reviewed in (89)). In contrast, atomic force microscopy (AFM) studies on two-dimensional OmpF crystals identified the extracellular loops as dynamic domains capable of folding over the lumen opening in response to voltage and acid (71). Additionally, the extracellular loop L6 of OmpG was shown to dynamically fold over the barrel lumen and spontaneously gate the pore. Loop-mediated gating was nearly absolved by restricting its motion via cysteine bond mutations at the loop base and enhancement of hydrogen bonding in its connecting β -strands (19). It could be hypothesized that similar motions in the L6 loop of MspA may undergo similar dynamic motions to gate the pore. The results described in this study show that the L6 periplasmic loop does influence, but is not solely responsible, for the voltage gating properties of MspA (29).

As the $\Delta 11$ mutant still exhibited voltage-dependent gating, it can be concluded that dynamic motions of the L6 loop to gate the pore do not occur in response to voltage. Because the vast majority of MspA is folded into rigid β -barrels (32), voltage dependent gating of MspA is likely electrostatic rather than via bulk dynamic motions. This is in agreement with the hypothesis that the electric field within the pore which allows for ion transport is perturbed by an externally applied voltage, ultimately disrupting ion flow (6). Consistent with this, molecular dynamics (MD) simulations of wild-type MspA showed no bulk movements in response to an applied electric field (Aksimentiev, *et. al.*, unpublished data). Interestingly, MD studies of MspA mutants devoid of the L6 loop showed reduced stability and eventual collapse of the constriction zone, suggesting the requirement of the L6 loop for a stable opening in the constriction zone in response to voltage. Thus, the mechanism of voltage-dependent closing for wild-type MspA and MspA L6 deletion mutants may be different.

It remains to be determined if dynamic motions of the L6 loop occur and are important for function under conditional stress. For instance, pH-induced loop closures of the major *E. coli* porin OmpF (71) were discovered to be a rapid response to pH changes. This may allow time for slower responses to initiate, such as switching to the alternative porin OmpC (83). AFM and/or nuclear magnetic resonance (NMR) structure studies may be able to demonstrate L6 loop movements. Alternatively, fluorescence resonance energy transfer (FRET) experiments may help to distinguish between dynamic loop motions from simple side chain realignment during *in vitro* translocation experiments. Due to MspA octamerization and the size restriction of FRET molecules, a single-chain *mspA*

gene encoding the octamer with single point mutations may be required for such experiments.

Role of the constriction zone in voltage gating. In addition to the role of the L6 loop in gating, charged residues within the barrel lumen also significantly contribute to gating. While the constriction zone leucine mutants (D90L and D90/91L) have not been evaluated for voltage sensitivity, triple mutation of the constriction zone aspartic acid residues D90, D91, and the proximal D93 to asparagine increased the critical gating voltage to at least -180 mV (14). This was approx. three-fold the limit of -60 mV for stable wt MspA pores. Deletion mutations in the constriction zone (also called the "eyelet") of OmpF similarly resulted in an increased critical voltage for gating but also failed to identify the constriction zone as the primary determinant of gating (80). Multiple contributing factors to gating were observed in *Haemophilus influenzae* porin in which the combinatorial effects of residues in two extracellular loops and within the channel lumen primarily account for voltage gating (1). Scanning mutagenesis of charged residues within the barrel combined with L6 loop deletions may help to further elucidate the various mechanistic components involved in voltage-induced MspA gating.

Implications of voltage gating for biotechnology. Understanding the gating mechanisms of MspA not only provides important insight into the transport dynamics of mycobacteria, but also has implications for biotechnological applications as well. Because of its inherent stability and pore properties (44), purified MspA can be utilized for nano-devices. Single-stranded DNA molecules can be threaded through the membrane-embedded MspA channel in a voltage-dependent manner (14) to decipher nucleotide base sequences in a process called nanopore DNA sequencing. As individual

bases pass through MspA, ionic conductance through the pore is transiently blocked. Detection of conductance blockade events, which are unique to each base, allows for the discrimination of bases in a strand of DNA, ultimately determining the sequence of the strand (reviewed in (12)). To date, all four DNA nucleotides can be resolved when temporarily stalled within the MspA constriction zone (Derrington, *et. al.*, submitted).

One caveat to nanopore sequencing involves the voltage dependent translocation of DNA through the pore and the counter-productive voltage dependent closing of the pore. In this regard, the MspA D90/91/93N triple mutant represents a significant advance in engineering a "quiet" or stable MspA pore for DNA translocation. The approach to stabilize the pore for nucleotide detection by charge alteration is also novel as previous attempts to successfully stabilize the OmpG pore involved immobilizing an extracellular loop and optimizing the hydrogen bonding network between β -strands (19). While nascent technology to resolve bases exists, further resolution may be obtained with increased voltage. For instance, increased voltage provides greater magnitudes of conductance blockade events. However, higher voltages also accelerate translocation such that sequential resolution of bases is poor. Several methods to slow down translocation include increased viscosity and salt concentration and decreased temperature (34), substitution of the electrolyte solution with organic salts such as butylmethylimidazolium chloride (26), stalling the strand in the pore via duplexed DNA (Derrington *et. al.*, submitted), and transient binding of nucleic acid polymers (as demonstrated with RNA) by a phage RNA packaging motor protein (5). If DNA translocation can be sufficiently slowed, increased voltage may assist in base discrimination. Therefore, it is of value to further delineate the mechanism(s) of voltage

gating to enhance engineering of an even "quieter" MspA pore. Perhaps the $\Delta 3$ mutation can be combined with the triple asparagine mutation, as the $\Delta 3$ mutant itself exhibited reduced gating. Thus, mutants can be constructed to have open pores but be stable against voltage, allowing for unrestricted passage of DNA and increased base resolution at higher applied voltages. The same concept applies for devices designed to detect nanoscale amounts of small molecules such as metal ion contaminants in drinking water.

The L6 loop is required for expression in the outer membrane. Reduced expression of MspA in the outer membrane was evident in large deletions of the L6 loop. Several reasons may account for this result including destabilization of the mRNA transcript or protein product, reduced membrane insertion efficiency, or instability in the outer membrane. Gram negative bacteria such as *E. coli* employ several systems to coordinate proper outer membrane protein insertion and removal of misfolded or superfluous proteins. Along with several other proteins, YaeT, a homologue of the Neisserial Omp85 protein (116), is required for correct insertion of proteins into the outer membrane while DegP and DegS are primarily responsible for recognizing and degrading misfolded or incorrectly inserted membrane proteins (67). In many cases, the C-terminal signal recognized by periplasmic chaperones and the YaeT membrane insertion machinery is the same signal exposed to the periplasmic DegS after misfolding in the membrane (10). No proteinaceous machinery for outer membrane protein insertion has been identified in mycobacteria and no known C-terminal signal is present in MspA. However, *M. tuberculosis* contains at least one exported protease that exhibits homology to DegP and DegS, chaperone activity, protein degradation activity, and is required for

virulence (69). Thus, functional analogues of outer membrane protein biogenesis and turn-over likely exist in mycobacteria.

In support of this hypothesis, the rim domain of MspA is surface accessible *in vivo* as determined by accessibility to the biotinylation reagent MPB (62) and to a monoclonal antibody specific for an extracellular epitope (unpublished results and this work). To the contrary, MspA reconstitutes unidirectionally into lipid vesicles and artificial bilayers in the opposite orientation via the more hydrophobic periplasmic end first (29). This same *in vitro* reverse insertion orientation phenomenon has been observed for OmpF of *E. coli* (88) and suggests the need for machinery to properly orient porins in the outer membrane. Additionally, membrane rigidity reduces the insertion capabilities of proteins (9). It has been experimentally shown that a fluidity gradient exists across the cell envelope of mycobacteria, with the inner leaflet being less fluid than the outer leaflet (61). This is due to covalent linkage of the mycolic acid heads to the arabinogalactan-peptidoglycan cell wall (60). It may be that outer membrane protein insertion through the rigid inner leaflet of mycobacteria is less efficient, suggesting that MspA requires other effectors for proper membrane insertion *in vivo*. Such insertion machinery likely also exists in *M. tuberculosis* as MspA can be functionally expressed in this organism (63). Identification of a functional Omp85 homologue in mycobacteria would be extremely beneficial as it would very likely interact with multiple outer membrane proteins. Cross-linking experiments with an Omp85-like protein may help to identify other yet-unknown outer membrane proteins of mycobacteria. As *omp85* is essential for the viability of *Niesseria meningitidis* (117), a mycobacterial functional homologue may represent an

attractive, surface-accessible drug target and greatly expand our understanding of protein biogenesis in the mycobacterial outer membrane.

An alternative explanation for reduced expression of MspA L6 loop deletion mutants in the outer membrane is that this loop may be required for stability of a putative aromatic belt. Membrane proteins typically contain aromatic residues positioned at the interface of hydrocarbon tails and charged phospholipid heads in the aqueous phase (56). Presumably, aromatic residues positioned at the membrane-water interface accommodate dielectric fluctuations (20), protect against slow membrane movements (96), mechanically stabilize the protein (59), and prevent aggregation (57). A strikingly clear aromatic belt is present at the extracellular interface of MspA which defines its surface accessible zone (62), suggesting that the physicochemical properties governing protein stability at the membrane-water interface also apply to the structurally unique mycobacterial outer membrane and its integral proteins. Several aromatic residues may contribute to this belt, which likely explains the tolerance to cysteine mutagenesis of each one individually. A single phenylalanine at position 99 is located in the L6 loop and has been suggested to form an aromatic belt at the inner leaflet interface (62). Upon deletion of five amino acids from the L6 loop, Phe99 is removed. Interestingly, the $\Delta 5$ mutation produced functional protein that complemented *in vivo* permeability defects without reduced expression. This demonstrates that a putative aromatic belt in the inner leaflet formed by Phe99 is not essential. This is in contrast to OmpA of *E. coli* where triple mutation to alanine of three out of the six aromatic residues in the outer leaflet belt greatly reduced thermodynamic stability (48). Perhaps the outer leaflet belt alone is sufficient for overall protein stability and large deletions destabilize β -structure and

hence, overall protein stability. In support, computer modeling suggests that large L6 deletions (such as $\Delta 9$ and $\Delta 11$) results in altered β -strand formation in the constriction zone (not shown). This may be because the correct strand tilt cannot be obtained without a sufficient linker. Alternatively, it may be possible that heterooligomerization with endogenous MspB donates enough stabilization via its Phe99. To our knowledge, no study has entirely eliminated an aromatic belt via mutagenesis nor do any crystal structures of outer membrane proteins show a missing belt. Thus, the absolute requirement for at least one aromatic residue at the lipid-water interface is not known. The direct role of Phe99 may therefore be examined by rescuing the viability defect of the quadruple *msp* porin mutant of *M. smegmatis* (which contains no Msp porins) with an integrated *mspA* F99A mutant.

If it can be directly shown that Phe99 does not form an essential aromatic belt, an alternative explanation for reduced expression in the outer membrane may be that large deletions in the L6 loop shorten the length of the protein such that it does not sufficiently span the outer membrane and make essential hydrophobic contacts, thus destabilizing integration into the bilayer. Though hydrophobic mismatching may warp the bilayer to align acyl chains with hydrophobic residues (25), severe warping stress may ultimately destabilize protein integration in the membrane. Putative destabilization, however, does not affect channel function as all mutants complemented *M. smegmatis* porin mutant phenotypes. It is important to note that while the interface region of MspA along the outer leaflet is well defined (62), the exact cross-sectional interface at the inner leaflet has only been postulated. Experiments determining the accessibility of cysteine mutants at

the periplasmic end of MspA when reconstituted into artificial membranes may help to determine the interface at this region.

The translocation properties of L6 deletion mutants were altered in regards to both small ions and larger molecules such as monosaccharides, identifying the L6 loop as a molecular determinant of translocation through the MspA channel. Despite extensive influence on the channel properties of MspA, the L6 loop was dispensable for porin function as even the $\Delta 11$ mutant complemented the growth defect of the triple porin mutant *M. smegmatis* ML16. As discussed, the transport properties of MspA are likely influenced by cumulative effects of multiple determinants.

The constriction zone is a molecular determinant of translocation.

Translocation determinants may be identified by expressing randomly mutagenized *mspA* genes in *M. smegmatis* ML16 in search of transformants without rescued growth.

However, the functions of MspA are relatively resistant to mutation (62) and mutations may affect expression or localization rather than channel function. Alternatively, a structure-based approach indicates that the constriction zone likely influences the channel properties of MspA. The constriction zone is a region lined with 16 aspartic acid residues with a narrowed diameter of 1 nm (32). Indeed, mutation of the constriction zone Asp90 to Leu resulted in a transport-impaired channel. Altered channel properties as opposed to other effects were likely the reason for translocation deficiency as a second mutation, Asp91→Leu partially complemented for transport and stabilized the pore. Formation of a stable pore via double mutation to leucine shows that charged residues are not required to repel the channel open and indicate maintenance of the gross quaternary structure of the protein octamer. Additionally, the single D90L mutant was detected on the cell surface,

indicating altered channel properties rather than incorrect localization. Circular dichroism (CD) spectra may confirm correct folding of MspA mutants. These results confirmed the constriction zone as a molecular determinant of translocation for MspA, in agreement with previous findings (14).

These results indicate that within this zone, coexistence of charged and hydrophobic residues result in a destabilized pore and resist passage of ions and small, hydrophilic molecules. To the contrary, existence of either charged or hydrophobic residues alone retain translocation capabilities, albeit with different channel properties. Partial complementation of glucose transport by MspA D90L/D91L may be due to resistance of passage by hydrophobic residues to larger hydrophilic molecules. Alternatively, hydrophobic effect may slightly collapse the constriction zone to sterically block passage of larger molecules but not smaller ions. An exhausted literary search did not identify any studies in which coexistence of charged and hydrophobic residues in the channel eyelet destabilized a porin from Gram negative bacteria. Thus, this work provides a novel approach to generate non-functional porin channels. It is unknown whether the influence of the L6 loop on the channel properties of MspA is due to direct contributions by the loop itself or stems from secondary effects imparted by the loop on the constriction zone.

***IN VIVO* EXAMINATION OF THE HYDROPHILIC PATHWAY ACROSS THE OUTER MEMBRANE OF *M. TUBERCULOSIS*.**

During infection, *M. tuberculosis* resides in macrophage phagosomes where it must acquire nutrients while resisting the uptake of toxic solutes. Because *M. tuberculosis* encounters both types of compounds *in vivo*, it was unclear whether the

growth of *M. tuberculosis* during animal infection would be enhanced due to increased nutrient acquisition or compromised due to increased toxic solute uptake. The results presented in this work show that expression of functional pores in the outer membrane drastically reduce the virulence of *M. tuberculosis* in mice.

Investigating the requirement of the cell wall for virulence. It has been shown by a multitude of experiments that an intact cell wall is required for virulence of *M. tuberculosis*, but these studies were not designed to isolate and examine the hydrophilic pathway across the outer membrane. For instance, inability to synthesize or correctly localize to the outer membrane a class of free lipids called phthiocerol dimycocerosates (DIMs) resulted in increased permeability (15) and decreased virulence (16, 21). However, DIM lipids also play a role in phagocytic uptake and inhibition of phagosome maturation (4), RNI resistance (90), and defense against an IFN- γ -independent immune response (73). Additionally, loss of DIM molecules would result in altered outer membrane architecture and thus, non-specific permeability defects. The multiple *in vivo* roles of DIM show that these molecules cannot be used to study the role of outer membrane permeability to hydrophilic compounds during infection. The same can be applied to many other free lipids such as trehalose dimycolate (TDM; also known as "cord factor"), which is also known to have immunomodulatory effects (92), as well as to covalently attached mycolic acids of which deletion mutants are not viable (82).

An appropriate approach to examining the role of the hydrophilic pathway across the outer membrane permeability barrier is via porins. However, no homologues of known general porins from other mycobacteria or Gram negative bacteria are found in *M. tuberculosis*. Yet, at least several channel forming proteins have been identified in the

outer membrane of *M. tuberculosis* (55, 98, 101). Of these, the virulence factor OmpATb was identified by weak homology to OmpA of *E. coli* (98) and was previously reported to be a porin with pH-dependent activity (87). Deletion of *ompATb* resulted in reduced uptake of several small, hydrophilic molecules. These results show that proteinaceous effectors exist in the outer membrane of *M. tuberculosis* to functionalize the hydrophilic pathway across this compartment. However, categorization of OmpATb as a general porin has been questioned (75) because both overall cellular permeability and OmpATb channel activity are reduced at pH 5.5 compared to pH 7.2, while strong induction of *ompATb* occurs under the same acidic conditions compared to neutral pH. Additionally, while uptake of serine was reduced in the mutant, uptake of glycine was enhanced. Delayed growth of the mutant also occurred at pH 5.5 while growth was identical to the wt at pH 7.2 (87). These results suggest that the primary function of OmpATb is not that of a porin and instead, an alternative function of OmpATb may be required for pH adaptation (75). Indeed, it was recently found that OmpATb has no general porin activity but is required for neutralization of acidic medium (Song *et. al.*, submitted), suggesting it may be involved in neutralizing excess protons in the phagosome. Fusion of a secretion signal to a pH-sensitive Gfp and expression of the construct in wild-type and *M. tuberculosis* Δ *ompATb* during macrophage infections may allow for direct measurements of phagosomal pH and examine the role of OmpATb in pH adaptation. Identification of putative secreted basic compounds via OmpATb would shed light on the mechanisms by which *M. tuberculosis* blocks phagosome acidification. Taken together, the role of the hydrophilic pathway in the virulence of *M. tuberculosis* has never been accurately assessed in animal infection experiments.

Outer membrane permeabilization by MspA reduces virulence. The results described here show that tipping the balance of nutrient and toxic solute uptake by increasing the efficiency of the hydrophilic pathway across the outer membrane is absolutely detrimental to the virulence of *M. tuberculosis*. Even slight perturbations to this balance create detrimental effects as only minute MspA expression significantly reduced virulence. The MspA D90L mutant served as a control to distinguish between virulence defects due to permeabilization of the outer membrane or other non-specific effects of MspA expression in the outer membrane. The partial complementation of the virulence defect by MspA D90L expression suggests that both permeabilization and other non-specific effects account for the reduced virulence of *M. tuberculosis* expressing functional MspA pores. Virulence defects arising from effects of MspA in the outer membrane other than permeabilization cannot be determined by these experiments, but may include local lipid packing disruptions or other membrane defects, effects on other membrane proteins, and/or effects on host cells. These results suggest that pathogenic mycobacteria such as *M. tuberculosis* may have resorted to reduced efficiency of the hydrophilic pathway across their outer membranes to resist influx of toxic solutes at the expense of reduced nutrient uptake. In agreement, *M. smegmatis* regulates porin expression to balance nutrient and toxic compound uptake (46). Similarly, *E. coli* switches from the more efficient ion conducting channel OmpF to the less efficient OmpC under adverse conditions in the intestinal tract, which includes concentrated bile salt exposure (78). However, it is unclear whether slow growth of pathogenic mycobacteria was at least partially a result of or a prerequisite for slow growth adaption.

Antimycobacterial phagosomal constituents. Expression of MspA porins in *M. tuberculosis* may allow for the identification of constituents capable of killing the organism *in vivo*. Killing of *M. tuberculosis* by a lysosomal ubiquitin-derived peptide is enhanced when MspA is expressed, although the mechanism of enhancement appears to be independent of the channel activity of MspA (84). Immunodepletion of ubiquitin-derived peptide from solubilized lysosomes only partially restored resistance to solubilized lysosomes, indicating either incomplete immunodepletion of the peptide below toxic levels or the presence of other molecules in solubilized lysosome extracts capable of killing *M. tuberculosis* expressing MspA pores.

While *M. tuberculosis* appears to have efficient mechanisms to resist the oxidative burst by macrophages (74), it is thought that reactive nitrogen species such as nitric oxide (NO) contribute to killing of *M. tuberculosis* (17). Expression of MspA may facilitate diffusion of NO in the same manner that aquaporin increases the diffusion rate of NO in both liposomes and mammalian ovary cells (45). *In vitro* NO killing assays may determine if MspA porins facilitate NO diffusion and hence, death of *M. tuberculosis* in the same manner that porin deletion mutants of *M. smegmatis* are more resistant to NO *in vitro* and have enhanced survival in macrophages (31). Decreased susceptibility of *M. tuberculosis* expressing MspA in iNOS $-/-$ mice may show translation of this phenomenon *in vivo*. It should be noted that *M. tuberculosis* contains additional mechanisms to cope with nitrosative stress not present in *M. smegmatis* (79).

It is unlikely that partial complementation of resistance to lysosomal extracts immunodepleted of ubiquitin-derived peptide is due to the presence of NO alone as its half-life is in the order of seconds (99), which renders NO too unstable for lysosome

extraction, solubilization, and immunodepletion. Therefore, compounds other than NO and ubiquitin-derived peptide with the capacity to kill *M. tuberculosis* expressing MspA pores may exist in the phagosome. For instance, a respiratory burst dependent on the NADPH oxidase complex is not required for killing wild-type *M. tuberculosis* as Phox *-/-* mice were still capable of controlling infection (52). While *M. tuberculosis* contains several effective reactive oxygen intermediate (ROI) detoxifying enzymes (28), decreased permeability may also be a passive defense mechanism against ROIs. Reduced survival of *M. tuberculosis* expressing MspA in wild-type mice compared to Phox *-/-* mice may indicate support for such a hypothesis. Alternatively, MspA pores may allow for increased proton influx. Experiments with IFN- γ activated macrophages treated with the V-ATPase proton pump inhibitor concanamycin A along with *in vitro* acid susceptibility assays may show whether resistance to proton uptake by impermeability is required for *M. tuberculosis* virulence. Results of these experiments may identify toxic phagosomal compounds to which *M. tuberculosis* at least partially defends itself against via low permeability.

Identification of *M. tuberculosis* outer membrane proteins and their physiological roles in nutrient acquisition. The identification of porins or other outer membrane proteins selective for nutrient uptake by *M. tuberculosis* would allow for the examination of how inversely tipping the balance of small and hydrophilic solute uptake across the outer membrane affects virulence. While our results show that unregulated influx of molecules is detrimental to virulence, it is unknown how reduced influx of hydrophilic molecules would affect growth *in vivo*. Identification of such outer membrane transport proteins would also shed light on the types of nutrients utilized by

M. tuberculosis during infection. Targeted deletions of bioinformatically predicted outer membrane proteins (105) may identify mutants with reduced or no growth on minimal media supplemented with single carbon nutrient sources. If these nutrients are required *in vivo*, such mutants with altered growth on plates should also have reduced virulence in mice. Transport defects as the probable cause for reduced virulence may be confirmed by radiolabeled uptake assays. For instance, the finding that the glyoxylate shunt is required for *in vivo* survival (72) suggests that *M. tuberculosis* must acquire fatty acids for growth. Fatty acids may be obtained by hydrolysis of host lipids (58) as evidenced by the joint requirement of secreted phospholipases for virulence (86). However, anionic fatty acid transport across membranes is slow (53, 95). Avirulent mutants of confirmed outer membrane proteins producing a similar inability to metabolize fatty acids may be candidates for a FadL functional homologue, the protein required for fatty acid uptake across outer membranes of Gram-negative bacteria (114). The SugABC and LpqY probable inner membrane sugar import proteins are required for early growth in mice (94), suggesting that carbohydrates are an important nutrient source early in infection. Mutants with reduced growth on carbohydrates *in vitro* may identify outer membrane sugar transporters. Screening such outer membrane protein mutants on an array of carbohydrates may identify which sugars are required for growth by *M. tuberculosis*. It is unknown how long carbohydrates are metabolized or when lipid metabolism becomes essential, but a metabolic switch from carbohydrates to lipids may occur during *M. tuberculosis* infection (76). Deletion of outer membrane sugar transporters may shed light on carbohydrate availability and metabolic adjustments to β -oxidation. Taken together, the identification of outer membrane transport proteins would help to understand the

physiology of *M. tuberculosis* during infection and elucidate which nutrients are available and required for growth *in vivo*.

An alternative paradigm for *M. tuberculosis* pathogenesis and its implication for solute uptake. Insight into *M. tuberculosis* metabolism and mechanisms of virulence may not be identified solely within the constraints of the phagosomal compartment of host cells. Recent evidence suggests that *M. tuberculosis* escapes from the phagosome into the cytosol (65, 115). The secreted protein ESAT-6 is required for virulence and lyses membranes in acidic conditions (24, 49). The closely related pathogen *Mycobacterium marinum* (107) requires ESAT-6 to escape vacuoles where it exhibits motility via actin polymerization in the cytosol (103). Later, it was shown that both cytosolic *M. marinum* and *M. tuberculosis* exhibit cell-to-cell spreading by ejection from cell membranes of *Dictyostelium*, an amoeba that maintains similar innate defense mechanisms as human macrophages. This process requires formation of an actin-based, non-lytic "ejectosome" that requires ESAT-6 secretion (41). These studies suggest *M. tuberculosis* may escape host vacuoles via secretion of ESAT-6 and gain access to the cytosol where cell-to-cell spreading can commence.

The apparent conundrum is why *M. tuberculosis* expressing MspA has reduced virulence if it can gain access to the nutrient rich, low-toxin environment of the cytosol. In this environment, MspA pores would be expected to be beneficial for increased nutrient uptake considering MspA increases the growth rate of *M. tuberculosis* in culture (63, 84). Additionally, several auxotrophic mutants are essentially avirulent in mice (39, 47, 50, 93, 102), suggesting these mutants cannot acquire nutrient supplements to complement auxotrophy. While it is widely accepted that *M. tuberculosis* survives and

replicates within macrophage phagosomes and spreads by cell lysis, it may be that the life cycle of the bacillus is more complex, involving a stage of persistence in phagosomes, subsequent escape into the cytosol, and initiation of direct cell-to-cell spreading. In both cases, the phagocytic vacuole is the first compartment the bacilli encounters and must adjust to (Dr. Thierry Soldati, personal communication), and it may be that this first phase persists for some time. ESAT-6 of *M. tuberculosis* must dissociate from its co-secreted counterpart Cfp-10 to exhibit membrane binding activity. Complex dissociation *in vitro* occurs slowly at pH 6.5, but is greatly enhanced between pH 4 and pH 5. Because *M. tuberculosis* is known to block phagosomal acidification (81), this may delay escape by prevention of ESAT-6/Cfp-10 dissociation. Along these lines, *M. tuberculosis* translocates to the cytosol less frequently than *M. marinum* (41).

It is plausible that auxotrophy or outer membrane permeabilization by MspA exerts detrimental effects within the phagocytic vacuole prior to escape. In support, ejectosome formation does not peak until after 24-36 hours (41, 42). Alternatively, it may be that permeabilization or auxotrophy inhibit phagosomal escape. Damage due to permeabilization or lack of essential nutrients due to auxotrophy may inhibit timely production of escape factors. Conversely, surface expression of MspA may influence the initial interaction with phagocytic cells as the outcome of infection may be linked with these early events (37, 118). Time course studies with electron microscopy may identify the presence of such *M. tuberculosis* mutants in the phagosome or the cytosol. To determine if phagosome residing bacteria cannot escape because they are quickly killed, bacteria may be harvested and plated for viability. Additionally, mycobacteria-containing

vacuoles may be purified and stained for late endosomal markers, indicating maturation of the endocytic pathway.

Postulates for translational research in the treatment of Tuberculosis. The compromised virulence of *M. tuberculosis* expressing MspA suggests that the influx of toxic solutes largely outweighs the benefits of increased nutrient uptake. Several translational applications may be conceived in light of these results. Integration of *mspA* in the *M. tuberculosis* chromosome may be beneficial for enhanced vaccine strain development. For instance, the BCG vaccine is primarily attenuated by loss of a genetic region encoding a Type VII secretion system required for release of the virulence factors ESAT-6 and Cfp-10 (100), yet these factors are also required for proper stimulation of T-cell mediated responses (64). Inclusion of *mspA* in a secretion competent strain may generate an attenuated vaccine that still expresses all key antigens and immunologically relevant factors. Alternatively, integration of *mspA* in a mycobacteriophage genome may increase phage-induced toxicity in phage therapy experiments. Studies have shown that delivery of mycobacteriophage TM4 via non-pathogenic mycobacteria vessels aids in killing infectious mycobacteria in mice (23). Phage-mediated expression of MspA may also enhance the chemotherapy of hydrophilic drugs. Results of this work also imply that drugs designed to block outer membrane biogenesis may lead to permeability defects and enhanced killing of *M. tuberculosis*. Along these lines, *M. tuberculosis* mutants compromised for cell wall biogenesis are attenuated *in vivo* (8). However, the high impermeability of the outer membrane presents a diffusion barrier to drugs that much reach intracellular targets of membrane biogenesis. Thus, surface targets are advantageous as drugs do not have to cross the notoriously impermeable outer

membrane. A novel approach to permeabilize the outer membrane of infectious *M. tuberculosis* bacilli is to design a drug that selectively binds to and alters mycolic acid cyclopropane rings in the outer membrane. Cyclopropane rings are required for virulence and loss of these lipid modifications results in compromised cell wall architecture and increased permeability (7). Additionally, cyclopropanation occurs on covalently attached mycolic acids which are not shed from the bacterium, and this modification does not exist in human cellular membranes. Permeabilization may possibly be enhanced by fusion of a cyclopropane ring-binding compound with a lipid packing disruption domain such as a lytic peptide, a short chain ceramide (33), or a dendromer (66).

A NEW SERIES OF INTEGRATION-PROFICIENT VECTORS.

Expression levels are often proportional to complementation levels and/or phenotypic severity. Consistent with this, low-level expression of *mspA* from an integrated cassette produced a modest but significant virulence defect while higher level expression from a multi-copy episomal vector resulted in drastic virulence defects. However, only stably integrated constructs may be maintained in the presence of selection pressure. Loss of the *mspA* episomal plasmid during infection in mice underscores that permeabilizing MspA porins are selected against by *M. tuberculosis*. Resultant (though delayed) death of infected mice due to reversion to wild-type *M. tuberculosis* highlights the challenges of examining genes with deleterious effects for the bacilli *in vivo*. Therefore, to better understand the role of the hydrophilic pathway during infection, stable, high-level expression of *mspA* is required. Thus, it is desirable to generate an *M. tuberculosis* strain carrying a stable, integrated *mspA* cassette producing

higher-level expression to generate similar phenotypes observed with multi-copy episomal constructs.

Chromosomal vs. episomal gene expression. To address the needs described above, the reasons for disproportionately lower expression yields of integrated constructs compared to episomal vectors (109) must be investigated. Similar Gfp fluorescence levels obtained when the gene is flanked by bi-directional intrinsic transcriptional terminators indicates that transcriptional interference does not strongly affect expression from the mycobacteriophage L5 attachment site. Similar expression yields from multiple sites within the chromosome also indicate that disparate nucleoid compaction does not account for reduced expression. Inactivity of the transcription terminators is unlikely as all bacterial RNA polymerases are highly homologous and are terminated by similar mechanisms (3) and similar terminators were shown to be functional in mycobacteria (111). However, direct transcriptional termination activity may be demonstrated by positioning the terminators between a promoter and a reporter gene. An alternative explanation may be that copy numbers of pAL5000-based episomal plasmid are higher than most estimates in the range of two to five (85, 108, 109). Gavigan *et. al.* observed a pAL5000-based plasmid to have a copy number of eight by counting single-cell kanamycin resistant clones (36). The use of qPCR may provide a more quantitative determination of copy number. The similar expression levels observed at different chromosomal locations indicates that no inexplicable phenomenon occurs at the commonly utilized L5 *attB* site which reduces expression.

Increased global expression from mycobacterial chromosomes. It is possible that disproportionately reduced expression from integrated cassettes may actually be the

result of inaccurate calculations of episomal copy numbers. More importantly, a method to increase expression by multiple integrations in the same strain was developed.

Interestingly, Gfp fluorescence did not increase proportionately with chromosomal copy number. The same phenomenon was observed when the copy number of an episomal vector was increased 10-fold but Gfp fluorescence increased only 4 to 6-fold (68).

Reduced fluorescence may possibly be the result of self aggregation of Gfp (22) or inner filter effects (27), suggesting that fluorescence measurements are not optimal methods for correlating plasmid copy numbers and expression levels. A more quantitative method should be to measure activity of an expressed enzyme. Nonetheless, superintegrating cassettes is a practical method to increase gene expression from the chromosome.

One drawback of increasing expression via multiple integrations is the time required to integrate a plasmid, excise the backbone, and integrate a second plasmid. In *M. tuberculosis*, this time requirement is in the order of months. One way to circumvent this hindrance is via co-transformation of at least two plasmids that simultaneously integrate at different attachment sites. However, such a shortcut is limited to the number of different resistance markers available as well as the number of attachment sites for which phage integration machinery has been identified and cloned. Additionally, it remains to be determined if backbone removal of multiple co-transformed plasmids can be achieved. This is theoretically possible, as a recombinase could be expected to perform two enzymatic reactions in the same cell prior to counter-selection. Thus, the frequency of obtaining dual antibiotic sensitive clones against a background of single sensitive or dual resistant clones should be determined. Site-directed recombination between a recombinase recognition site from one plasmid to the same site on another

plasmid elsewhere in the chromosome would excise large chromosomal regions and render these clones non-viable. Alternatively, integrating plasmids may be adapted to two different recombinase-mediated excision systems. Therefore, subsequent transformation of a vector expressing two different recombinases may independently excise each backbone.

Alternative means of increasing gene expression. If chromosomal expression can be increased by multiple integrations but is limited by available resistance cassettes and phage integration machinery, one must resort to other means if expression yields remain insufficient. Much of these mechanisms are well studied in model organisms such as *E. coli*, but are at best only poorly understood or absent in mycobacteria. For instance, expression of genes driven by phage RNA polymerase has exhibited a profound level of success in *E. coli* (110). The T7 RNA polymerase (RNAP) is a simplistic, single-subunit polymerase capable of transcribing DNA independent of other cellular factors five times faster than the multi-subunit bacterial RNAP of *E. coli* (18, 38). Unfortunately, no mycobacteriophage is known to encode a phage RNAP to date (Dr. Graham Hatfull, personal communication), and earlier reports that mycobacteriophage D29 was an exception (51), were later proven otherwise (35, 43).

However, other alternatives to increase expression in mycobacteria do exist. Aside from encoding consensus promoter and Shine-Delgarno sequences, expression of an integrated gene may be enhanced by inclusion of a promoter UP element. These sequences are located upstream of σ factor binding sites, are A/T rich, and bind the α subunit of RNA polymerase (RNAP) to enhance promoter binding (40). Encoding the consensus UP element in the promoter can increase expression by over 300-fold in *E. coli*

(30). The highly conserved region of the α -subunit which binds UP elements suggests that this may be an efficient, functional feature in most bacteria (40). However, the *rrnB* upstream activating region (UAR) of *M. smegmatis* does not appear to contain a factor-independent UP element (2), while the *rrnB* operon of *E. coli* serves as a paradigm for promoter UP elements (40). To the contrary, the UAR of *katG* increases *katG* expression, its expression enhancement properties are transferrable when fused to other mycobacterial promoters, and it displays some sequence resemblance to UP elements (70). Determination of whether consensus UP elements enhance promoter activity in mycobacteria would be beneficial for expression studies. This may be accomplished by encoding known promoter UP elements from both Gram-positive and Gram-negative bacteria in upstream regions of mycobacterial promoters. Additionally, it would be interesting to determine if the *katG* UAR enhances gene expression from highly active, constitutive mycobacterial promoters such as *p_{smyc}* (54) and *p_{hsp60}* (109).

Codon optimization of the gene sequence may also increase expression (104), but does not appear to be beneficial if the original sequence is G + C rich and void of rare codons, as was observed for the ~58 % G + C rich *xylE* (not shown). Thus, this would not be expected to increase *mspA* expression in *M. tuberculosis* but may apply for other non-mycobacterial A + T rich genes. Interestingly, codon optimization may allow for efficient expression of i.e. T7 RNAP in mycobacteria, thus indirectly opening new avenues for modifications of gene expression. Though the strategies to improve gene expression are countless, listed above are several approaches that may help to curb low chromosomal expression in mycobacteria.

CONCLUSIONS.

The outer membrane of mycobacteria presents an efficient permeability barrier which must be functionalized by proteins for the transport of nutrients while resisting the uptake of toxic compounds. As *M. tuberculosis* resides in a subcellular compartment where molecules of both value and toxicity exist, our understanding of the functional effectors in the outer membrane diffusion barrier is of paramount importance. This work has identified and characterized the periplasmic L6 loop and the constriction zone as molecular determinants for the activity of the channel protein MspA. These results aid in building a model of small and hydrophilic molecule transport in mycobacteria. While MspA is highly beneficial for the growth of *M. smegmatis*, its permeabilizing effects are absolutely detrimental to *in vivo* survival of *M. tuberculosis*, thus explaining the absence of general porin homologues in this pathogen. The direct relationship between expression levels and toxicity of MspA highlight the need for efficient methods to produce stable integration cassettes with high expression levels in mycobacteria. Therefore, a series of integration proficient vectors were constructed which, when used in tandem, increase the global expression of integrated genes. Thus, the identification of outer membrane transport proteins and characterization of their functional mechanisms is of critical importance to understanding the balance between selective nutrient uptake and resulting virulence and the resistance to toxic compound influx. Future research in this area may identify drug targets for which low diffusion kinetics across the outer membrane are not pertinent or the generation of novel attenuated vaccine strains which do not require deletion of virulence factors that double as antigenic targets.

REFERENCES

1. **Arbing, M. A., J. W. Hanrahan, and J. W. Coulton.** 2001. Mutagenesis identifies amino acid residues in extracellular loops and within the barrel lumen that determine voltage gating of porin from *Haemophilus influenzae* type b. *Biochemistry* **40**:14621-8.
2. **Arnvig, K. B., B. Gopal, K. G. Papavinasundaram, R. A. Cox, and M. J. Colston.** 2005. The mechanism of upstream activation in the *rrnB* operon of *Mycobacterium smegmatis* is different from the *Escherichia coli* paradigm. *Microbiology* **151**:467-73.
3. **Artsimovitch, I., V. Svetlov, L. Anthony, R. R. Burgess, and R. Landick.** 2000. RNA polymerases from *Bacillus subtilis* and *Escherichia coli* differ in recognition of regulatory signals in vitro. *J Bacteriol* **182**:6027-35.
4. **Astarie-Dequeker, C., L. Le Guyader, W. Malaga, F. K. Seaphanh, C. Chalut, A. Lopez, and C. Guilhot.** 2009. Phthiocerol dimycocerosates of *M. tuberculosis* participate in macrophage invasion by inducing changes in the organization of plasma membrane lipids. *PLoS Pathog* **5**:e1000289.
5. **Astier, Y., D. E. Kainov, H. Bayley, R. Tuma, and S. Howorka.** 2007. Stochastic detection of motor protein-RNA complexes by single-channel current recording. *Chemphyschem* **8**:2189-94.
6. **Bainbridge, G., I. Gokce, and J. H. Lakey.** 1998. Voltage gating is a fundamental feature of porin and toxin beta-barrel membrane channels. *FEBS Lett* **431**:305-8.
7. **Barkan, D., Z. Liu, J. C. Sacchettini, and M. S. Glickman.** 2009. Mycolic acid cyclopropanation is essential for viability, drug resistance, and cell wall integrity of *Mycobacterium tuberculosis*. *Chem Biol* **16**:499-509.
8. **Barry, C. E.** 2001. Interpreting cell wall 'virulence factors' of *Mycobacterium tuberculosis*. *Trends Microbiol* **9**:237-41.
9. **Booth, P. J., M. L. Riley, S. L. Flitsch, R. H. Templer, A. Farooq, A. R. Curran, N. Chadborn, and P. Wright.** 1997. Evidence that bilayer bending rigidity affects membrane protein folding. *Biochemistry* **36**:197-203.
10. **Bos, M. P., V. Robert, and J. Tommassen.** 2007. Biogenesis of the gram-negative bacterial outer membrane. *Annu Rev Microbiol* **61**:191-214.
11. **Boshoff, H. I., and C. E. Barry, 3rd.** 2005. Tuberculosis - metabolism and respiration in the absence of growth. *Nat Rev Microbiol* **3**:70-80.
12. **Branton, D., D. W. Deamer, A. Marziali, H. Bayley, S. A. Benner, T. Butler, M. Di Ventra, S. Garaj, A. Hibbs, X. Huang, S. B. Jovanovich, P. S. Krstic, S. Lindsay, X. S. Ling, C. H. Mastrangelo, A. Meller, J. S. Oliver, Y. V. Pershin, J. M. Ramsey, R. Riehn, G. V. Soni, V. Tabard-Cossa, M. Wanunu, M. Wiggins, and J. A. Schloss.** 2008. The potential and challenges of nanopore sequencing. *Nat Biotechnol* **26**:1146-53.
13. **Brennan, P. J., and H. Nikaido.** 1995. The envelope of mycobacteria. *Annu. Rev. Biochem.* **64**:29-63.
14. **Butler, T. Z., M. Pavlenok, I. M. Derrington, M. Niederweis, and J. H. Gundlach.** 2008. Single-molecule DNA detection with an engineered MspA protein nanopore. *Proc Natl Acad Sci U S A* **105**:20647-52.

15. **Camacho, L. R., P. Constant, C. Raynaud, M. A. Laneelle, J. A. Triccas, B. Gicquel, M. Daffé, and C. Guilhot.** 2001. Analysis of the phthiocerol dimycocerosate locus of *Mycobacterium tuberculosis*. Evidence that this lipid is involved in the cell wall permeability barrier. *J. Biol. Chem.* **276**:19845-54.
16. **Camacho, L. R., D. Ensergueix, E. Perez, B. Gicquel, and C. Guilhot.** 1999. Identification of a virulence gene cluster of *Mycobacterium tuberculosis* by signature-tagged transposon mutagenesis. *Mol Microbiol* **34**:257-67.
17. **Chan, E. D., J. Chan, and N. W. Schluger.** 2001. What is the role of nitric oxide in murine and human host defense against tuberculosis? Current knowledge. *Am J Respir Cell Mol Biol* **25**:606-12.
18. **Cheetham, G. M., and T. A. Steitz.** 2000. Insights into transcription: structure and function of single-subunit DNA-dependent RNA polymerases. *Curr Opin Struct Biol* **10**:117-23.
19. **Chen, M., S. Khalid, M. S. Sansom, and H. Bayley.** 2008. Outer membrane protein G: Engineering a quiet pore for biosensing. *Proc Natl Acad Sci USA* **105**:6272-7.
20. **Cowan, S. W., T. Schirmer, G. Rummel, M. Steiert, R. Ghosh, R. A. Paupit, J. N. Jansonius, and J. P. Rosenbusch.** 1992. Crystal structures explain functional properties of two *E. coli* porins. *Nature* **358**:727-33.
21. **Cox, J. S., B. Chen, M. McNeil, and W. R. Jacobs, Jr.** 1999. Complex lipid determines tissue-specific replication of *Mycobacterium tuberculosis* in mice. *Nature* **402**:79-83.
22. **Cramer, A., E. A. Whitehorn, E. Tate, and W. P. Stemmer.** 1996. Improved green fluorescent protein by molecular evolution using DNA shuffling. *Nat. Biotechnol.* **14**:315-319.
23. **Danelishvili, L., L. S. Young, and L. E. Bermudez.** 2006. In vivo efficacy of phage therapy for *Mycobacterium avium* infection as delivered by a nonvirulent mycobacterium. *Microb Drug Resist* **12**:1-6.
24. **de Jonge, M. I., G. Pehau-Arnaudet, M. M. Fretz, F. Romain, D. Bottai, P. Brodin, N. Honore, G. Marchal, W. Jiskoot, P. England, S. T. Cole, and R. Brosch.** 2007. ESAT-6 from *Mycobacterium tuberculosis* dissociates from its putative chaperone CFP-10 under acidic conditions and exhibits membrane-lysing activity. *J Bacteriol* **189**:6028-34.
25. **de Planque, M. R., and J. A. Killian.** 2003. Protein-lipid interactions studied with designed transmembrane peptides: role of hydrophobic matching and interfacial anchoring. *Mol Membr Biol* **20**:271-84.
26. **de Zoysa, R. S., D. A. Jayawardhana, Q. Zhao, D. Wang, D. W. Armstrong, and X. Guan.** 2009. Slowing DNA translocation through nanopores using a solution containing organic salts. *J Phys Chem B* **113**:13332-6.
27. **Eftink, M. R.** 1997. Fluorescence methods for studying equilibrium macromolecule-ligand interactions. *Methods Enzymol* **278**:221-57.
28. **Ehrt, S., and D. Schnappinger.** 2009. Mycobacterial survival strategies in the phagosome: defence against host stresses. *Cell Microbiol.*
29. **Engelhardt, H., C. Heinz, and M. Niederweis.** 2002. A tetrameric porin limits the cell wall permeability of *Mycobacterium smegmatis*. *J. Biol. Chem.* **277**:37567-37572.

30. **Estrem, S. T., T. Gaal, W. Ross, and R. L. Gourse.** 1998. Identification of an UP element consensus sequence for bacterial promoters. *Proc Natl Acad Sci USA* **95**:9761-6.
31. **Fabrino, D. L., C. K. Bleck, E. Anes, A. Hasilik, R. C. Melo, M. Niederweis, G. Griffiths, and M. G. Gutierrez.** 2009. Porins facilitate nitric oxide-mediated killing of mycobacteria. *Microbes Infect* **11**:868-75.
32. **Faller, M., M. Niederweis, and G. E. Schulz.** 2004. The structure of a mycobacterial outer-membrane channel. *Science* **303**:1189-92.
33. **Flynn, J. L., and J. Chan.** 2001. Immunology of tuberculosis. *Annu Rev Immunol* **19**:93-129.
34. **Fologea, D., J. Uplinger, B. Thomas, D. S. McNabb, and J. Li.** 2005. Slowing DNA translocation in a solid-state nanopore. *Nano Lett* **5**:1734-7.
35. **Ford, M. E., G. J. Sarkis, A. E. Belanger, R. W. Hendrix, and G. F. Hatfull.** 1998. Genome structure of mycobacteriophage D29: implications for phage evolution. *J Mol Biol* **279**:143-64.
36. **Gavigan, J. A., J. A. Ainsa, E. Perez, I. Otal, and C. Martin.** 1997. Isolation by genetic labeling of a new mycobacterial plasmid, pJAZ38, from *Mycobacterium fortuitum*. *J Bacteriol* **179**:4115-22.
37. **Geijtenbeek, T. B., S. J. Van Vliet, E. A. Koppel, M. Sanchez-Hernandez, C. M. Vandenbroucke-Grauls, B. Appelmelk, and Y. Van Kooyk.** 2003. Mycobacteria target DC-SIGN to suppress dendritic cell function. *J Exp Med* **197**:7-17.
38. **Golomb, M., and M. Chamberlin.** 1974. Characterization of T7-specific ribonucleic acid polymerase. IV. Resolution of the major in vitro transcripts by gel electrophoresis. *J Biol Chem* **249**:2858-63.
39. **Gordhan, B. G., D. A. Smith, H. Alderton, R. A. McAdam, G. J. Bancroft, and V. Mizrahi.** 2002. Construction and phenotypic characterization of an auxotrophic mutant of *Mycobacterium tuberculosis* defective in L-arginine biosynthesis. *Infect Immun* **70**:3080-4.
40. **Gourse, R. L., W. Ross, and T. Gaal.** 2000. UPs and downs in bacterial transcription initiation: the role of the alpha subunit of RNA polymerase in promoter recognition. *Mol Microbiol* **37**:687-95.
41. **Hagedorn, M., K. H. Rohde, D. G. Russell, and T. Soldati.** 2009. Infection by tubercular mycobacteria is spread by nonlytic ejection from their amoeba hosts. *Science* **323**:1729-33.
42. **Hagedorn, M., and T. Soldati.** 2007. Flotillin and RacH modulate the intracellular immunity of Dictyostelium to Mycobacterium marinum infection. *Cell Microbiol* **9**:2716-33.
43. **Hatfull, G. F., and G. J. Sarkis.** 1993. DNA sequence, structure and gene expression of mycobacteriophage L5: a phage system for mycobacterial genetics. *Mol Microbiol* **7**:395-405.
44. **Heinz, C., H. Engelhardt, and M. Niederweis.** 2003. The core of the tetrameric mycobacterial porin MspA is an extremely stable beta-sheet domain. *J. Biol. Chem.* **278**:8678-8685.
45. **Herrera, M., N. J. Hong, and J. L. Garvin.** 2006. Aquaporin-1 transports NO across cell membranes. *Hypertension* **48**:157-64.

46. **Hillmann, D., I. Eschenbacher, A. Thiel, and M. Niederweis.** 2007. Expression of the major porin gene *mspA* is regulated in *Mycobacterium smegmatis*. *J Bacteriol* **189**:958-67.
47. **Hondalus, M. K., S. Bardarov, R. Russell, J. Chan, W. R. Jacobs, Jr., and B. R. Bloom.** 2000. Attenuation of and protection induced by a leucine auxotroph of *Mycobacterium tuberculosis*. *Infect. Immun.* **68**:2888-98.
48. **Hong, H., S. Park, R. H. Jimenez, D. Rinehart, and L. K. Tamm.** 2007. Role of aromatic side chains in the folding and thermodynamic stability of integral membrane proteins. *J Am Chem Soc* **129**:8320-7.
49. **Hsu, T., S. M. Hingley-Wilson, B. Chen, M. Chen, A. Z. Dai, P. M. Morin, C. B. Marks, J. Padiyar, C. Goulding, M. Gingery, D. Eisenberg, R. G. Russell, S. C. Derrick, F. M. Collins, S. L. Morris, C. H. King, and W. R. Jacobs, Jr.** 2003. The primary mechanism of attenuation of bacillus Calmette-Guerin is a loss of secreted lytic function required for invasion of lung interstitial tissue. *Proc Natl Acad Sci USA* **100**:12420-5.
50. **Jackson, M., S. W. Phalen, M. Lagranderie, D. Ensergueix, P. Chavarot, G. Marchal, D. N. McMurray, B. Gicquel, and C. Guilhot.** 1999. Persistence and protective efficacy of a *Mycobacterium tuberculosis* auxotroph vaccine. *Infect Immun* **67**:2867-73.
51. **Jones, W. D., Jr., and H. L. David.** 1971. Inhibition by rifampin of mycobacteriophage D29 replication in its drug-resistant host, *Mycobacterium smegmatis* ATCC 607. *Am Rev Respir Dis* **103**:618-24.
52. **Jung, Y. J., R. LaCourse, L. Ryan, and R. J. North.** 2002. Virulent but not avirulent *Mycobacterium tuberculosis* can evade the growth inhibitory action of a T helper 1-dependent, nitric oxide Synthase 2-independent defense in mice. *J Exp Med* **196**:991-8.
53. **Kampf, J. P., D. Cupp, and A. M. Kleinfeld.** 2006. Different mechanisms of free fatty acid flip-flop and dissociation revealed by temperature and molecular species dependence of transport across lipid vesicles. *J Biol Chem* **281**:21566-74.
54. **Kaps, I., S. Ehrt, S. Seeber, D. Schnappinger, C. Martin, L. W. Riley, and M. Niederweis.** 2001. Energy transfer between fluorescent proteins using a co-expression system in *Mycobacterium smegmatis*. *Gene* **278**:115-24.
55. **Kartmann, B., S. Stenger, and M. Niederweis.** 1999. Porins in the cell wall of *Mycobacterium tuberculosis*. *J. Bacteriol.* **181**:6543-6546. (Authors' correction appeared in *J. Bacteriol.* **181**, 7650).
56. **Kelkar, D. A., and A. Chattopadhyay.** 2006. Membrane interfacial localization of aromatic amino acids and membrane protein function. *J Biosci* **31**:297-302.
57. **Killian, J. A., I. Salemink, M. R. de Planque, G. Lindblom, R. E. Koeppe, 2nd, and D. V. Greathouse.** 1996. Induction of nonbilayer structures in diacylphosphatidylcholine model membranes by transmembrane alpha-helical peptides: importance of hydrophobic mismatch and proposed role of tryptophans. *Biochemistry* **35**:1037-45.
58. **Kondo, E., and K. Kanai.** 1976. An attempt to cultivate mycobacteria in simple synthetic liquid medium containing lecithin-cholesterol liposomes. *Jpn J Med Sci Biol* **29**:109-21.

59. **Kreusch, A., and G. E. Schulz.** 1994. Refined structure of the porin from *Rhodopseudomonas blastica*. Comparison with the porin from *Rhodobacter capsulatus*. *J. Mol. Biol.* **243**:891-905.
60. **Liu, J., C. E. Barry, 3rd, G. S. Besra, and H. Nikaido.** 1996. Mycolic acid structure determines the fluidity of the mycobacterial cell wall. *J. Biol. Chem.* **271**:29545-51.
61. **Liu, J., E. Y. Rosenberg, and H. Nikaido.** 1995. Fluidity of the lipid domain of cell wall from *Mycobacterium chelonae*. *Proc. Natl. Acad. Sci. U S A* **92**:11254-8.
62. **Mahfoud, M., S. Sukumaran, P. Hülsmann, K. Grieger, and M. Niederweis.** 2006. Topology of the porin MspA in the outer membrane of *Mycobacterium smegmatis*. *J Biol Chem* **281**:5908-15.
63. **Mailaender, C., N. Reiling, H. Engelhardt, S. Bossmann, S. Ehlers, and M. Niederweis.** 2004. The MspA porin promotes growth and increases antibiotic susceptibility of both *Mycobacterium bovis* BCG and *Mycobacterium tuberculosis*. *Microbiology* **150**:853-864.
64. **Majlessi, L., P. Brodin, R. Brosch, M. J. Rojas, H. Khun, M. Huerre, S. T. Cole, and C. Leclerc.** 2005. Influence of ESAT-6 secretion system 1 (RD1) of *Mycobacterium tuberculosis* on the interaction between mycobacteria and the host immune system. *J Immunol* **174**:3570-9.
65. **McDonough, K. A., Y. Kress, and B. R. Bloom.** 1993. Pathogenesis of tuberculosis: interaction of *Mycobacterium tuberculosis* with macrophages [published erratum appears in *Infect Immun* 1993 Sep61(9):4021-4]. *Infect Immun* **61**:2763-73.
66. **Mecke, A., S. Uppuluri, T. M. Sassanella, D. K. Lee, A. Ramamoorthy, J. R. Baker, Jr., B. G. Orr, and M. M. Banaszak Holl.** 2004. Direct observation of lipid bilayer disruption by poly(amidoamine) dendrimers. *Chem Phys Lipids* **132**:3-14.
67. **Meltzer, M., S. Hasenbein, N. Mamant, M. Merdanovic, S. Poepsel, P. Hauske, M. Kaiser, R. Huber, T. Krojer, T. Clausen, and M. Ehrmann.** 2009. Structure, function and regulation of the conserved serine proteases DegP and DegS of *Escherichia coli*. *Res Microbiol* **160**:660-6.
68. **Mo, Y., N. M. Quanquin, W. H. Vecino, U. D. Ranganathan, L. Tesfa, W. Bourn, K. M. Derbyshire, N. L. Letvin, W. R. Jacobs, Jr., and G. J. Fennelly.** 2007. Genetic alteration of *Mycobacterium smegmatis* to improve mycobacterium-mediated transfer of plasmid DNA into mammalian cells and DNA immunization. *Infect Immun* **75**:4804-16.
69. **Mohamedmohaideen, N. N., S. K. Palaninathan, P. M. Morin, B. J. Williams, M. Braunstein, S. E. Tichy, J. Locker, D. H. Russell, W. R. Jacobs, Jr., and J. C. Sacchettini.** 2008. Structure and function of the virulence-associated high-temperature requirement A of *Mycobacterium tuberculosis*. *Biochemistry* **47**:6092-102.
70. **Mulder, M. A., H. Zappe, and L. M. Steyn.** 1999. The *Mycobacterium tuberculosis* katG promoter region contains a novel upstream activator. *Microbiology* **145**:2507-18.

71. **Müller, D. J., and A. Engel.** 1999. Voltage and pH-induced channel closure of porin OmpF visualized by atomic force microscopy. *J. Mol. Biol.* **285**:1347-51.
72. **Munoz-Elias, E. J., and J. D. McKinney.** 2005. *Mycobacterium tuberculosis* isocitrate lyases 1 and 2 are jointly required for *in vivo* growth and virulence. *Nat Med* **11**:638-44.
73. **Murry, J. P., A. K. Pandey, C. M. Sasseti, and E. J. Rubin.** 2009. Phthiocerol dimycocerosate transport is required for resisting interferon-gamma-independent immunity. *J Infect Dis* **200**:774-82.
74. **Ng, V. H., J. S. Cox, A. O. Sousa, J. D. MacMicking, and J. D. McKinney.** 2004. Role of KatG catalase-peroxidase in mycobacterial pathogenesis: countering the phagocyte oxidative burst. *Mol Microbiol* **52**:1291-302.
75. **Niederweis, M.** 2003. Mycobacterial porins - new channel proteins in unique outer membranes. *Mol. Microbiol.* **49**:1167-77.
76. **Niederweis, M.** 2008. Nutrient acquisition by mycobacteria. *Microbiology* **154**:679-692.
77. **Niederweis, M., S. Ehrt, C. Heinz, U. Klöcker, S. Karosi, K. M. Swiderek, L. W. Riley, and R. Benz.** 1999. Cloning of the *mspA* gene encoding a porin from *Mycobacterium smegmatis*. *Mol. Microbiol.* **33**:933-945.
78. **Nikaido, H.** 2003. Molecular basis of bacterial outer membrane permeability revisited. *Microbiol. Mol. Biol. Rev.* **67**:593-656.
79. **Ohno, H., G. Zhu, V. P. Mohan, D. Chu, S. Kohno, W. R. Jacobs, Jr., and J. Chan.** 2003. The effects of reactive nitrogen intermediates on gene expression in *Mycobacterium tuberculosis*. *Cell Microbiol* **5**:637-48.
80. **Phale, P. S., T. Schirmer, A. Prilipov, K. L. Lou, A. Hardmeyer, and J. P. Rosenbusch.** 1997. Voltage gating of *Escherichia coli* porin channels: role of the constriction loop. *Proc Natl Acad Sci USA* **94**:6741-5.
81. **Pieters, J.** 2008. *Mycobacterium tuberculosis* and the macrophage: maintaining a balance. *Cell Host Microbe* **3**:399-407.
82. **Portevin, D., C. De Sousa-D'Auria, C. Houssin, C. Grimaldi, M. Chami, M. Daffe, and C. Guilhot.** 2004. A polyketide synthase catalyzes the last condensation step of mycolic acid biosynthesis in mycobacteria and related organisms. *Proc. Natl. Acad. Sci. USA* **101**:314-9.
83. **Pratt, L. A., W. Hsing, K. E. Gibson, and T. J. Silhavy.** 1996. From acids to *osmZ*: multiple factors influence synthesis of the OmpF and OmpC porins in *Escherichia coli*. *Mol Microbiol* **20**:911-7.
84. **Purdy, G. E., M. Niederweis, and D. G. Russell.** 2009. Decreased outer membrane permeability protects mycobacteria from killing by ubiquitin-derived peptides. *Mol Microbiol* **73**:844-57.
85. **Ranes, M. G., J. Rauzier, M. Lagranderie, M. Gheorghiu, and B. Gicquel.** 1990. Functional analysis of pAL5000, a plasmid from *Mycobacterium fortuitum*: construction of a "mini" *mycobacterium-Escherichia coli* shuttle vector. *J Bacteriol* **172**:2793-7.
86. **Raynaud, C., C. Guilhot, J. Rauzier, Y. Bordat, V. Pelicic, R. Manganeli, I. Smith, B. Gicquel, and M. Jackson.** 2002. Phospholipases C are involved in the virulence of *Mycobacterium tuberculosis*. *Mol Microbiol* **45**:203-17.

87. **Raynaud, C., K. G. Papavinasasundaram, R. A. Speight, B. Springer, P. Sander, E. C. Böttger, M. J. Colston, and P. Draper.** 2002. The functions of OmpATb, a pore-forming protein of *Mycobacterium tuberculosis*. *Mol. Microbiol.* **46**:191-201.
88. **Robert, V., E. B. Volokhina, F. Senf, M. P. Bos, P. Van Gelder, and J. Tommassen.** 2006. Assembly factor Omp85 recognizes its outer membrane protein substrates by a species-specific C-terminal motif. *PLoS Biol* **4**:e377.
89. **Robertson, K. M., and D. P. Tieleman.** 2002. Molecular basis of voltage gating of OmpF porin. *Biochem Cell Biol* **80**:517-23.
90. **Rousseau, C., N. Winter, E. Pivert, Y. Bordat, O. Neyrolles, P. Ave, M. Huerre, B. Gicquel, and M. Jackson.** 2004. Production of phthiocerol dimycocerosates protects *Mycobacterium tuberculosis* from the cidal activity of reactive nitrogen intermediates produced by macrophages and modulates the early immune response to infection. *Cell Microbiol* **6**:277-87.
91. **Russell, D. G.** 2007. Who puts the tubercle in tuberculosis? *Nat Rev Microbiol* **5**:39-47.
92. **Ryll, R., Y. Kumazawa, and I. Yano.** 2001. Immunological properties of trehalose dimycolate (cord factor) and other mycolic acid-containing glycolipids--a review. *Microbiol Immunol* **45**:801-11.
93. **Sambandamurthy, V. K., X. Wang, B. Chen, R. G. Russell, S. Derrick, F. M. Collins, S. L. Morris, and W. R. Jacobs, Jr.** 2002. A pantothenate auxotroph of *Mycobacterium tuberculosis* is highly attenuated and protects mice against tuberculosis. *Nat Med* **8**:1171-4.
94. **Sassetti, C. M., and E. J. Rubin.** 2003. Genetic requirements for mycobacterial survival during infection. *Proc Natl Acad Sci USA* **100**:12989-12994.
95. **Schmider, W., A. Fahr, H. E. Blum, and G. Kurz.** 2000. Transport of heptafluorostearate across model membranes. Membrane transport of long-chain fatty acid anions I. *J Lipid Res* **41**:775-87.
96. **Schulz, G. E.** 1993. Bacterial porins: structure and function. *Curr. Opin. Cell Biol.* **5**:701-7.
97. **Sen, K., J. Hellman, and H. Nikaido.** 1988. Porin channels in intact cells of *Escherichia coli* are not affected by Donnan potentials across the outer membrane. *J. Biol. Chem.* **263**:1182-7.
98. **Senaratne, R. H., H. Mobasheri, K. G. Papavinasasundaram, P. Jenner, E. J. Lea, and P. Draper.** 1998. Expression of a gene for a porin-like protein of the OmpA family from *Mycobacterium tuberculosis* H37Rv. *J. Bacteriol.* **180**:3541-3547.
99. **Sharma, J. N., A. Al-Omran, and S. S. Parvathy.** 2007. Role of nitric oxide in inflammatory diseases. *Inflammopharmacology* **15**:252-9.
100. **Simeone, R., D. Bottai, and R. Brosch.** 2009. ESX/type VII secretion systems and their role in host-pathogen interaction. *Curr Opin Microbiol* **12**:4-10.
101. **Siroy, A., C. Mailaender, D. Harder, S. Koerber, F. Wolschendorf, O. Danilchanka, Y. Wang, C. Heinz, and M. Niederweis.** 2008. Rv1698 of *Mycobacterium tuberculosis* represents a new class of channel-forming outer membrane proteins. *J. Biol. Chem.* **283**:17827-37.

102. **Smith, D. A., T. Parish, N. G. Stoker, and G. J. Bancroft.** 2001. Characterization of auxotrophic mutants of *Mycobacterium tuberculosis* and their potential as vaccine candidates. *Infect Immun* **69**:1142-50.
103. **Smith, J., J. Manoranjan, M. Pan, A. Bohsali, J. Xu, J. Liu, K. L. McDonald, A. Szyk, N. LaRonde-LeBlanc, and L. Y. Gao.** 2008. Evidence for pore formation in host cell membranes by ESX-1-secreted ESAT-6 and its role in *Mycobacterium marinum* escape from the vacuole. *Infect Immun* **76**:5478-87.
104. **Song, H., and M. Niederweis.** 2007. Functional expression of the Flp recombinase in *Mycobacterium bovis* BCG. *Gene* **399**:112-9.
105. **Song, H., R. Sandie, Y. Wang, M. A. Andrade-Navarro, and M. Niederweis.** 2008. Identification of outer membrane proteins of *Mycobacterium tuberculosis*. *Tuberculosis* **88**:526-44.
106. **Stahl, C., S. Kubetzko, I. Kaps, S. Seeber, H. Engelhardt, and M. Niederweis.** 2001. MspA provides the main hydrophilic pathway through the cell wall of *Mycobacterium smegmatis*. *Mol. Microbiol.* **40**:451-464 (Authors' correction appeared in *Mol. Microbiol.* **57**, 1509).
107. **Stinear, T. P., T. Seemann, P. F. Harrison, G. A. Jenkin, J. K. Davies, P. D. Johnson, Z. Abdellah, C. Arrowsmith, T. Chillingworth, C. Churcher, K. Clarke, A. Cronin, P. Davis, I. Goodhead, N. Holroyd, K. Jagels, A. Lord, S. Moule, K. Mungall, H. Norbertczak, M. A. Quail, E. Rabinowitsch, D. Walker, B. White, S. Whitehead, P. L. Small, R. Brosch, L. Ramakrishnan, M. A. Fischbach, J. Parkhill, and S. T. Cole.** 2008. Insights from the complete genome sequence of *Mycobacterium marinum* on the evolution of *Mycobacterium tuberculosis*. *Genome Res* **18**:729-41.
108. **Stolt, P., and N. G. Stoker.** 1996. Functional definition of regions necessary for replication and incompatibility in the *Mycobacterium fortuitum* plasmid pAL5000. *Microbiology* **142**:2795-802.
109. **Stover, C. K., V. F. de la Cruz, T. R. Fuerst, J. E. Burlein, L. A. Benson, L. T. Bennett, G. P. Bansal, J. F. Young, M. H. Lee, G. F. Hatfull, and et al.** 1991. New use of BCG for recombinant vaccines. *Nature* **351**:456-60.
110. **Terpe, K.** 2006. Overview of bacterial expression systems for heterologous protein production: from molecular and biochemical fundamentals to commercial systems. *Appl Microbiol Biotechnol* **72**:211-22.
111. **Timm, J., E. M. Lim, and B. Gicquel.** 1994. *Escherichia coli*-mycobacteria shuttle vectors for operon and gene fusions to *lacZ*: the pJEM series. *J. Bacteriol.* **176**:6749-53.
112. **Trias, J., V. Jarlier, and R. Benz.** 1992. Porins in the cell wall of mycobacteria. *Science* **258**:1479-81.
113. **Ulrichs, T., and S. H. Kaufmann.** 2006. New insights into the function of granulomas in human tuberculosis. *J Pathol* **208**:261-9.
114. **van den Berg, B.** 2005. The FadL family: unusual transporters for unusual substrates. *Curr Opin Struct Biol* **15**:401-7.
115. **van der Wel, N., D. Hava, D. Houben, D. Fluitsma, M. van Zon, J. Pierson, M. Brenner, and P. J. Peters.** 2007. *M. tuberculosis* and *M. leprae* translocate from the phagolysosome to the cytosol in myeloid cells. *Cell* **129**:1287-98.

116. **Voulhoux, R., M. P. Bos, J. Geurtsen, M. Mols, and J. Tommassen.** 2003. Role of a highly conserved bacterial protein in outer membrane protein assembly. *Science* **299**:262-5.
117. **Voulhoux, R., and J. Tommassen.** 2004. Omp85, an evolutionarily conserved bacterial protein involved in outer-membrane-protein assembly. *Res Microbiol* **155**:129-35.
118. **Wieland, C. W., E. A. Koppel, J. den Dunnen, S. Florquin, A. N. McKenzie, Y. van Kooyk, T. van der Poll, and T. B. Geijtenbeek.** 2007. Mice lacking SIGNR1 have stronger T helper 1 responses to *Mycobacterium tuberculosis*. *Microbes Infect* **9**:134-41.